Dynamic analysis of serum tumor marker decline during anti-cancer treatment using population kinetic modeling approach

Benoît You

N° d'ordre : 42-2011 Année 2011

THESE DE L'UNIVERSITE DE LYON

Délivrée par

L'UNIVERSITE CLAUDE BERNARD LYON I

ECOLE DOCTORALE : ED 205 Interdisciplinaire Sciences-Santé (EDISS)

DIPLOME DE DOCTORAT
(Arrêté du 7 août 2006)

Présentée et soutenue publiquement le 11 mars 2011

Par

M. YOU Benoît

DYNAMIC ANALYSIS OF SERUM TUMOR MARKER DECLINE DURING ANTI-CANCER TREATMENT USING POPULATION KINETIC MODELING APPROACH

ANALYSE DYNAMIQUE DE LA CINETIQUE DE DECROISSANCE DES MARQUEURS TUMORAUX SERIQUES EN COURS DE TRAITEMENT AU MOYEN DE LA MODELISATION ET DE LA CINETIQUE DE POPULATION

Président de thèse : Prof. FREYER Gilles (Lyon, France)
Directeur de thèse : Dr. TRANCHAND Brigitte (Lyon, France)
Co-Directeur de thèse : Prof. TOD Michel (Lyon, France)

Jury : Rapporteur : Prof. SPANO Jean-Philippe (Paris, France)
Rapporteur : Prof. BARBOLOSI Dominique (Marseille, France)
Invité international : Prof. OZA Amit (Toronto, Canada)

UNIVERSITE CLAUDE BERNARD - LYON 1

Président de l'Université	**M. le Professeur A. Bonmartin**
Vice-président du Conseil Scientifique	M. le Professeur J-F. Mornex
Vice-président du Conseil d'Administration	M. le Professeur G. Annat
Vice-président du Conseil des Etudes et de la Vie Universitaire	M. le Professeur D. Simon
Secrétaire Général	M. G. Gay

COMPOSANTES SANTE

Faculté de Médecine Lyon Est – Claude Bernard	Directeur : M. le Professeur J. Etienne
Faculté de Médecine et de Maïeutique Lyon Sud – Charles Mérieux	Directeur : M. le Professeur F-N. Gilly
UFR d'Odontologie	Directeur : M. le Professeur D. Bourgeois
Institut des Sciences Pharmaceutiques et Biologiques	Directeur : M. le Professeur F. Locher
Institut des Sciences et Techniques de la Réadaptation	Directeur : M. le Professeur Y. Matillon
Département de formation et Centre de Recherche en Biologie Humaine	Directeur : M. le Professeur P. Farge

COMPOSANTES ET DEPARTEMENTS DE SCIENCES ET TECHNOLOGIE

Faculté des Sciences et Technologies	Directeur : M. le Professeur F. Gieres
Département Biologie	Directeur : M. le Professeur F. Fleury
Département Chimie Biochimie	Directeur : Mme le Professeur H. Parrot
Département GEP	Directeur : M. N. Siauve
Département Informatique	Directeur : M. le Professeur S. Akkouche
Département Mathématiques	Directeur : M. le Professeur A. Goldman
Département Mécanique	Directeur : M. le Professeur H. Ben Hadid
Département Physique	Directeur : Mme S. Fleck
Département Sciences de la Terre	Directeur : Mme le Professeur I. Daniel
UFR Sciences et Techniques des Activités Physiques et Sportives	Directeur : M. C. Collignon
Observatoire de Lyon	Directeur : M. B. Guiderdoni
Ecole Polytechnique Universitaire de Lyon 1	Directeur : M. P. Fournier
Institut Universitaire de Technologie de Lyon 1	Directeur : M. le Professeur C. Coulet
Institut de Science Financière et d'Assurances	Directeur : M. le Professeur J-C. Augros
Institut Universitaire de Formation des Maîtres	Directeur : M. R. Bernard

Remerciements / aknowledgements

A Monsieur le Professeur Gilles Freyer,

Tu me fais pour la deuxième fois l'honneur d'accepter la Présidence de mon jury de thèse et je t'en remercie. Avec les années, notre collaboration n'a cessé de s'enrichir et les projets de foisonner. Chaque jour, avec patience et confiance, tu me guides à l'hôpital comme à l'université et me permets de m'épanouir un peu plus dans ma vie professionnelle. Comme tu me l'as souvent dit, la carrière hospitalo-universitaire est d'une richesse incroyable. Sur ce chemin, je fais de mon mieux pour te suivre à la hauteur de l'estime et de l'amitié que je te porte. Je tiens à te remercier très chaleureusement de l'honneur que tu me fais en m'encadrant, en espérant que nous ouvrirons un jour cette très bonne bouteille souvent évoquée ensemble.

A Madame le Docteur Brigitte Tranchand,

Depuis le début, tu as dirigé mes projets et as su développer en moi un goût pour les activités de recherche. Ton oreille attentive, ta disponibilité, ton professionnalisme et ta rigueur m'ont été très chers pendant ces quelques années d'encadrement. J'essaierai de faire fructifier tout ce que tu m'as enseigné avec beaucoup de patience. Je te souhaite une heureuse retraite dans le sud que tu aimes tant.

A Monsieur le Professeur Tod,

Depuis quelques temps, nous travaillons ensemble sur des projets qui nous animent. Je mesure chaque jour la chance qui m'est donnée de pouvoir collaborer avec toi. J'ai encore beaucoup de choses à apprendre de toi.

A Messieurs les Professeurs Jean-Philippe Spano et Dominique Barbolosi,

J'ai été extrêmement touché que vous ayez accepté d'être les rapporteurs de ma thèse. Respectivement experts en oncologie et en modélisation, vous me faites l'honneur de bien vouloir juger mon travail. Il sera incontestablement enrichi de vos commentaires. J'espère qu'il constitue le début de longues collaborations.

To Professor Amit Oza,

I feel extremely honored and delighted that you have accepted to come from Canada to evaluate my PhD work. By supporting me and introducing me to GOG and GINECO, you have taken a great part in the extension of my research projects. I shall never forget your strong and sustained help: repetitive emails to GOG trophoblastic committee, visit to Ray at Sunnybrook Hospital, phone calls to NCIC and GINECO staffs, the January week-end at GOG meeting in San Diego, and now your trip to Lyon from Toronto ... I had a great time working with you at DDP and in gyne. clinics during my fellowship. You taught me so many things. I feel very grateful to you. I hope I have the pleasure and the honour to collaborate with you for very long.

RESUME en français

Plusieurs cancers sont associés à des concentrations sériques anormales de marqueurs tumoraux, tels que le prostate specific antigen (PSA) dans le cancer de prostate, l'alfa-foetoproteine (AFP) ou l'human chorionic gonadotrophin (hCG) dans les tumeurs germinales ou les maladies trophoblastiques gestationnelles (MTG). Le traitement du cancer doit s'accompagner d'une chute de leurs concentrations. Les valeurs prédictives de nombreux paramètres cinétiques censés caractériser la décroissance des marqueurs ont été publiées dans la littérature (nadir, valeur seuil, demi-vie, temps à normalisation etc…) Cependant très peu de ces paramètres sont utilisés en pratique par manque de reproductibilité.

La modélisation en approche de cinétique de population, déjà utilisée dans les études pharmacocinétiques, permettrait de caractériser de façon dynamique la décroissance des marqueurs tumoraux sériques et de compenser les limites des autres méthodes. Nous avons étudié la faisabilité et l'intérêt de cette approche dans 4 études portant sur le PSA après chirurgie d'adénome ou de cancer de la prostate, l'hCG-AFP dans les tumeurs germinales non-séminomateuses traitées par polychimiothérapie de type Bléomycine-Etoposide-Cisplatine (BEP) et l'hCG dans les MTG traitées par méthotrexate. La modélisation de la décroissance des marqueurs tumoraux a été possible dans toutes les études en adaptant la méthodologie aux spécificités de chaque marqueur. Il apparaît que les clairances apparentes du PSA et de l'hCG permettraient d'identifier les patients ayant des profils cinétiques défavorables et donc à haut risque de rechute. Des études de validation sur des cohortes indépendantes sont nécessaires.

TITRE en anglais

Dynamic analysis of serum tumor marker decline during anti-cancer treatment using population kinetic modelling approach.

RESUME en anglais

Several cancers are associated with abnormal serum concentrations of tumor markers such as prostate specific antigen (PSA) in prostate tumor diseases, alfa-fetoprotein (AFP) or human chorionic gonadotrophin (hCG) in germ cell tumors or persistent gestational trophoblastic diseases (GTD). Cancer treatment should induce decline of serum tumor marker concentrations. The predictive values of many kinetic parameters supposed to characterize tumor marker declines such as nadir, time-point cutoff, half-life, time to normalization etc…, have been reported in previous studies. However very few of them have been used in routine due to the lack of outcome reproducibility.

Population pharmacokinetic approach-based modeling is already used in pharmacokinetic studies. It might be helpful to characterize tumor marker decline equations dynamically and overcome limitations of previous studies. The feasibility and the relevance of this approach were assessed in 4 studies involving: PSA titers in patients with prostate adenoma or cancer treated with surgery; hCG-AFP in non-seminomatous germ cell tumor patients treated with BEP regimen (Bleomycin-Etoposide-Cisplatin) and hCG in GTD patients treated with methotrexate. Tumor marker decline modeling was feasible in all studies provided the methodology was adjusted to marker specificities. Apparent clearance of hCG and PSA might enable identification of patients with unfavorable decline profiles and thereby with high risk of relapse. Confirmatory studies with independent cohorts of patients are warranted.

DISCIPLINE

Médecine (Oncologie) ; Modélisation

MOTS-CLES

Marqueur tumoral ; Cancer de prostate ; Adénome de prostate ; Tumeurs germinales non-séminomateuses ; Tumeurs trophoblastiques gestationnelles ; Prostate specific antigen ; PSA ; Alfa-foetoproteine ; AFP ; Human chorionic gonadotrophin ; hCG ; Cinétique de population ; Modélisation ; Décroissance ; Pronostique ; Facteur prédictif ; Rechute ; Résistance.

KEY-WORDS

Tumor markers ; Prostate cancer ; Prostate adenoma ; Non-seminomatous germ cell tumors; Gestational trophoblastic disease; Prostate specific antigen ; PSA ; Alfa-fetoprotein ; AFP ; Human chorionic gonadotrophin ; hCG ; Population kinetics ; Modeling ; Decline ; Prognosis ; Predictive factor ; Relapse ; Resistance.

INTITULE ET ADRESSE DE L'U.F.R. OU DU LABORATOIRE :

EMR UCBL/HCL 3738 : Ciblage Thérapeutique en Oncologie (CTO)
Equipe 2 : Modélisation de la biologie tumorale et optimisation de l'effet des anticancéreux
Faculté de Médecine et de Maïeutique Lyon-Sud – Charles Mérieux
165, chemin du Petit Revoyet ; BP 12
69921 Oullins Cedex
France

Les marqueurs tumoraux sont des molécules retrouvées en quantités anormales dans certains tissus, tels que le sang, les urines ou le tissu tumoral, chez des patients atteints de cancer. Ils sont généralement produits par les cellules tumorales mais peuvent-être également sécrétés par l'organisme en réponse à la présence d'un cancer. Les marqueurs tumoraux sont plus ou moins spécifiques des cancers qu'ils sont supposés caractériser. Par exemple le *prostate specific antigen* (PSA) est très spécifique du tissu prostatique mais pas du cancer de prostate. En effet, il peut-être produit par les cellules normales, par les cellules adénomateuses ou par les cellules cancéreuses à des taux différents. Le traitement du cancer doit s'accompagner d'une chute des marqueurs tumoraux dont on peut suivre les cinétiques de décroissance. Ainsi de nombreux auteurs ont cherché à caractériser la décroissance des marqueurs tumoraux aux moyens de différentes techniques. Certains investigateurs se sont intéressés à une valeur spécifique de concentration sur la courbe de décroissance, telle que la valeur basale pré-thérapeutique, le nadir, la normalisation du marqueur ou une valeur seuil à un temps t. D'autres auteurs ont utilisé des approches cinétiques basées sur un minimum de 2 valeurs de concentration telles que le pourcentage de décroissance, la pente de décroissance, la demi-vie d'élimination, le temps au nadir ou encore le temps à normalisation. Enfin l'aire sous la courbe des concentrations en fonction du temps (*area under the curv*e ou AUC) a été analysée dans une étude portant sur le CA 125 chez des patientes traitées pour un cancer de l'ovaire. Dans la plupart des études, les investigateurs ont cherché à mettre en évidence une valeur prédictive aux marqueurs cinétiques étudiés par rapport au risque de rechute ou à la survie globale. En revanche, le rôle de la modélisation mathématique pour analyser la décroissance de marqueurs tumoraux en cours de traitement a été très peu évalué.

Dans ce projet de recherche, nous proposons d'utiliser la modélisation en approche de cinétique de population pour étudier la décroissance de marqueurs tumoraux à la suite ou pendant un traitement anticancéreux. En effet cette technique permet de modéliser l'équation de la décroissance d'un marqueur tumoral dans une population de patients, de quantifier les variabilités inter et intra-individuelles, d'évaluer l'influence de covariables individuelles sur la variabilité inexpliquée et de prédire le profil de décroissance individuel chez chaque patient. Cette méthode présente un certain nombre d'avantages puisqu'elle permet de travailler dans des conditions de *sparse data* (peu de points par patient) et de travailler rétrospectivement sur des données hétérogènes, provenant de patients non sélectionnés.

Dans 4 travaux publiés, la modélisation en approche de cinétique de population a été utilisée avec succès pour étudier la décroissance de marqueurs tumoraux, en adaptant la méthodologie aux caractéristiques du marqueur étudié. Dans la première étude, la faisabilité de la modélisation de la décroissance du PSA après adénomectomie de prostate selon la technique de Millin a été évaluée. Deux méthodologies basées sur une approche similaire (modèle basé sur la clairance du PSA et modèle multiparamétrique) ont été comparées. L'approche multiparamétrique a permis d'évaluer la production de PSA par les différentes zones prostatiques ainsi que la production de PSA résiduelle après adénomectomie. L'approche basée sur la clairance apparente du PSA est apparue plus simple et plus précise. La deuxième étude a confirmé la décroissance bi-exponentielle du PSA après prostatectomie radicale chez des patients atteints de cancer de prostate. La clairance apparente du PSA était le seul facteur prédictif significatif indépendant de rechute biologique. Dans la mesure où ce paramètre a pu être défini précocement dans le mois qui suivait la chirurgie, nous pensons qu'il pourrait être utilisé pour adapter le traitement chez les patients présentant un profil de décroissance défavorable du PSA. Dans la troisième étude, les cinétiques particulières de l'AFP et l'hCG, comportant une ascension initiale du marqueur durant la première semaine de traitement suivie d'une décroissance, ne nous a pas permis d'analyser la clairance apparente du marqueur comme dans les études antérieures. Nous avons donc caractérisé l'aire sous la courbe des concentrations en fonction du temps des 2 marqueurs. Deux groupes pronostiques ont pu être définis en fonction des AUCs de chaque marqueur tumoral. Les résultats de la quatrième étude impliquant des patientes atteintes de maladies trophoblastiques gestationnelles traitées par méthotrexate ont suggéré que la clairance apparente de l'hCG pourrait permettre de prédire le risque de résistance au méthotrexate. L'identification des patientes présentant un faible risque de résistance permettrait de réduire la dose-intensité de la chimiothérapie, comme cela a été proposé par certains experts.

Les études présentées ici présentent un certain nombre de limites susceptibles de réduire l'intérêt de l'approche utilisée. La complexité des analyses pourrait contribuer à réduire la faisabilité et l'extension de cette approche pour l'étude d'autres marqueurs tumoraux. De plus, contrairement aux études classiques de pharmacocinétique, il n'était pas possible de caractériser les taux de production de marqueur tumoral par le cancer. C'est la raison pour laquelle nous avons dû poser des hypothèses concernant ces productions. Par ailleurs, la précision des paramètres cinétiques estimés a pu être réduite par le caractère non-centralisé des mesures de concentration des marqueurs tumoraux. En effet en dehors de l'étude portant sur les tumeurs germinales non-séminomateuses, les concentrations avaient été mesurées dans plusieurs laboratoires en utilisant des trousses de dosage différents. Ceci pourrait avoir contribué à augmenter l'hétérogénéité des données et les

variabilités inter et intra-individuelles des estimations. Cependant la modélisation en approche de cinétique de population, capable d'évaluer les paramètres cinétiques de façon dynamique, indépendamment des points de temps-concentration, et de quantifier ces variabilités, a dû être moins pénalisée par ce problème que les autres méthodes rapportées antérieurement.

L'intérêt de l'approche de cinétique de population dans l'analyse de la cinétique des marqueurs tumoraux doit être encore confirmé sur les données d'études rétrospectives ou prospectives impliquant des cohortes de patients indépendantes. Une étude prospective a été prévue avec le service d'urologie du Centre Hospitalier Lyon-Sud. Près d'une centaine de patients, dont les PSA ont été mesurés à 4 reprises dans le mois qui suivait la chirurgie, ont été inclus dans une étude prospective entre octobre 2007 et octobre 2008. De plus des collaborations ont été mises en place avec des équipes internationales pour confirmer la faisabilité de la modélisation de l'hCG ainsi que la valeur prédictive de la clairance apparente de l'hCG dans les tumeurs trophoblastiques.

Enfin, nous avons prévu d'analyser les cinétiques des marqueurs tumoraux avec des modèles mécanistiques. Cette approche permettra de décrire la production de marqueur tumoral par la tumeur au moyen d'un *set* d'équations alors que la cinétique d'élimination du marqueur sera décrite par un autre *set* d'équations. L'interaction entre les 2 systèmes sera caractérisée par une inhibition du taux de production de marqueur tumoral induite par le traitement.

En conclusion, les cinétiques de décroissance des marqueurs tumoraux, supposées refléter l'efficacité des traitements anticancéreux, ont été très largement étudiées avec des stratégies différentes. Cependant très peu des marqueurs cinétiques rapportés jusqu'à ce jour sont reconnus et utilisés en routine. La modélisation mathématique pourrait permettre de mieux caractériser la décroissance des marqueurs tumoraux. De plus elle pourrait permettre de distinguer des groupes de patients selon leurs risques de rechute en vue d'un ajustement thérapeutique.

Table of Contents

I. Introduction and Background

Tumor markers are molecules, generally proteins, which are associated with cancers. They can be measured at normal or abnormal titers in different tissues including tumor, urine or blood. Tumor markers are generally produced by cancer cells or can be released by organism in response to cancer's presence [1-2].

Depending on their features and activities, 3 types of tumor markers can be distinguished [1-2]. Cancer antigens (CA) represent the majority of tumor markers and include carcinoembryonic antigen (CEA); alfa-fetoprotein (AFP); CA 125; CA 19-9; CA 15-3; CYFRA 21-1 and squamous cell carcinoma (SCC). Hormone tumor markers characterized by endocrine functions include human chorionic gonadotropin (hCG); thyrocalcitonin; thyroglobulin and chromogranin A. Enzyme tumor markers comprise lactate deshydrogenase (LDH); prostate specific antigen (PSA) and neuron specific enolase (NSE).

Tumor markers are more or less specific of cancers that they are supposed to characterize. For instance, PSA is a 33 kDa glycoprotein released by prostate cells. If PSA is very specific of prostate tissue, it is not specific of prostate cancer. Indeed it is produced by prostate normal cells, adenoma cells and cancer cells at different rates [3-4]. High blood PSA titers frequently found in cancer patients can be understood by the higher PSA release rate by prostate cancer cells. Changes in PSA titers are generally linked to alteration in prostate cancer growth induced by treatment. However high PSA values can also be related to benign prostate inflammation such as prostatitis [5].

HCG is a 37.5 kDa glycoprotein produced by placenta syncitiotrophoblastic cells during pregnancy. This marker is frequently released by seminomatous or non-seminomatous germ cell tumors (NSGCTs) and gestational trophoblastic diseases (GTD), rarely by breast, small cell lung, gastro-intestinal and urothelial cancers [6-7].

CA 125 is a 200 kDa protein which is expressed in 80% of epithelial ovarian cells. This marker is poorly specific of ovarian cancer. Indeed high CA 125 serum titer can be found in patients with ovarian carcinoma, endometrial cancer, breast cancer or lung cancer along with benign diseases such as endometriosis, renal failure, pancreatitis, pregnancy or any peritoneal inflammation [8-9].

Parallel evolution of serum tumor marker titers and cancer growth has been reported in many cancers. The role of tumor markers in screening or staging of cancer has been extensively analyzed and is still under debate. The kinetics of tumor marker titers following cancer treatment, considered as a reflection of treatment efficacy, has also been largely

investigated. Indeed the need for prognostic or predictive factors able to inform on treatment efficacy early and on risk of relapse/progression prompted the development of such studies.

« Prévoir consiste à projeter dans l'avenir ce qu'on a perçu dans le passé »
« Prediction is projecting in the future what has been seen in the past»

Henri Bergson, French philosopher (1859-1941)

II. Approaches Used to Analyze Tumor Marker Declines During Anti-Cancer Treatment in the Literature

Different approaches have been used to analyze tumor marker decrease following anti-cancer treatment. However the most adequate method has not been determined yet. Figure 1 is an illustration of the kinetics of a serum tumor marker to be investigated.

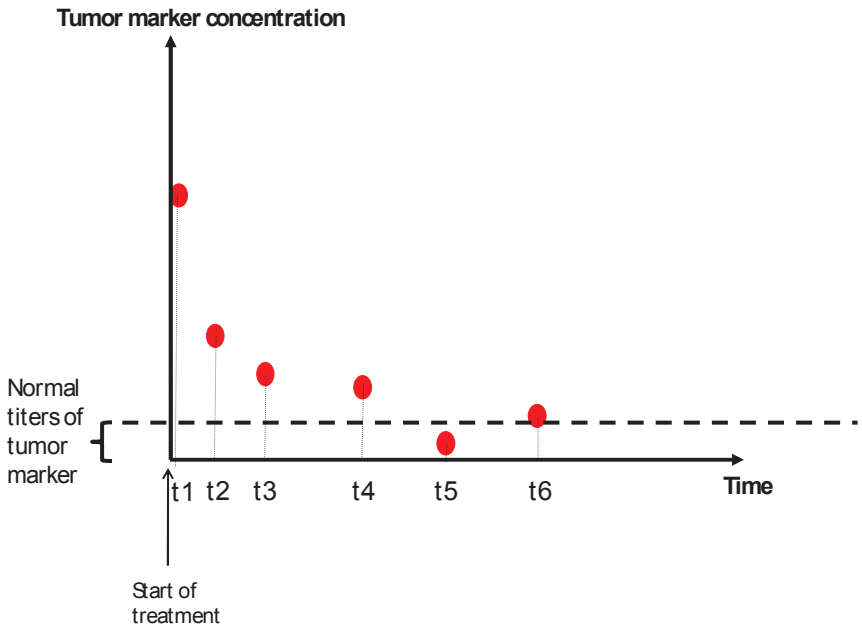

Figure 1. Typical example of serum tumor marker concentration decline profile to be analyzed.

II.1. Approaches based on a single time-point

Several authors reported the predictive value of one specific time-point supposed to characterize the tumor marker decline profile, including baseline titer; normalization of tumor marker value; nadir and cut-off at a time t.

II.1.1. Baseline (pre-treatment) titer

The predictive or prognostic value of the baseline concentration measured prior to the start of treatment has been described for most tumor markers (Figure 2). Indeed it has been reported for ACE in colorectal cancers [10-11]; CA 125 in ovarian cancers [12-15]; AFP in hepatocellular carcinoma [7, 16] and germ cell tumors [17]; CA 15-3 in breast cancers [18-21]; CA 19-9 in colorectal cancer [22-23] and pancreatic cancers [24-26]; CYFRA 21-1 in lung cancers [27]; SCC in head and neck carcinomas [28]; hCG in germ cell tumors [17] and trophoblastic tumors [29]; chromogranin A in neuroendocrine tumors [30]; LDH in germ cell tumors [17]; PSA in prostate cancers [5, 31-32] or NSE in lung cancers [33]. Across studies, the reported cut-offs were heterogeneous.

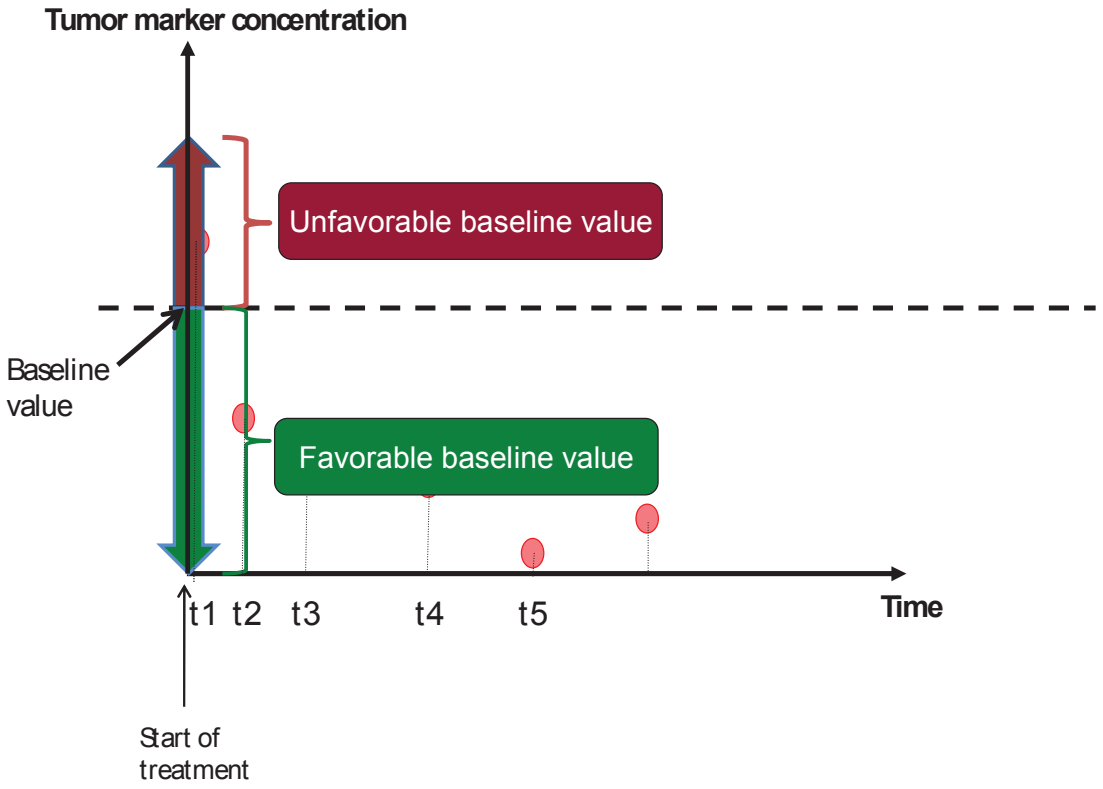

Figure 2. Prognostic value of the baseline tumor marker concentration. According to a cut-off, patients are classified into favorable or unfavorable groups regardless of further tumor marker kinetics.

Only the baseline serum concentrations of hCG & AFP in germ cell tumors and hCG in trophoblastic tumors have been consensually recognized. They are now used for treatment decision making in routine [17, 29]. The baseline values of the other tumor makers have not been considered reliable enough to be used for treatment adjustment.

This approach, although being simple to apply, presents several limitations able to explain the lack of reproducibility of reported results. First it relies on a time-point measured before the start of treatment but not on further tumor marker titers. As a result, the tumor marker baseline value does not integrate the effect of treatment, and thereby embodies a prognostic factor rather than a predictive factor. Moreover this strategy relies on the value of a single time-point prone to unexplained inter- and intra-individual variability. A single time-point outside normal decline curve might lead to wrong conclusions of abnormal decrease. As a consequence this approach is static and inaccurate to assess the decrease of tumor marker concentrations following anti-cancer treatment.

II.1.2. Normalization of tumor marker

Using this approach, a tumor marker titer is supposed to be in the normal range at a time t that is the end of treatment or another time frame defined by the authors (Figure 3). A tumor marker value outside normal values at that time means treatment failure and thereby higher risk of relapse. This strategy was mainly used for analysis of CA 125 decline during chemotherapy treatment. For instance, the predictive value of CA 125 normalization in ovarian cancers was described in 3 studies: at the end of 6 chemotherapy cycles in a review of 7 Gynecology Oncology Group (GOG) trials [34] or by the third cycle in 2 other studies [35-36]. Similar conclusions were drawn with CA 125 concentration measured after neo-adjuvant chemotherapy in ovarian cancer patients [37-38] and CA 125 after 3 chemotherapy cycles in endometrial cancers [39]. In another study including pancreatic cancer patients treated with surgery, normalization of CA 19-9 within 2 months after surgery was a positive predictor of survival [40]. The predictive value of tumor marker normalization was also reported with CA 15-3 in breast cancer patients [41-42] as well as with CEA, CA 19-9 and CA 125 in non-small cell lung cancer patients [43] along with SCC in cervix carcinoma patients treated with chemotherapy [44].

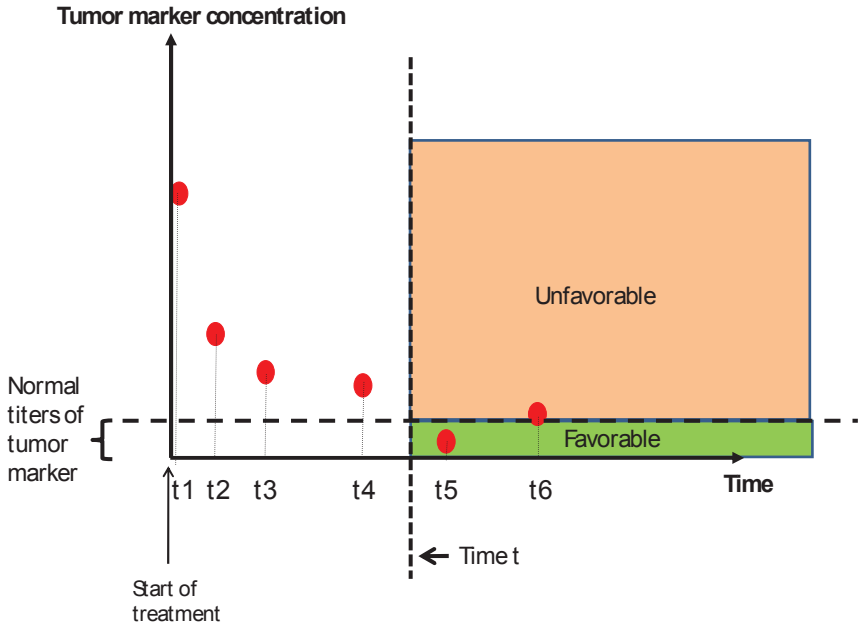

Figure 3. Predictive value of tumor marker normalization at a time t. Patients are classified into favorable or unfavorable groups according to normalization of tumor marker (yes/no) at a time t.

None of these parameters are currently used in routine due to the lack of reproducibility of this approach. It might be understood by some limitations. First this strategy is static and relies on a single time-point prone to inter- and intra-individual variability. Moreover

normalization can be expected in curative intent treatment only. As a consequence, this approach can not be applied in the cases of most of metastatic cancer patients.

II.1.3. Nadir

In this case, normalization of tumor marker is not necessarily expected. The minimum titer observed at a time t, frequently at the end of treatment, during the period of observation is considered as a predictive factor of treatment efficacy (Figure 4). This strategy has mainly been used for analysis of CA 125 concentrations in patients with ovarian cancer and of PSA values in patients with prostate cancer.

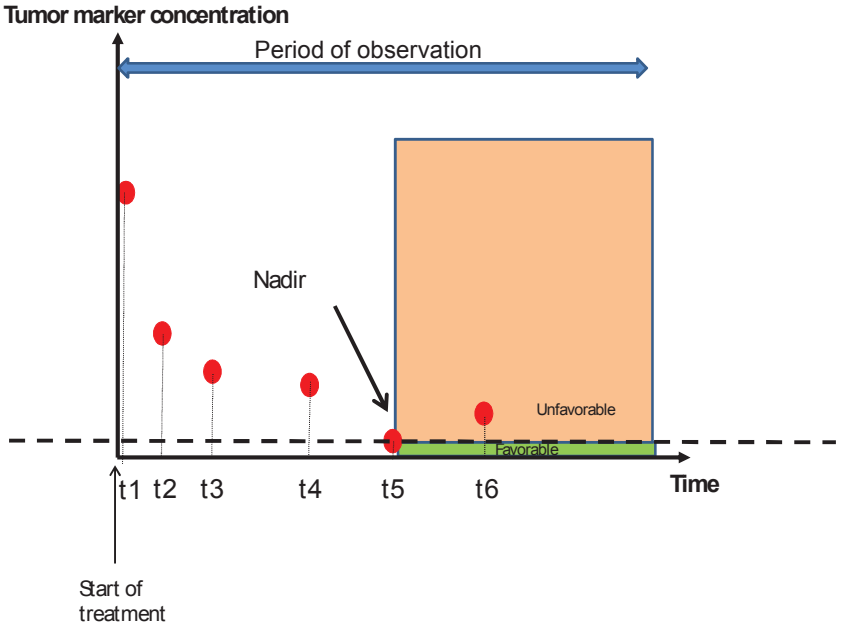

Figure 4. Predictive value of tumor marker nadir. According to the minimum tumor marker value observed during tumor marker concentration monitoring, patient are classified into favorable or unfavorable groups.

The predictive value of CA 125 nadir regarding overall survival was reported in patients with ovarian cancer at the end of neo-adjuvant chemotherapy (20 IU/mL[45]); after surgery (5 IU/mL [46]; 10 IU/mL [47]); at the end of adjuvant chemotherapy (10 IU/mL [48-49]) or before maintenance chemotherapy (10 IU/mL [49]).

Different predictive PSA nadirs were reported in prostate cancer patients treated with radiotherapy regarding biochemical relapse free survival or disease free survival[50] (0.2 ng/mL [51]; 0.4 ng/mL [52]; 0.4-2.0 ng/mL [53]; 0.5 ng/mL [54-56]; 1.0 ng/mL[56-58]; 1.2 ng/mL [59], 1.5 ng/mL[60]; 3 ng/mL [61] or nadir + 2 ng/mL [62] measured 3 months to 5 years after start of treatment). PSA nadirs predictive of biochemical recurrence were also reported in prostate cancer patients treated with radical prostatectomy (no cut-off due to continuous predictive value [63]; 0.01

ng/mL[64]; 0.4 ng/mL[65]) or treated with hormonotherapy (0.1 ng/mL[66-67]; 0.2 ng/mL [68-69]; 0.4 ng/mL [70]). In addition, a PSA nadir less than 0.2 ng/mL during first line treatment was described as a predictor of second line treatment efficacy in metastatic prostate cancer patients [71].

The CA 19-9 nadir after radiotherapy was also described as a predictive factor of survival (162.5 IU/mL [72]) in patients with pancreatic cancers, as was the CEA nadir during chemotherapy in patients with colorectal cancer regarding disease free survival (DFS) [73].

None of these parameters are currently used in routine. Indeed the nadir-based strategy is limited by dependence on a single time-point prone to inter- and intra-individual variability. Moreover it is necessarily influenced by the time frame of observation. Outside a clearly defined monitoring time window, it is difficult to know if tumor marker nadir has been reached or not.

II.1.4. Cut-off at a time t

A threshold, different from assay normal limit or nadir, is sought as a predictive factor (Figure 5). The cut-off time is generally arbitrarily defined by authors.

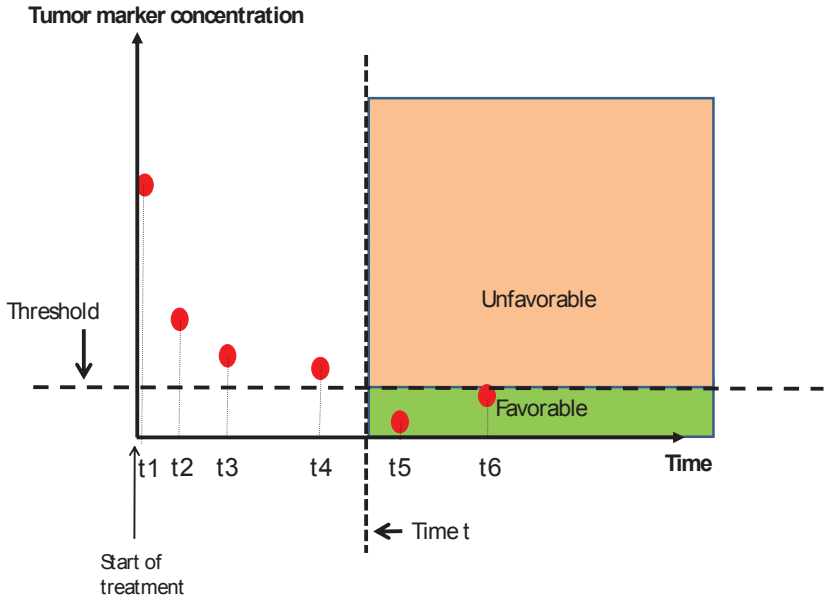

Figure 5. Predictive value of tumor marker threshold at a time t. Patients are classified into favorable or unfavorable groups depending on the value of their tumor marker with respect to this cut-off.

Different methodologies have been used to determine the cut-offs reported so far:

- Arbitrarily set thresholds. Authors compared the predictive values of different time-point cut-offs that they consider of interest and then selected the best one to predict the risk of relapse or death [48, 74-76].

- Thresholds determined according to distribution of tumor marker concentrations at a time t. Authors calculated the distribution of tumor marker values at a time t to select some percentiles of interest. Subsequently they assessed the predictive values of these cut-offs using different tests [77].

- Corridor-based approach (Figure 6). Distributions of tumor marker concentration time curves were calculated in patients with favorable outcomes and/or in patients with unfavorable outcomes. Time-point cut-offs able to discriminate patients with adequate and patients with inadequate decline profiles were inferred from observation of corridors. The predictive values of these cut-offs were sometimes subsequently tested using receiver operating characteristic (ROC) curve analyses [78-79].

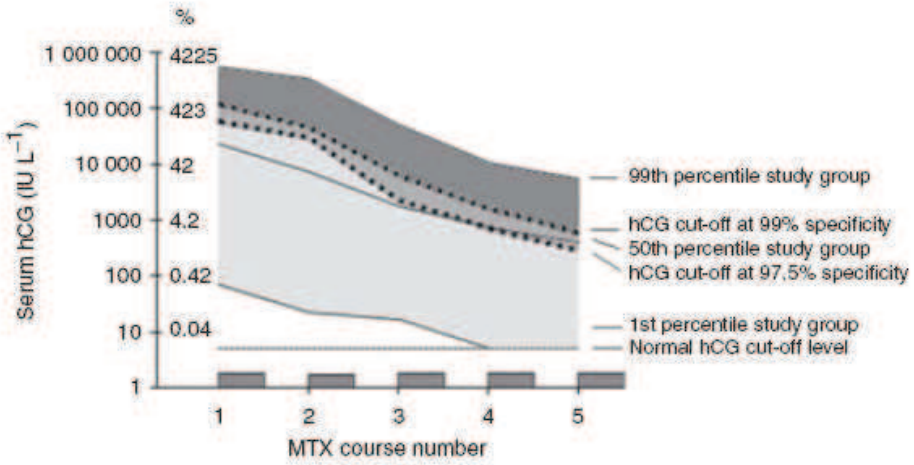

Figure 6. Typical example of tumor marker corridor analysis in patients with gestational trophoblastic disease treated with methotrexate. Distributions of serum hCG titers at different times were represented in patient population to identify cut-offs able to discriminate patients with favorable tumor decreases and those with unfavorable tumor marker declines [79].

Time-point cut-offs were reported for PSA in patients with prostate cancer after surgery regarding the risk of relapse (0.2 ng/mL [74]). As well, CA 125 cutoffs predictive of overall survival were found at the end of adjuvant chemotherapy (35 IU/mL [75]; 10 IU/mL [48]) or before maintenance chemotherapy (10 IU/mL[76, 80]) in patients with ovarian cancers. Predictive cut-offs were also described for post-operative CA 19-9 in patients with pancreatic cancer regarding overall survival (37 IU/mL [77]; 90 or 180 IU/mL [81]). Different predictive thresholds were reported for 7th week hCG titers in patients with trophoblastic tumors treated with methotrexate regarding the risk of relapse or resistance (56 µg/L [78]; 737 IU/L [79] or 500 mIU/mL [82]).

None of reported cut-offs are used in routine. As mentioned above with other single time-point-based parameters, this approach is limited by dependence on the unique value of tumor markers prone to inter- and intra-individual variability. Moreover thresholds and times were arbitrarily selected by authors in most studies. It may explain the high inconsistency in cut-offs reported so far.

II.2. Kinetic approach based on minimum 2 time-points

Many authors reported the predictive values of kinetic parameters calculated with at least 2 time-points and supposed to characterize the tumor marker concentration-time profile. The following parameters were reported: percentage change in tumor marker concentrations; decline slope; decline half-life(ves); time to normalization, time to nadir and area under the curve.

II.2.1. Percentage change in tumor marker concentrations

Using this strategy, the tumor marker percentage decrease was assessed, with or without consideration of time frame required to observe this decline. A predictive percentage cut-off was sought to discriminate patients with favorable decline and those with unfavorable decline (Figure 7).

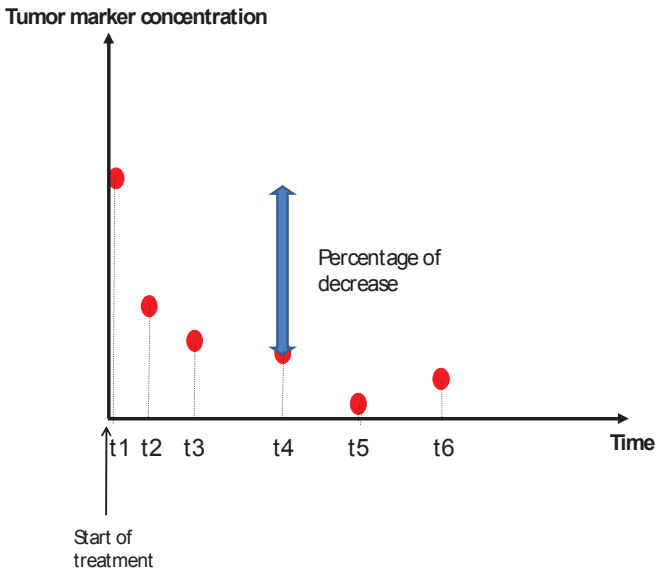

Figure 7. Predictive value of tumor marker decrease percentage. According to decrease percentage, patients are classified into favorable or unfavorable groups.

CA 125 decrease percentage by 50% or 75% correlated with response to chemotherapy in ovarian cancer patients [83-86]. A reduction of CEA, CA 15-3 or NCC-ST-439 levels by 10 or 20% or more during the 8th or 12th week of treatment was associated with better time to progression (TTP) in patients with localized or metastatic breast cancers [87-90]. A decline of

CA 19-9 by 20% or more was the only predictor of survival in advanced pancreatic cancer patients treated with chemotherapy [91].

Percentage change in tumor marker value is mainly used for assessment of tumor response in prostate cancer patients. Several studies showed that the decrease of PSA more than 50% over a 8-12 week treatment period was associated with longer median survivals in castration-resistant prostate cancer patients treated with systemic treatments [92-94]. In 1999, PSA working group declared PSA decline ≥ 50% on 2 measurements separated by ≥ 4 weeks was the official definition of PSA biochemical response for clinical trials [95]. Since then, this surrogate marker has been widely used to assess the efficacy of systemic treatments in prostate cancer patients [96-106]. For instance, a PSA decrease of ≥ 50% during at least 1 month was associated with better overall survival (OS) and progression free survival (PFS) in patients with advanced prostate cancer treated with suramine [96].

This strategy enables an easy quantification of tumor marker value decrease and comparison of decline profiles among patients, especially if times frames of measurements are homogeneous. However the calculation of tumor marker percentage decrease requires 2 time-points. It is also influenced by the inter- and intra-individual variability of tumor marker values. Because it is not possible to integrate more that 2 time-points to calculate tumor marker percentage decline, a dynamic assessment of tumor marker decline using this strategy is impossible.

II.2.2. Decline slope

The predictive value of the tumor marker decrease slope has been reported in a few studies (Figure 8). It was always determined using linear regression tests.

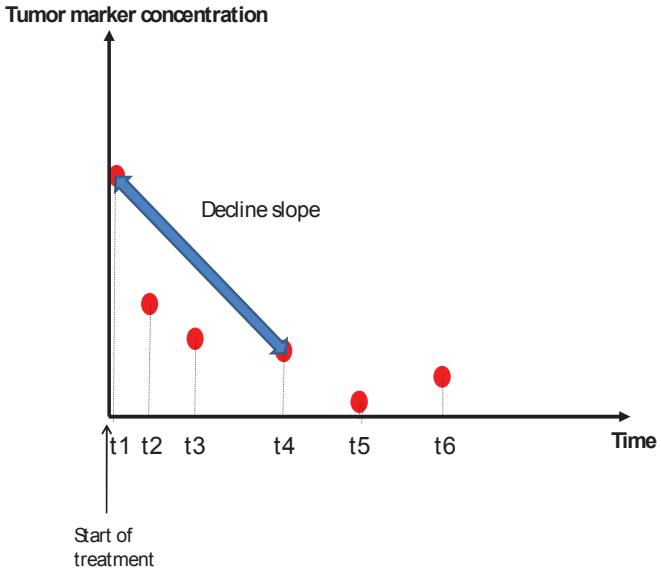

Figure 8. Predictive value of tumor marker decline slope calculated using linear regression.

The linear regression slope of CA 15-3 correlated with PFS in 122 patients with metastatic breast cancer treated with chemotherapy [107]. In addition, the linear regression slope of CA 125 correlated with overall survival in 126 patients with ovarian cancer treated by chemotherapy [108-109].

No tumor marker decline slope is currently used in routine for treatment adjustment. Although this strategy might offer an interesting assessment of tumor marker decline profile in some situations, it has been poorly used. Indeed if the studied tumor marker decrease is linear or mono-exponential, linear regression may enable an accurate assessment of tumor marker decrease rate provided several time-points have been measured to counterbalance variability. However the interpretation of tumor marker decrease slopes would not have been clear to clinicians and patients. This might have contributed to investigation of other time-dependent kinetic parameters.

II.2.3. Time to events

This strategy, which has been the most widely used, relies on calculation of the time required to observe a tumor marker event such as:

- Decrease by 50%: Half-life (HL)
- Minimum value: Time to nadir
- Normalization: Time to normalization (TTN)

II.2.3.1. Half-life/lives (HL)

The half-life is the length of time required to observe a decrease of tumor marker values by 50%. Depending on the shape of tumor marker decline, one or more elimination half-lives can be sought. If the decrease curve is mono-exponential, only one half-life can be found (e.g. $Titer(t) = A * e^{-\alpha * t} + B$). A bi-exponential decline profile can be characterized by two HLs (e.g. HL_{α} and HL_{β} if $Titer(t) = A * e^{-\alpha * t} + B * e^{-\beta * t} + C$). As shown in Figure 9, HL value may depend on time-points selected to calculate it in the case of multi-exponential decline curve.

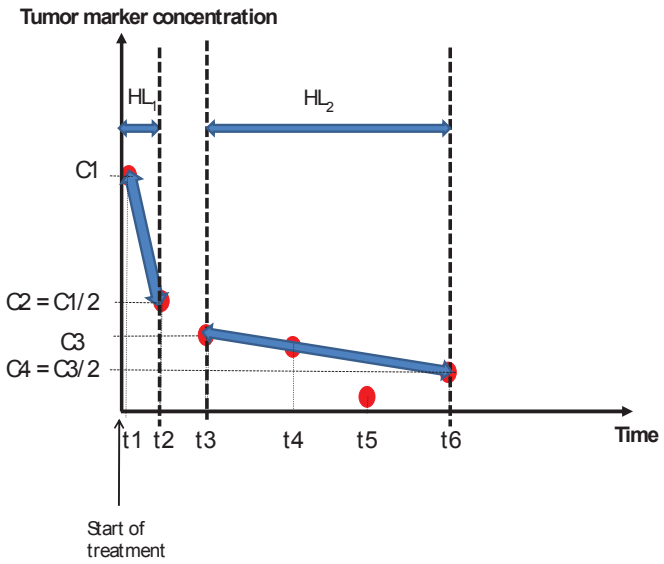

Figure 9. Predictive value of tumor marker half-lives (HLs). Half-life value depends on the time-points selected to calculate it.

The number of exponentials was arbitrarily defined on the basis of authors' assumptions or on observations of concentration-time curves. Across studies, the methodologies used to calculate tumor marker elimination half-lives differed significantly. Indeed the method was sometimes poorly reported [110-111]. In other studies, graphical representation of tumor marker concentrations versus time were used to estimate one or two decline slopes ("s") depending on author assumptions regarding tumor marker decrease profiles [112-115]. Then half-life could be calculated using *Formula 1*:

$$HL = Ln\ 2 / s \qquad (Formula\ 1)$$

An example of graphical calculation of tumor marker HL is shown in Figure 10.

In some studies, HL between time-point A and time-point B was calculated using the following *Formula 2* [116-120]:

$$HL = (Ln\ 2 * (Time\ A - Time\ B)) / (Ln\ (Titer\ A) - Ln\ (Titer\ B)) \qquad (Formula\ 2)$$

Elsewhere, linear regression tests were applied to assess decline slopes using multiple time-points when tumor maker decline profiles were assumed to be mono-exponential [121-122 123 124-129]. Reported HL values were inferred from *Formula 1*. An example of linear regression approach is shown in Figure 10.

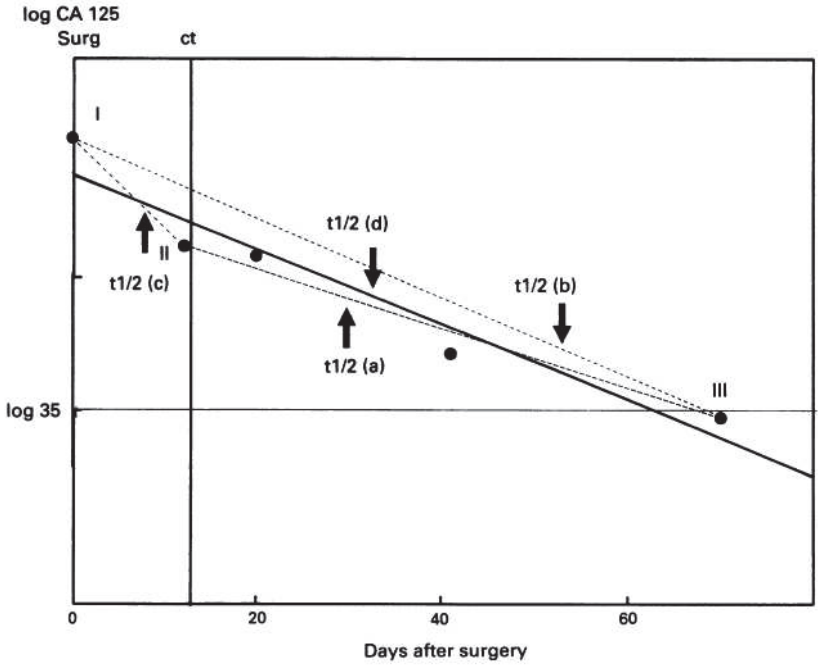

Figure 10. Typical example of half-life calculation using graphical representation and linear regression of tumor marker concentrations versus time [114]. CA 125 were measured after surgery (time-point I), before chemotherapy (ct) (time-point II) and during chemotherapy (last time-point III) in patients with ovarian cancers. Different half-lives were calculated during pre-chemotherapy period (t1/2(c)), during chemotherapy (t1/2(a)) or between the first and the last time-point (t1/2(b)) using graphical representation. Linear regression was used to assess decline slope using all time-points (t1/2(d)).

Non-linear least-square regression analyses were occasionally used to fit tumor decline profiles according to mono- or bi-exponential equations and then to calculate 1 or 2 decline slopes [130] [131-134].

Half-lives were frequently calculated to assess PSA, CA 125 and hCG-AFP declines following anti-cancer treatments.

II.2.3.1.1. PSA in patients with prostate cancer

Decrease of PSA after prostate cancer surgery or radiation treatment has been extensively analyzed using half-lives. The first study was reported in 1988 by Oesterling et al. who reported a mono-exponential decrease using a log-linear regression model in 178 patients with prostate cancer. The HL was 3.15 +/-0.09 days [123]. Other authors subsequently reported different values of PSA HL ranging from 1.9 days to 3.4 days (Table 1).

Table 1. Results of studies in which PSA decline in patients with prostate cancer after radical prostatectomy was investigated using mono-exponential models.

Study	Equation $PSA(t)=PSA_0 * e^{-kt}$	Number of patients	HL (SD) days	Disease	Predictive value
Oesterling et al. [123]	k= 0.219	178	3.15 (0.09)	Prostate cancer	Not assessed
Haab et al. [124]	ND	10 10	1.92 (1.20) 2.50 (1.33)	Bladder cancer Prostate cancer	Not assessed
Ravery et al. [122]	ND	27	3.39 (2.33) 2.15 (1.79)	Prostate benign hypertrophia Prostate cancer	Not assessed
Vollmer et al. [135]	k=0.216	27	3.20 (ND)	Prostate cancer	Not assessed

PSA_0: Initial value of PSA; HL: Half-life; SD: Standard Deviation; ND: Not Defined

When PSA decrease after radical prostatectomy was fit to bi-exponential decline curves, the 2 HLs (HL_α and HL_β) were reported in between 1.4 and 45.4 hours and 52.8 and 182.9 hours respectively (Table 2).

Table 2. Results of studies in which PSA decline in patients with prostate cancer after radical prostatectomy was investigated using bi-exponential models.

Study	Equation $PSA(t)= Ae^{-\alpha t} + Be^{-\beta t}$	Number of patients	HL_α (SD) hours	HL_β (SD) hours	Predictive value; cut-off
Stamey et al. [113]	ND	378	12.60 (19.7)	52.80 (ND)	Not assessed
Van Straalen et al. [136]	ND	8	1.63 (ND)	111.12 (ND)	Not assessed
Haab et al. [124]	ND	7	22.56 (19.2)	182.88 (152.0)	Not assessed
Lein et al. [137]	ND	11	6.30 (6.1)	85.60 (11.0)	Not assessed
Brandle et al. [130]	$PSA(t)=51.5e^{-0.0079t}+48.5e^{-0.000177t}$	11	1.45 (0.3)	65.26 (ND)	Not assessed
Gregorakis et al. [112]	$PSA(t)=3{,}34^{e-0{,}859t}+0{,}167^{e-0{,}0212t}$	9	1.75 (0.26)	71.96 (ND)	Not assessed
May et al. [116]	N.D.	77	45.36 (0.7)	81.36 (8.4)	RFS ; 3.8 days

PSA_0: Initial value of PSA; HL: Half-life; ND: Not Defined; SD: Standard Deviation; RFS: Relapse free survival

Mono-exponential models were used to describe PSA decrease after radiation treatment. In many studies, an additional exponential rate rise was incorporated in the equation. PSA HL ranged in between 0.33 and 6.93 months (Table 3).

Table 3. Results of studies in which PSA decline after radiotherapy in patients with prostate cancer was investigated

Study	Equation	Number of patients	K	HL of decrease months (SD)	Predictive value
Meek et al. [138]	$PSA(t)=PSA_0e^{-kt}$	81	ND	1.43 (0.36)	Not assessed
Kaplan et al. [134]	$PSA(t)= PSA_0*e^{-kt}$	25	2.07	0.33	Metastatic relapse
Ritter et al. [139]	$PSA(t)= PSA_0+Be^{-kt}$	63	ND	2.60	Not assessed

Zagars et al. [133]	$PSA(t)= PSA_0e^{-kt} + Be^{rt}$	154	ND	1.9	Not assessed
Zagars et al. [131]	$PSA(t)= PSA_0e^{-kt} + Be^{rt}$	578	ND	1.60	Not assessed
Hanlon et al. [140]	$PSA(t)= PSA_0e^{-kt} + B*(t-20)*It$	153	0.10	6.93	Not assessed
Vollmer et al. [135]	$PSA(t)= 22.8e^{-kt} +0.9e^{0.048t}$	164	0.37	1.87	

PSA_0: Initial value of PSA; HL: Half-life; ND: Not Defined; SD: Standard Deviation

Few studies investigated the predictive values of PSA half-lives during systemic anti-cancer treatments. Treatments and results were heterogeneous among studies (Table 4).

Table 4. Results of studies in which PSA decline in patients with prostate cancer during systemic treatment was investigated

Study	Treatment	Number of patients	HL (months)	Predictive value and cut-off
Malik et al. [141]	Neo-adjuvant hormonotherapy	117	0.5	Biochemical relapse; 2 weeks
Hanninen et al. [119]	Chemotherapy	154	13.2	Overall survival; 70 days
Banu et al. [124]	Chemotherapy	256	ND	Time to failure; Not reported
Lin et al. [70]	Hormonotherapy	153	0.5	Overall survival; 0.5 months

ND: Not Defined, SD: Standard Deviation; HL: Half-life

II.2.3.1.2. CA 125 in patients with ovarian cancer

Assessments of CA 125 half-lives in patients with ovarian cancer treated with chemotherapy were reported in several studies. CA 125 HLs along with predictive cut-offs were inconsistent among studies (Table 5). Riedinger et al. first introduced the concept of CA 125 bi-exponential decrease. In a study involving 130 ovarian patients, a mono-exponential decline profile was found in 54 patients and a bi-exponential decrease in 38 patients. They concluded the initial half-life (cut-off = 14 days) and decline profiles (mono- versus bi-exponential) were predictive factors of disease free survival and overall survival [142].

Table 5. Results of studies in which CA 125 decline during treatment in patients with ovarian cancers was investigated.

Study	Treatment	Number of patients	Mono-exponential	Bi-exponential		Predictive value and cut-off
			HL (days)	HL_α (SD) hours	HL_β (SD) hours	
Buller et al. [143]	Surgery		10			
Markowska et al. [144]	Adjuvant chemotherapy	130				OS ; ND
Yedema et al. [114]	Adjuvant chemotherapy	60	10			OS; 20 days
Gadducci et al. [118]	Palliative chemotherapy	225	25			OS; 25 days
Colakovic et al.	Palliative Chemotherapy	222				OS; 20 days
Mano et al. [120]	Adjuvant chemotherapy	63	Not reported			OS; 16 days
Gadducci et al. [117]	Palliative chemotherapy	71	14			OS; 14 days
Riedinger et al. [45]	Induction chemotherapy	631	15.8			DFS and OS; 14 days

Riedinger et al. [142]	Induction chemotherapy	54	17.0			OS; initial half-life 14 days
		38		13.6	53.1	

ND: Not defined; HL: Half-life; OS: Overall survival; DFS: Disease free survival

II.2.3.1.3. hCG and AFP in germ cell tumor patients

Most works that have assessed the predictive value of tumor marker kinetics in patients with non-seminomatous germ cell tumors relied on hCG and/or AFP half-lives (Table 6). The leading HL-based model, described by Murphy et al. [126], was based on HL_{hCG} and/or HL_{AFP} calculated between day 7 (D7; day 1 was the first day of chemotherapy) and D42 (completion of the second cycle of treatment). It was used by the Memorial Sloan-Kettering Cancer Center (MSKCC) in 2 chemotherapy dose-densification clinical trials [126, 128, 145].

Table 6. Results of studies in which AFP and hCG declines following treatment in patients with non seminomatous germ cell tumors were investigated.

Study	Treatment	Number of patients	Mono-exponential	Predictive value and cut-off
			HL (days)	
Lange et al. [125]	Surgery	36	AFP: 5.0-7.0 days hCG: 0.5–2.0 days	Overall response rate
Vogelzang et al. [146]	Induction chemotherapy	37	AFP: 6.0-7.9 days hCG: 3.1 days	Relapse rate
Toner et al. [111]	Surgery	198		OS; AFP 7 days, hCG 3 days
Murphy et al. [126]	Salvage chemotherapy	54		OS; AFP 7 days, hCG 3 days
Gerl et al. [121]	Induction chemotherapy	263	AFP: 6.2 days hCG: 2.8 days	OS, PFS; AFP 7 days, hCG 2.5 days
Inanc et al. [127]	Induction chemotherapy	34	AFP: 3.3 days hCG: 4.4 days	EFS, OS: AFP 7 days
Stevens et al. [147]	Induction chemotherapy	183	AFP: 6 days hCG: 2.6 days	OS; AFP 7 days, hCG 3 days
Mazumadar et al. [148]	Induction chemotherapy	189		OS, EFS; AFP 7 days, hCG 3.5 days

ND: Not defined; HL: Half-life; OS: Overall survival; EFS: Event free survival; PFS: Progression free survival; SD: Standard deviation

II.2.3.1.4. Other tumor markers

CEA half-life after colorectal cancer surgery correlated with risk of relapse [149-151].

Despite extensive publications, none of predictive HLs reported so far have been used for treatment adjustment in routine. Heterogeneity in methods used to assess HL and in outcomes among studies might have contributed to reduce the reproducibility of reported results. HL outcomes were very dependent on the time-points selected for HL calculation. In most works, a few time-points different among studies were retrospectively used to calculate one or two half-lives. Moreover the high unexplained inter- and intra-individual variability of tumor marker values might have introduced additional inaccuracy in HL calculations. No authors showed the predictive value of a HL was reproducible in independent cohorts of patients.

II.2.3.2. Time to nadir

This is the length of time required to observe decline of tumor markers to the minimum value during a period of observation (Figure 11). The calculation of this kinetic parameter was based on longitudinal observations of tumor markers.

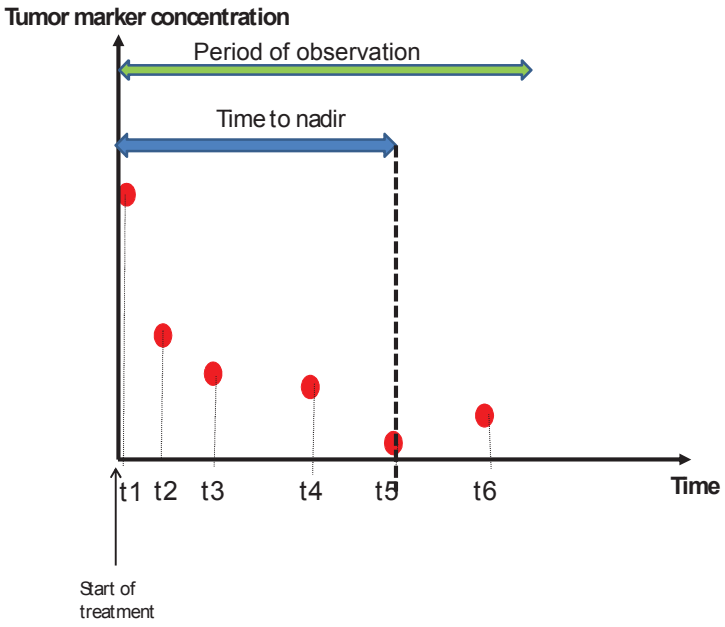

Figure 11. Time to nadir defined as the length of time required to observe minimum value of tumor marker.

This kinetic parameter has mainly been investigated for analysis of PSA in patients with prostate cancer treated with radiation treatment. It sometimes correlated with biochemical relapse free survival (cut-off at 1 year [58], 2 years [52], 1-3 years [53]; no cut-off defined [50, 61]) or not [56-57, 152] . As well, PSA time to nadir was assessed in prostate cancer patients treated with hormonotherapy [153] and correlated with disease specific survival (cut-off of 6 months [154]) or with biochemical relapse free survival (cut-off of 24 months [66]).

Time to nadir was assessed in patients with ovarian cancer treated with induction chemotherapy or adjuvant chemotherapy but had no real predictive value [45, 155].

None of these parameters are currently used in routine. This strategy presents the same limitations as nadir-based approach. Its relevance is reduced by dependence on a nadir time-point prone to inter- and intra-individual variability. Moreover it is necessarily influenced by the period of observation of tumor marker values. Outside a clearly defined monitoring time window, it is difficult to know if tumor marker nadir has been reached or not.

II.2.3.3. Time to normalization (TTN)

This kinetic parameter is defined as the length of time required for normalization of tumor marker titer (Figure 12).

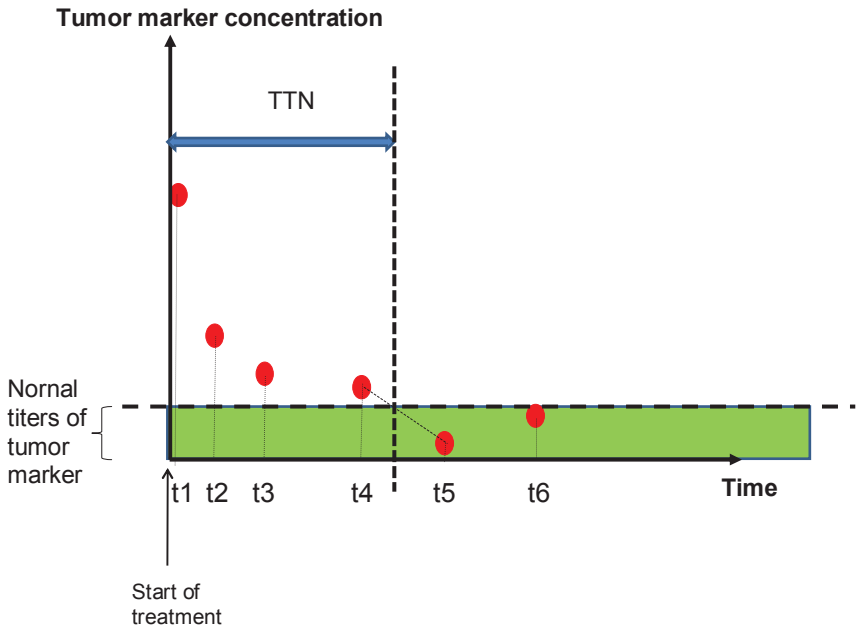

Figure 12. Definition of time to normalization (TTN).

Different methodologies were used to determine time to normalization. In some studies, it resulted from observations of patients who normalized their tumor markers [155-157]. In other studies, it was calculated using the following formula [158]:

$$TTN\ (weeks) = 3 * (\log C_0 - \log C_N) / (\log C_0 - \log C_1) \qquad \textit{(Formula 3)}$$

where C_0 is the baseline tumor marker titer; C_N is normal upper bound of tumor marker; C1 is tumor marker value after 1 cycle of chemotherapy.

TTN has mainly been assessed in patients with non-seminomatous germ cell tumors (NSGCT) by Fizazi et al. In a retrospective study involving 654 NSGCT patients treated by chemotherapy, hCG and AFP TTNs were used to determine 2 prognostic groups regarding risks of progression. Indeed the patients with hCG TTN < 6 weeks and AFP TTN < 9 weeks had better PFS than the other patients [158]. This classification has been used to adjust treatment in the on-going GETUG 13 trial in which dose-dense chemotherapy is administered in the case of unfavorable tumor marker decline profile. Similar results were

reported in a TTN-based study involving 75 patients with relapsed NSGCTs treated with salvage chemotherapy [159].

CA 125 TTN correlated with survival of ovarian cancer patients treated with surgery and adjuvant chemotherapy. The authors suggested a second look surgery was not required in patients classified into the favorable group (TTN < 1 month) in terms of overall survival [156]. Furthermore CA 125 TTNs were used to compare efficacies of 2 adjuvant chemotherapy regimens [160] or treatment route [155] in ovarian cancers. As well, PSA TTN was used to compare 2 radiation treatment modalities in patients with prostate cancer [157].

The TTN-based strategy is limited by dependence on 2 unique time-points prone to unexplained inter- and intra-individual variability. Moreover it is not applicable to treatment of most of metastatic cancers in which normalization of tumor marker is not necessarily expected.

II.2.4. Area under the curve (AUC)

The area under the concentration-time curve (AUC) was investigated in only one study [161]. Calculation of AUC was based on the sum of trapezoid areas (Figure 13).

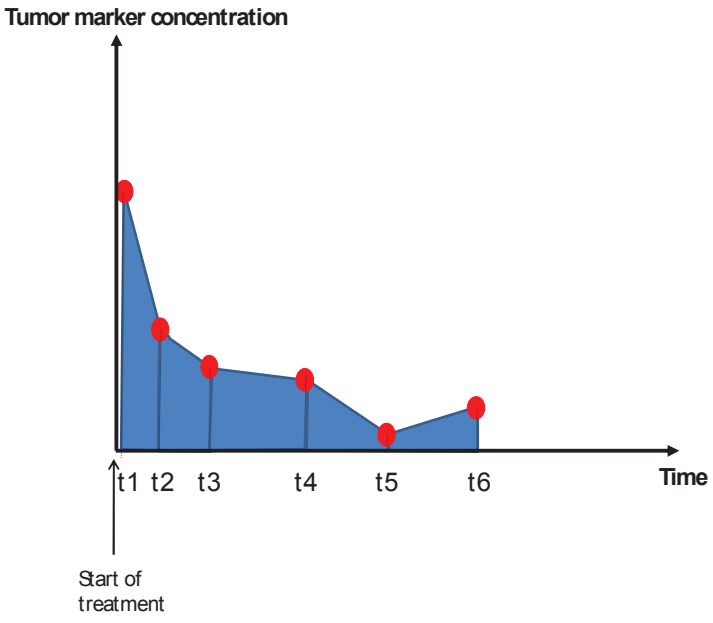

Figure 13. Calculation of tumor marker AUC between t1 and t6 using the sum of trapezoid areas.

In Mano et al., the area under CA 125 concentration-time curve was assessed in ovarian cancer patients treated with surgery followed by post-operative chemotherapy. Individual

AUCs were estimated using trapezoid areas with at least 3 time-points (Figure 14). ROC curve analysis was used to discriminate the best AUC cut-off in terms of tumor response and survival. The best CA 125 AUC able to predict patient overall survival was 1000 IU/mL*days [161].

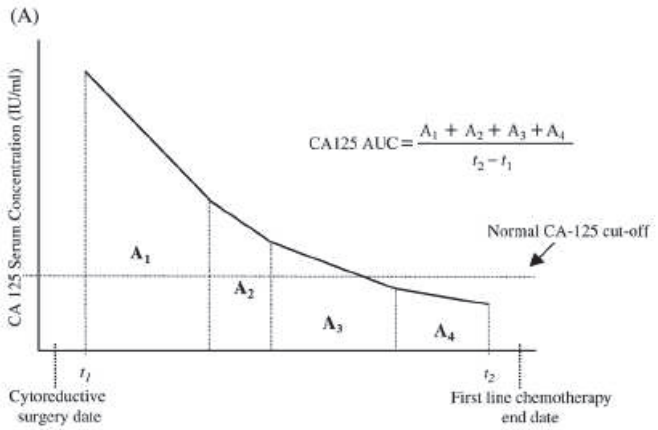

Figure 14. Trapezoid area-based approach used to calculate the AUC of CA 125 during post-operative chemotherapy in patients with locally advanced ovarian cancer in Mano et al. study [161].

A better integration of the whole decline curve might be offered by this kinetic parameter calculated with several time-points. It should be less influenced by inter- and intra-individual variability of tumor marker values than above methods. However the number of trapezoids is directly linked to the number of time-points used to calculate AUCs. As a result the accuracy of this method is influenced by the selected time-points.

II.2.5. Tumor marker modeling studies

In occasional studies, modeling was used to characterize decline profile with or without production and/or elimination of tumor marker. None of the results reported in these studies are used in routine for treatment decision.

Hanlon used non-linear mixed effect modeling (Nlinmix macro under the SAS System.17) to analyze decrease of PSA concentrations after radiation treatment in 153 prostate cancer patients [140]. PSA decline was fit to mono-exponential or bi-exponential models. Estimation was done using maximum likelihood. The authors concluded PSA was well described by a mono-exponential decline curve including an additional parameter to integrate the slight PSA increase related to repopulation of normal epithelial prostate cells

$$[PSA(t)= 4.65e^{-0.10t}+0.02*(time-20)*I(time<20)] \qquad (\textit{Formula 4})$$

The indicator function, I(time<20), specifies that the ‘‘tail’’ be considered only for PSA levels observed more than 20 months after treatment. They found that equation parameters were influenced by Gleason score and baseline PSA value [140].

Vollmer built a first-order kinetic semi-mechanistic model using non-linear least square algorithm to describe PSA decline in prostate cancer patients after radical prostatectomy and to discriminate PSA produced by benign tissues from PSA released by cancer tissues [135] (Figure 15). Both PSA production and elimination were considered in the model:

$$PSA(t)=\alpha/\beta*(1-e^{-\beta t}) + PSA_0*e^{-\beta t} \qquad \textit{(Formula 5)}$$

where PSA_0 is baseline PSA; α relates to the release of PSA by prostate cells into the prostate tissue, β relates to the excretion of PSA from the prostate to the serum compartment, k is coefficient controlling the loss of PSA from the serum. Using this model, Vollmer et al. estimated PSA productions by prostate normal and cancer tissues at 100 ng/mL.day and 1070 ng/mL.day respectively [135].

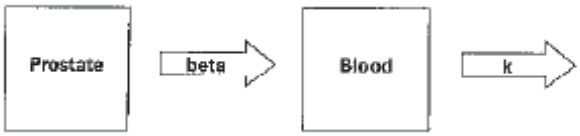

Figure 15.The 2 compartment model used by Vollmer et al. [135].

In 1994, Cappelli et al. defined the basic principles of a mechanistic modeling study for analysis of tumor marker kinetics after treatment, meant to go “beyond the cut-off”. They presented different mathematical models potentially available to describe tumor marker increase related to tumor growth (logistics models, Gomperz model) or tumor marker decrease after radical treatment (non-linear regression models, half-lives) [162]. However, they did not apply these principles for the analysis of a tumor marker.

II.3. Limitations of methods used to analyze tumor marker decline in the literature

As shown above, many studies meant to analyze tumor marker decline following cancer treatment were published over the last 30 years. Different approaches based on baseline value; cut-off at a time t; half-life; time to normalization etc… were used to find predictive factors of treatment efficacy. However very few of them have been validated on independent cohorts of patients and consensually adopted for management of cancer [17, 29 95]. It might be linked to the high heterogeneity in outcomes and the low reproducibility of reported results. For instance, in gestational trophoblastic disease patients treated with methotrexate, 3 different hCG cut-offs measured during the 7th week of treatment were predictive of resistance: 56 µg/L equivalent to 520.24 mIU/mL for Van Trommel et al. [78]; 500 mIU/mL for

Savage et al. [82] and 737 mIU/mL for Kerkmeijer et al. [79]. The lack of reproducibility of results reported in the literature might be understood by:

- Intra-individual variability of biological marker titers. Despite the advantage of its simplicity, the use of a single time-point for characterizing the complex kinetics of tumor markers is a cause of inaccuracy. A single time-point outside normal decline curve might lead to false conclusions of abnormal decrease. As a result dynamic analysis of tumor marker kinetics integrating several time-points is warranted.

- Inconsistency in time-points selected to assess time-dependent parameters such as HLs, TTNs or decline slopes. If the actual tumor-marker decline curve is not mono-exponential, as it seems to be for PSA or CA 125, HL depend on the time-points selected for analysis. No guidelines have been defined for the time-points that had to be selected to assess half-lives. As a consequence, variable time-points were chosen and heterogeneous results were reported.

- Inaccurate determination of equation parameters due to limited number of time-points in non-linear regression models. A few time-points per patient are not enough to calculate with accuracy more than 4 kinetic parameters (decrease rates along with intercepts) in the case of pluri-exponential decreases.

- Lack of assessment of inter-individual variability.

- Lack of search for individual covariates able to explain parts of unexplained variability.

Population kinetic approach might enable to overcome most of these limitations. Indeed this strategy offers a dynamic analysis of tumor marker decline curve independently on selected time-points, even in sparse data conditions; allows to quantify inter & intra-individual variability and enables determination of individual covariates able to reduce unexplained variability.

III. Population Kinetic Approach for Analysis of Tumor Marker Declines

III.1.Principles of population pharmacokinetics

III.1.1. Definition

Population pharmacokinetics describe:

-The typical relationships between physiology (both normal and disease altered) and pharmacokinetics (PK)/pharmacodynamics (PD),
-The inter-individual variability in these relationships, and
-Their residual intra-individual variability.

Sheiner-LB
Drug Metab Rev. 1984; 15(1-2): 153-71

III.1.2. General principles

Population kinetic approach is commonly used to analyze the pharmacokinetic (PK) parameters of drugs administered to study subjects. The general principles have already been described elsewhere [163-165].

On the basis of a few concentration time-points per patient exposed to a drug, this approach enables (Figure 16):

- To determine the drug concentration kinetic profile of patient population,
- To quantify inter- and intra-individual variability,
- To assess the influence of patient covariates on unexplained inter- and intra-individual variability,
- To predict drug concentration kinetic profile of every patient.

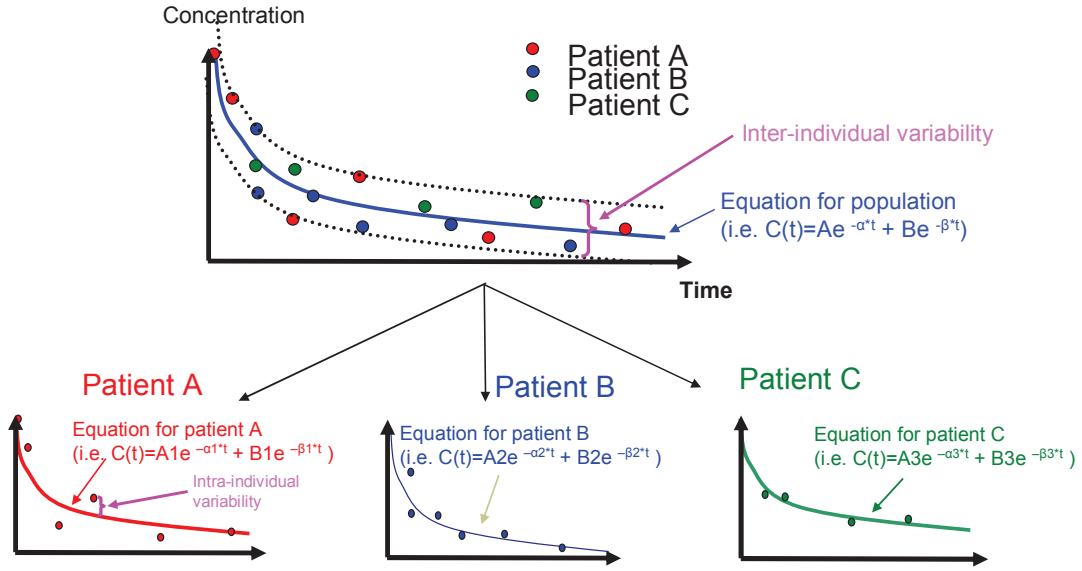

Figure 16. Principles of population kinetic approach: assessment of population decline profile using all available data, quantification of inter- and inter-individual variability, investigation of influence of individual covariates on unexplained inter-individual variability and prediction of individual decline profiles.

This approach presents several advantages:

- Sparse sampling strategy. Because all patient time-points are grouped to determine the population kinetic profile, a few data per patient (2-3 concentrations/subject) are sufficient to perform accurate PK analyses.

- Identification of covariates able to explain inter-individual variability. It is possible to test the influences of individual covariates such as renal function, liver function, age, weight, etc … on unexplained inter-individual variability of parameter estimates and thereby to increase accuracy of individual predictions.

- Large selection of patients. In opposition with other strategies that require enrollment of highly selected patients to reduce variability able to alter study outcomes, result accuracy is improved by inclusion of patients with different characteristics. As a consequence, results are more applicable to general population.

- Independence on selected time-points. The model relies on the mathematical equation of decline curves. As a result it is possible to predict the tumor marker values in any time-point of the curve.

However the population PK strategy presents some limitations:

- Complexity of analyses. Implementation of population PK models requires skills to deal with mathematical and pharmacological concepts along with computer programs.

- Time consuming analyses. This strategy requires time to format the database, design the model, to implement models in computer program, to analyze the data along with the results and to ensure external & internal validation of results.

We performed 4 studies to assess the feasibility and the relevance of population kinetic approach for analyzing decline of different tumor markers in cancer patients treated with surgery or chemotherapy.

III.2.Studies and Articles

III.2.1. PSA decline after adenomectomy in patients prostate benign hypertrophia:

You B, Perrin P, Freyer G, et al. Advantages of prostate-specific antigen (PSA) clearance model over simple PSA half-life computation to describe PSA decrease after prostate adenomectomy. Clin Biochemistry 2008;41:785-95 [166].

Study details and outcomes are shown in the article presented in pages 63 to 73.

III.2.2. PSA decrease after radical prostatectomy in patients with prostate cancer:

You B, Girard P, Paparel P, et al. Prognostic value of modeled PSA clearance on biochemical relapse free survival after radical prostatectomy. Prostate 2009;69:1325-33 [167]**.**

Study details and outcomes are shown in the article presented in pages 74 to 82.

III.2.3. hCG and AFP declines during chemotherapy in patients with non seminomatous germ cell tumors treated with BEP regimen:

You B, Fronton L, Boyle H, et al. Predictive value of modeled AUC(AFP-hCG), a dynamic kinetic parameter characterizing serum tumor marker decline in patients with nonseminomatous germ cell tumor. Urology 2010;76:423-9 e2 [168].

Study details and outcomes are shown in the article presented in pages 83 to 90.

III.2.4. hCG decrease in patients with gestational trophoblastic disease treated with methotrexate:

You B, Pollet-Villard M, Fronton L, et al. Predictive values of hCG clearance for risk of methotrexate resistance in low-risk gestational trophoblastic neoplasias. Ann Oncol 2010;21:1643-50 [169].

Study details and outcomes are shown in the article presented in pages 91 to 98.

III.3.Implementation of models with NONMEM software®

The versions V and VI of NONMEM software® (NON linear Mixed Effect Model, University of San Francisco, California, USA) compiled with Digital Visual Fortran 5.0 were used to analyze tumor marker concentration-time data with first order (FO) and first order conditional event interaction (FOCEI) methods. The following parameters were estimated:

- Fixed effects parameters:
  - Intercepts & decrease constants in multi-exponential models [166, 168-169].
  - Clearance, central compartment volume (V1) & inter-compartmental transfer rates (K12, K21) in clearance-based models [166-167].
- . Random effects:
  - Inter-individual variability.
  - Intra-individual residual variability arising from assay errors and model misspecifications.

Extensive graphical analyses of predicted versus observed concentrations were performed to test the value of each model. The search was also guided by looking at the differences between the objective functions (OF) given by NONMEM. The NONMEM OF is an approximation of twice the logarithm of the likelihood. When a model could be reduced to a simpler one by fixing some parameters to a given value (e.g., 0), the difference between the 2 NONMEM OF was approximately distributed according to a χ^2 with n degrees of freedom, n being equal to the number of additional fixed parameters in the reduced model. In addition, the hypotheses of independence or dependence of parameter inter-individual variability were investigated.

Subsequently, the main individual covariates such as patient age, weight, blood cell counts, sodium, total protein, serum creatinine clearance etc… were tested to estimate their impacts on kinetic parameters. When a covariate demonstrated significant relationships with any kinetic parameters, it was introduced into the model describing the fixed effects by forward inclusion. The covariate was kept in the model only if the decrease in the NONMEM OF was at least greater than 7, corresponding to a nominal p value < 0.01.

For instance, the influence of the “age” covariate on CL_{PSA} was tested with the following equations [166-167]:

$$CL_{PSA} = \Theta 1 * (age)^{\Theta 2} * \exp(\eta 1) \qquad (\textit{Formula 6})$$

Or

$$CL_{PSA} = \Theta 1 * (age / age_{med})^{\Theta 2} * \exp(\eta 1) \qquad (\textit{Formula 7})$$

where:

- age is the patient age and age_{med} is the median age of all patients among the cohort;
- Θ1 and Θ2 are the fixed-effect parameters

- η1 is the random-effect parameter.

The latter equation gives an easy parameter interpretation because Θ1 is the clearance of a patient whose age equals the age_{med}. Afterwards, a stepwise backward elimination procedure was performed to keep in the model only the significant covariates, producing an OF decrease of at least 11, corresponding to a $p < 0.001$.

III.4.Qualifications of the models

In efforts to qualify model abilities to predict correctly tumor marker distribution values [170-171], 100 to 500 tumor marker decline profiles were simulated across studies using the final parameters of the different models. They were subsequently compared with associated observed data using visual predictive checks (VPC) regarding the whole curves [166-169] with or without statistical predictive checks (SPC) regarding the first portion and the last portion of decline curve [166] or the decrease slope [167-168], as previously described [172].

IV. Discussion and Projects

In four studies involving 3 different tumor markers, population kinetic approach-based models could be implemented with success to assess decline of tumor markers after or during treatment. In each study, methodology was adjusted to the specific characteristics of the tumor marker analyzed.

The first study mainly investigated the feasibility of PSA decline assessment after prostate adenomectomy [166]. Two methodologies based on a similar approach were compared to prepare the second study involving PSA decline after radical prostatectomy. The clearance-based model was simpler due to the reduced number of model parameters. However the multi-parameter approach gave the opportunity to assess PSA productions by the different prostate zones along with the residual PSA release after surgery, which was requested by urologists [166].

The second study was an extension of the latter study. Consistently with studies previously reported [113, 124, 130, 136-137 112, 116], a bi-exponential decline profile best fit PSA decrease after radical prostatectomy. In addition, PSA apparent clearance was the only significant predictive factor of biochemical relapse. Given this parameter was determined with serum PSA concentrations measured early, during the first month following surgery, we assumed it could be used for treatment adjustment in patients with unfavorable PSA decline profiles. However this hypothesis will have to be validated prospectively.

In the third study, the specific shape of AFP and hCG kinetics including an initial surge during the first week of treatment avoided calculation of tumor marker apparent clearance. Areas under the tumor marker concentration-time curves were selected as predictive kinetic markers. Modeling of hCG decline curve was less accurate than AFP decrease curve. The results of this study should be considered with caution due to the limited numbers of patients & time-points, the significant number of missing data and the lack of multivariate analysis. Moreover the AUCs of 2 tumor markers had to be combined to define predictive groups, which contributed to increase uncertainty.

Given treatment of gestational trophoblastic disease has to be adjusted on hCG concentration evolution only, determination of a hCG kinetic parameter able to inform on the risk of treatment failure is warranted. The results the fourth study involving patients with trophoblastic tumors treated with methotrexate suggested hCG clearance might offer an early prediction of methotrexate resistance risk. Identification of patients with low resistance risk might enable treatment reduction, as advocated by some authors. Confirmation of the predictive value of modeled hCG clearance is warranted.

Did the population kinetic approach implemented improve assessment of tumor marker declines following anti-cancer treatment?

Several limitations able to reduce the relevance of population kinetic approach for analysis of tumor marker kinetics were identified. Compared with the simple algorithms used in studies reported in section II (graphical measurements, linear or non-linear regression), our modeling analyses were complex and time-consuming. This might contribute to reduce the feasibility and spread of such analyses on a large scale.

Moreover, in opposition with traditional population PK studies in which drug dose administered to organism is known, it was not possible to characterize tumor marker released by cancer in blood. Ideally we would have identified the production rate (Kp), the starting date of production and the steady state concentration so that we could discriminate Kp and elimination rates as showed in Figure 17 in the case of prostate cancer. However it was not possible to perform such an analysis due to unavailable data prior to the start of treatment. As a consequence, we had to do assumptions regarding tumor marker production. In prostate disease studies, PSA production was assimilated into an intravenous bolus arbitrarily set at 1, with an unknown bioavailability F that was greater than 1. As a result, the apparent volume of distribution and clearance corresponding to Clearance/F=Ke*V1 and V1/F respectively were determined, where V1 and CL were the unknown actual volume of distribution and clearance.

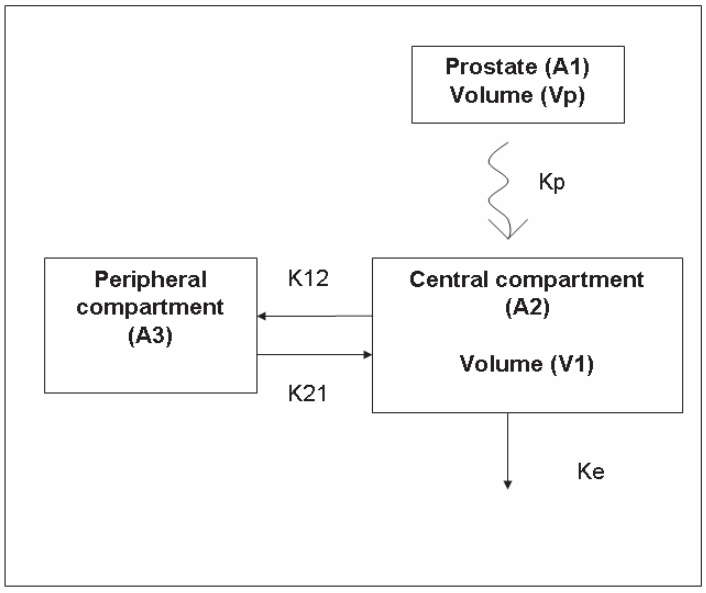

Figure 17. The optimal specification for PSA decrease model. Kp is the rate constant of PSA release from prostate to serum; K12 and K21 are the PSA transfer rate constants between the peripheral compartment and central compartment; and Ke is the elimination rate constant. PSA concentration is assayed in the central compartment [166].

In the trophoblastic tumor study, we decided to implement multi-exponential equations. Subsequently we calculated the individual apparent clearance (CL_{hCGi}) which was equal to the product of Ki and the volume of distribution (Vd) based on a previous estimation of Vd [173].

In NSGCT study, the area under the time-concentration curve between day 0 and day 42 was assessed by the sum of a trapezoid area (between day 0 and day 7) and area under the modeled tumor marker concentration-time curve (between day 7 and day 42). Indeed this study was complicated by the initial surge of hCG and AFP following start of treatment found in about 25% patients, consistently with previous reports [174-175], and led us to split tumor marker kinetics in 2 parts. The same phenomenon was reported with CEA, CA 15-3 or CA 19-9 [107, 176-178]. It might limit the exploration of these markers by population kinetic approach.

In addition, the accuracy of kinetic parameter assessment might have been reduced by the non-centralized measurement of tumor marker concentrations. Indeed except in NSGCT study, tumor marker concentrations were determined in different laboratories using variable assay kits. Many authors highlighted the large variability in tumor marker titers provided by different assays and thereby the risk of treatment making based on tumor marker values measured using different methods [179-183]. Variability related to use of different immunoassays might have contributed to increase inter- and intra-individual variability and to scatter kinetic parameter results. This might explain failures in previous studies investigating the predictive values of tumor marker kinetic parameters [184-187]. However population kinetic approach able to quantify inter- and intra-individual variability and to calculate kinetic parameters dynamically, independently on selected time-points, is supposed to be less involved by this issue. It might explain that the results regarding predictive values of modeled kinetic parameters were encouraging against those previously published.

The relevance of population kinetic approach has still to be confirmed with retrospective studies along with prospective analyses involving independent cohorts of patients. A prospective confirmatory study has been planned with Department of Urology at Centre Hospitalier Lyon-Sud. Four PSA were assayed on day 0, day 1, day 3, day 7 and day 30 after surgery in 101 patients treated with radical prostatectomy between October 2007 and October 2008. Analysis of results is planned in October 2011.

International collaborations were developed to assess the reproducibility of hCG modeling and of hCG clearance predictive value in trophoblastic tumors treated with chemotherapy. The gynecology team at Charing Cross Hospital provided with a database including hCG titers from 200 patients with low risk trophoblastic tumors treated with methotrexate. An abstract with promising results was submitted to the 2011 Annual Meeting of American Society of Clinical Oncology (Chicago, USA).

Moreover, the US Gynecology Oncology Group has recently planned to analyze decrease of hCG titers using population kinetic approach in patients enrolled in GOG 174 phase 3 trial, in which 2 chemotherapy regimens were compared. In addition, the prospective assessment of hCG clearance using population kinetic approach will be included in the protocol of the future UC 1005 phase 3 trial aiming at comparing 3 chemotherapy regimens in low risk trophoblastic tumors (GOG Semi-Annual Meeting, Boston, July 2010).

A way of improving modeling of tumor marker titer evolution would rely on mechanistic modeling approach. Using this strategy, tumor marker production related to the tumour size and proliferation would be described by one set of equation while the kinetics and the effect of chemotherapy on tumor proliferation and tumor marker production would be described by another set of equations as proposed by Cappelli et al. [162]. The interaction between the two systems would then be characterized as an inhibition of the marker production rate by the treatment. In an effort to improve characterization of tumor marker production by cancers, Sostelly et al. developed a mechanistic model describing PSA production rates by the different prostate compartments after combining the 2 post-operative PSA kinetic databases (Figure 18) [188]. They showed this approach was feasible and relevant. However their conclusions were limited due to the high number of missing PSA data before prostate surgery.

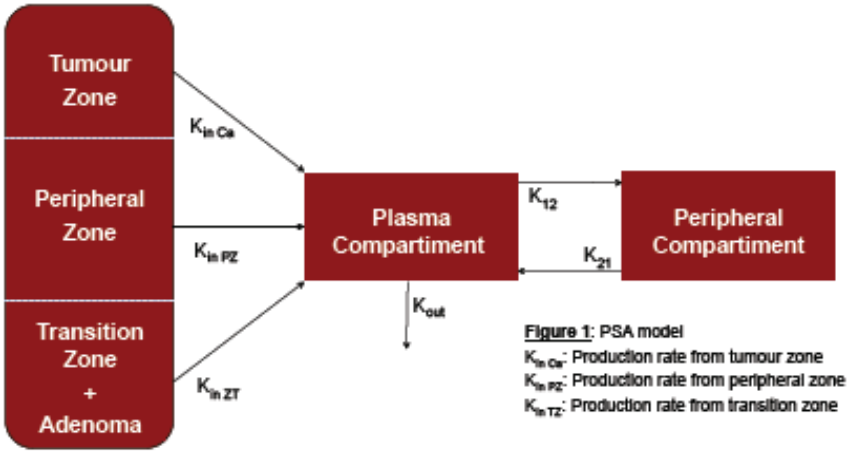

Figure 18. Schema of model used to describe PSA productions by prostate compartments as well as PSA elimination, in Sostelly et al. [188].

In addition, we are assessing the role of semi-mechanistic mathematical modeling for analysis of CA 125 kinetics in patients enrolled in the international CALYPSO phase III trial. In this study coordinated by ARCAGY-GINECO-IGCG Intergroup, the efficacies of two carboplatin-based regimens were compared. An abstract with promising results was

submitted to the 2011 Annual Meeting of American Society of Clinical Oncology (Chicago, USA).

In conclusion, tumor marker kinetics following cancer treatment, considered as a reflection of treatment efficacy, has been studied by many authors using variable methodologies. Very few of these kinetic parameters have been adopted in routine. Mathematical modeling might help better characterize the accurate equation of tumor marker decline curve. Moreover it might contribute to discriminate patients with favorable or unfavorable decrease profiles, to predict risk of relapse and thereby to adjust treatment early.

« Savoir pour prévoir, afin de pouvoir »
« Knowledge to foresee in order to be able»

Auguste Comte, French philosopher (1798-1857)

V. References

1. Sturgeon C. Practice guidelines for tumor marker use in the clinic. Clin Chem 2002;48:1151-9.
2. You B, Freyer G. Du bon usage des principaux biomarqueurs tumoraux. In: Maloine, ed. Diagnostic difficile en médecine interne. Third ed; 2008.
3. Aus G, Bergdahl S, Frosing R, Lodding P, Pileblad E, Hugosson J. Reference range of prostate-specific antigen after transurethral resection of the prostate. Urology 1996;47:529-31.
4. Recker F, Kwiatkowski MK, Pettersson K, et al. Enhanced expression of prostate-specific antigen in the transition zone of the prostate. A characterization following prostatectomy for benign hyperplasia. Eur Urol 1998;33:549-55.
5. Lilja H, Ulmert D, Vickers AJ. Prostate-specific antigen and prostate cancer: prediction, detection and monitoring. NatRevCancer 2008;8:268-78.
6. Mottet N, Berger N, Droz JP. [Diagnosis and staging of germ-cell tumours of the testis]. RevPrat 2007;57:365-78.
7. Voorzanger-Rousselot N, Garnero P. Biochemical markers in oncology. Part I: molecular basis. Part II: clinical uses. Cancer TreatRev 2007;33:230-83.
8. Gadducci A, Cosio S, Carpi A, Nicolini A, Genazzani AR. Serum tumor markers in the management of ovarian, endometrial and cervical cancer. BiomedPharmacother 2004;58:24-38.
9. Rapkiewicz AV, Espina V, Petricoin EF, III, Liotta LA. Biomarkers of ovarian tumours. EurJCancer 2004;40:2604-12.
10. Park YJ, Youk EG, Choi HS, et al. Experience of 1446 rectal cancer patients in Korea and analysis of prognostic factors. IntJColorectal Dis 1999;14:101-6.
11. Wang WS, Lin JK, Chiou TJ, et al. Preoperative carcinoembryonic antigen level as an independent prognostic factor in colorectal cancer: Taiwan experience 2. JpnJClin Oncol 2000;30:12-6.
12. Bast RC, Jr., Badgwell D, Lu Z, et al. New tumor markers: CA125 and beyond. IntJGynecolCancer 2005;15 Suppl 3:274-81.
13. Paramasivam S, Tripcony L, Crandon A, et al. Prognostic importance of preoperative CA-125 in International Federation of Gynecology and Obstetrics stage I epithelial ovarian cancer: an Australian multicenter study. JClinOncol 2005;23:5938-42.
14. Vorgias G, Iavazzo C, Savvopoulos P, et al. Can the preoperative Ca-125 level predict optimal cytoreduction in patients with advanced ovarian carcinoma? A single institution cohort study. Gynecol Oncol 2009;112:11-5.
15. Zorn KK, Tian C, McGuire WP, et al. The prognostic value of pretreatment CA 125 in patients with advanced ovarian carcinoma: a Gynecologic Oncology Group study. Cancer 2009;115:1028-35.
16. Jeng KS, Sheen IS, Tsai YC. Does the presence of circulating hepatocellular carcinoma cells indicate a risk of recurrence after resection? AmJGastroenterol 2004;99:1503-9.
17. International Germ Cell Consensus Classification: a prognostic factor-based staging system for metastatic germ cell cancers. International Germ Cell Cancer Collaborative Group. JClinOncol 1997;15:594-603.
18. Clinical practice guidelines for the use of tumor markers in breast and colorectal cancer. Adopted on May 17, 1996 by the American Society of Clinical Oncology 1. JClin Oncol 1996;14:2843-77.
19. Gion M, Boracchi P, Dittadi R, et al. Prognostic role of serum CA15.3 in 362 node-negative breast cancers. An old player for a new game 5. EurJCancer 2002;38:1181-8.
20. Shering SG, Sherry F, McDermott EW, O'Higgins NJ, Duffy MJ. Preoperative CA 15-3 concentrations predict outcome of patients with breast carcinoma 1. Cancer 1998;83:2521-7.
21. Uehara M, Kinoshita T, Hojo T, Akashi-Tanaka S, Iwamoto E, Fukutomi T. Long-term prognostic study of carcinoembryonic antigen (CEA) and carbohydrate antigen 15-3 (CA 15-3) in breast cancer. Int J Clin Oncol 2008;13:447-51.

22. Eche N, Pichon MF, Quillien V, et al. [Standards, options and recommendations for tumor markers in colorectal cancer]. BullCancer 2001;88:1177-206.
23. Kouri M, Nordling S, Kuusela P, Pyrhonen S. Poor prognosis associated with elevated serum CA 19-9 level in advanced colorectal carcinoma, independent of DNA ploidy or SPF 1. EurJCancer 1993;29A:1691-6.
24. Hess V, Glimelius B, Grawe P, et al. CA 19-9 tumour-marker response to chemotherapy in patients with advanced pancreatic cancer enrolled in a randomised controlled trial 1. Lancet Oncol 2008;9:132-8.
25. Steinberg W. The clinical utility of the CA 19-9 tumor-associated antigen 2. AmJGastroenterol 1990;85:350-5.
26. Reni M, Cereda S, Balzano G, et al. Carbohydrate antigen 19-9 change during chemotherapy for advanced pancreatic adenocarcinoma. Cancer 2009;115:2630-9.
27. Pujol JL, Molinier O, Ebert W, et al. CYFRA 21-1 is a prognostic determinant in non-small-cell lung cancer: results of a meta-analysis in 2063 patients. BrJCancer 2004;90:2097-105.
28. Torre GC. SCC antigen in malignant and nonmalignant squamous lesions. TumourBiol 1998;19:517-26.
29. FIGO staging for gestational trophoblastic neoplasia 2000. FIGO Oncology Committee. IntJ GynaecolObstet 2002;77:285-7.
30. Nobels FR, Kwekkeboom DJ, Coopmans W, et al. Chromogranin A as serum marker for neuroendocrine neoplasia: comparison with neuron-specific enolase and the alpha-subunit of glycoprotein hormones. JClinEndocrinolMetab 1997;82:2622-8.
31. Kattan MW, Wheeler TM, Scardino PT. Postoperative nomogram for disease recurrence after radical prostatectomy for prostate cancer. JClinOncol 1999;17:1499-507.
32. Han M, Partin AW, Zahurak M, Piantadosi S, Epstein JI, Walsh PC. Biochemical (prostate specific antigen) recurrence probability following radical prostatectomy for clinically localized prostate cancer. J Urol 2003;169:517-23.
33. Bonner JA, Sloan JA, Rowland KM, Jr., et al. Significance of neuron-specific enolase levels before and during therapy for small cell lung cancer. ClinCancer Res 2000;6:597-601.
34. Tian C, Markman M, Zaino R, et al. CA-125 change after chemotherapy in prediction of treatment outcome among advanced mucinous and clear cell epithelial ovarian cancers: a Gynecologic Oncology Group study. Cancer 2009;115:1395-403.
35. Rocconi RP, Matthews KS, Kemper MK, Hoskins KE, Huh WK, Straughn JM, Jr. The timing of normalization of CA-125 levels during primary chemotherapy is predictive of survival in patients with epithelial ovarian cancer. Gynecol Oncol 2009;114:242-5.
36. Wong C, Dai ZM, Lele SB, Natarajan N. Comparison of CA 125 after three courses of chemotherapy and results of second-look surgery. Eur J Gynaecol Oncol 2000;21:70-3.
37. Le T, Faught W, Hopkins L, Fung-Kee-Fung M. Importance of CA125 normalization during neoadjuvant chemotherapy followed by planned delayed surgical debulking in patients with epithelial ovarian cancer. J Obstet Gynaecol Can 2008;30:665-70.
38. Tate S, Hirai Y, Takeshima N, Hasumi K. CA125 regression during neoadjuvant chemotherapy as an independent prognostic factor for survival in patients with advanced ovarian serous adenocarcinoma. Gynecol Oncol 2005;96:143-9.
39. Hoskins PJ, Le N, Correa R. CA 125 normalization with chemotherapy is independently predictive of survival in advanced endometrial cancer. Gynecol Oncol 2010.
40. Motoi F, Rikiyama T, Katayose Y, Egawa SI, Unno M. Retrospective Evaluation of the Influence of Postoperative Tumor Marker Status on Survival and Patterns of Recurrence After Surgery for Pancreatic Cancer Based on RECIST Guidelines. Ann Surg Oncol 2010.
41. Vizcarra E, Lluch A, Cibrian R, et al. Value of CA 15.3 in breast cancer and comparison with CEA and TPA: a study of specificity in disease-free follow-up patients and sensitivity in patients at diagnosis of the first metastasis. Breast Cancer Res Treat 1996;37:209-16.
42. Repetto L, Onetto M, Gardin G, et al. Serum CEA, CA 15-3, and MCA in breast cancer patients: a clinical evaluation. Cancer Detect Prev 1993;17:411-5.

43. Spiridonidis CH, Laufman LR, Stydnicki KA, et al. Decline of posttreatment tumor marker levels after therapy of nonsmall cell lung cancer. A useful outcome predictor. Cancer 1995;75:1586-93.
44. Rose PG, Baker S, Fournier L, Nelson BE, Hunter RE. Serum squamous cell carcinoma antigen levels in invasive cervical cancer: prediction of response and recurrence. Am J Obstet Gynecol 1993;168:942-6.
45. Riedinger JM, Wafflart J, Ricolleau G, et al. CA 125 half-life and CA 125 nadir during induction chemotherapy are independent predictors of epithelial ovarian cancer outcome: results of a French multicentric study. Ann Oncol 2006;17:1234-8.
46. van Altena AM, Kolwijck E, Spanjer MJ, Hendriks JC, Massuger LF, de Hullu JA. CA125 nadir concentration is an independent predictor of tumor recurrence in patients with ovarian cancer: a population-based study. Gynecol Oncol 2010;119:265-9.
47. Kang S, Seo SS, Park SY. Nadir CA-125 level is an independent prognostic factor in advanced epithelial ovarian cancer. J Surg Oncol 2009;100:244-7.
48. Prat A, Parera M, Peralta S, et al. Nadir CA-125 concentration in the normal range as an independent prognostic factor for optimally treated advanced epithelial ovarian cancer. Ann Oncol 2008;19:327-31.
49. Liu PY, Alberts DS, Monk BJ, Brady M, Moon J, Markman M. An early signal of CA-125 progression for ovarian cancer patients receiving maintenance treatment after complete clinical response to primary therapy. J Clin Oncol 2007;25:3615-20.
50. Sandler HM, Dunn RL, McLaughlin PW, Hayman JA, Sullivan MA, Taylor JM. Overall survival after prostate-specific-antigen-detected recurrence following conformal radiation therapy. Int J Radiat Oncol Biol Phys 2000;48:629-33.
51. Critz FA, Williams WH, Holladay CT, et al. Post-treatment PSA < or = 0.2 ng/mL defines disease freedom after radiotherapy for prostate cancer using modern techniques. Urology 1999;54:968-71.
52. Kestin LL, Vicini FA, Ziaja EL, Stromberg JS, Frazier RC, Martinez AA. Defining biochemical cure for prostate carcinoma patients treated with external beam radiation therapy. Cancer 1999;86:1557-66.
53. Martinez AA, Kestin LL, Stromberg JS, et al. Interim report of image-guided conformal high-dose-rate brachytherapy for patients with unfavorable prostate cancer: the William Beaumont phase II dose-escalating trial. Int J Radiat Oncol Biol Phys 2000;47:343-52.
54. Critz FA, Levinson AK, Williams WH, Holladay DA, Holladay CT. The PSA nadir that indicates potential cure after radiotherapy for prostate cancer. Urology 1997;49:322-6.
55. Ogawa K, Nakamura K, Sasaki T, et al. Postoperative radiotherapy for localized prostate cancer: clinical significance of nadir prostate-specific antigen value within 12 months. Anticancer Res 2009;29:4605-13.
56. Ellis RJ, Vertocnik A, Kim E, et al. Four-year biochemical outcome after radioimmunoguided transperineal brachytherapy for patients with prostate adenocarcinoma. Int J Radiat Oncol Biol Phys 2003;57:362-70.
57. Kavadi VS, Zagars GK, Pollack A. Serum prostate-specific antigen after radiation therapy for clinically localized prostate cancer: prognostic implications. Int J Radiat Oncol Biol Phys 1994;30:279-87.
58. Aref I, Eapen L, Agboola O, Cross P. The relationship between biochemical failure and time to nadir in patients treated with external beam therapy for T1-T3 prostate carcinoma. Radiother Oncol 1998;48:203-7.
59. Doyle KL, Roach M, Weinberg V, McLaughlin P, Sandler H. What Does the Post Radiotherapy Prostate Specific Antigen (PSA) Nadir Tell Us About Progression-Free-Survival in Patients with Localized Cancer. Int J Radiat Oncol Biol Phys;51.
60. Buyyounouski MK. Radiotherapy: PSA nadir predicts long-term mortality. Nat Rev Clin Oncol 2010;7:188-90.
61. Cavanaugh SX, Kupelian PA, Fuller CD, et al. Early prostate-specific antigen (PSA) kinetics following prostate carcinoma radiotherapy: prognostic value of a time-and-PSA threshold model. Cancer 2004;101:96-105.

62. Kuban DA, Levy LB, Potters L, et al. Comparison of biochemical failure definitions for permanent prostate brachytherapy. Int J Radiat Oncol Biol Phys 2006;65:1487-93.
63. Moreira DM, Presti Jr JC, Aronson WJ, et al. Postoperative prostate-specific antigen nadir improves accuracy for predicting biochemical recurrence after radical prostatectomy: Results from the Shared Equal Access Regional Cancer Hospital (SEARCH) and Duke Prostate Center databases. Int J Urol 2010.
64. Hong SK, Park HZ, Lee WK, et al. Prognostic significance of undetectable ultrasensitive prostate-specific antigen nadir after radical prostatectomy. Urology 2010;76:723-7.
65. Stephenson AJ, Kattan MW, Eastham JA, et al. Defining biochemical recurrence of prostate cancer after radical prostatectomy: a proposal for a standardized definition. JClinOncol 2006;24:3973-8.
66. Hori S, Jabbar T, Kachroo N, Vasconcelos JC, Robson CN, Gnanapragasam VJ. Outcomes and predictive factors for biochemical relapse following primary androgen deprivation therapy in men with bone scan negative prostate cancer. J Cancer Res Clin Oncol 2010.
67. Alexander A, Crook J, Jones S, et al. Is biochemical response more important than duration of neoadjuvant hormone therapy before radiotherapy for clinically localized prostate cancer? An analysis of the 3- versus 8-month randomized trial. Int J Radiat Oncol Biol Phys 2010;76:23-30.
68. Morote J, Trilla E, Esquena S, Abascal JM, Reventos J. Nadir prostate-specific antigen best predicts the progression to androgen-independent prostate cancer. Int J Cancer 2004;108:877-81.
69. Soga N, Arima K, Sugimura Y. Undetectable level of prostate specific antigen (PSA) nadir predicts PSA biochemical failure in local prostate cancer with delayed-combined androgen blockade. Jpn J Clin Oncol 2008;38:617-22.
70. Lin GW, Yao XD, Zhang SL, et al. Prostate-specific antigen half-life: a new predictor of progression-free survival and overall survival in Chinese prostate cancer patients. Asian J Androl 2009;11:443-50.
71. Kobayashi M, Suzuki K, Kurokawa S, Yuzawa M, Morita T. Second-Line Antiandrogen Therapy in Japanese Men with Advanced Prostate Cancer Relapsed after Primary Combined Androgen Blockade: Who Will Benefit from Second-Line Hormonal Therapy? Urol Int 2010.
72. Katz A, Hanlon A, Lanciano R, Hoffman J, Coia L. Prognostic value of CA 19-9 levels in patients with carcinoma of the pancreas treated with radiotherapy. Int J Radiat Oncol Biol Phys 1998;41:393-6.
73. Grem JL, Steinberg SM, Chen AP, et al. The utility of monitoring carcinoembyronic antigen during systemic therapy for advanced colorectal cancer. Oncol Rep 1998;5:559-67.
74. Freedland SJ, Sutter ME, Dorey F, Aronson WJ. Defining the ideal cutpoint for determining PSA recurrence after radical prostatectomy. Prostate-specific antigen. Urology 2003;61:365-9.
75. Krivak TC, Tian C, Rose GS, Armstrong DK, Maxwell GL. A Gynecologic Oncology Group Study of serum CA-125 levels in patients with stage III optimally debulked ovarian cancer treated with intraperitoneal compared to intravenous chemotherapy: an analysis of patients enrolled in GOG 172. Gynecol Oncol 2009;115:81-5.
76. Micha JP, Goldstein BH, Rettenmaier MA, Brown JV, 3rd, John CR, Markman M. Clinical utility of CA-125 for maintenance therapy in the treatment of advanced stage ovarian carcinoma. Int J Gynecol Cancer 2009;19:239-41.
77. Kondo N, Murakami Y, Uemura K, et al. Prognostic impact of perioperative serum CA 19-9 levels in patients with resectable pancreatic cancer. Ann Surg Oncol 2010;17:2321-9.
78. van Trommel NE, Massuger LF, Schijf CP, ten Kate-Booij MJ, Sweep FC, Thomas CM. Early identification of resistance to first-line single-agent methotrexate in patients with persistent trophoblastic disease. J Clin Oncol 2006;24:52-8.

79. Kerkmeijer LG, Thomas CM, Harvey R, et al. External validation of serum hCG cutoff levels for prediction of resistance to single-agent chemotherapy in patients with persistent trophoblastic disease. BrJ Cancer 2009;100:979-84.
80. Markman M, Liu PY, Rothenberg ML, Monk BJ, Brady M, Alberts DS. Pretreatment CA-125 and risk of relapse in advanced ovarian cancer. J Clin Oncol 2006;24:1454-8.
81. Berger AC, Garcia M, Jr., Hoffman JP, et al. Postresection CA 19-9 predicts overall survival in patients with pancreatic cancer treated with adjuvant chemoradiation: a prospective validation by RTOG 9704. J Clin Oncol 2008;26:5918-22.
82. Savage P, Seckl M, Short D. Practical issues in the management of low-risk gestational trophoblast tumors. J Reprod Med 2008;53:774-80.
83. Rustin GJ, Nelstrop AE, McClean P, et al. Defining response of ovarian carcinoma to initial chemotherapy according to serum CA 125. J Clin Oncol 1996;14:1545-51.
84. Bhoola SM, Coleman RL, Herzog T, et al. Retrospective analysis of weekly topotecan as salvage therapy in relapsed ovarian cancer. Gynecol Oncol 2004;95:564-9.
85. Bodnar L, Wcislo G, Nasilowska A, et al. Salvage therapy with topotecan in heavily pretreated ovarian cancer patients. J Cancer Res Clin Oncol 2009;135:815-21.
86. Riedinger JM, Bonnetain F, Basuyau JP, et al. Change in CA 125 levels after the first cycle of induction chemotherapy is an independent predictor of epithelial ovarian tumour outcome. AnnOncol 2007;18:881-5.
87. Kurebayashi J, Nishimura R, Tanaka K, et al. Significance of serum tumor markers in monitoring advanced breast cancer patients treated with systemic therapy: a prospective study. Breast Cancer 2004;11:389-95.
88. Cheung KL, Evans AJ, Robertson JF. The use of blood tumour markers in the monitoring of metastatic breast cancer unassessable for response to systemic therapy. Breast Cancer Res Treat 2001;67:273-8.
89. Dixon AR, Jackson L, Chan SY, Badley RA, Blamey RW. Continuous chemotherapy in responsive metastatic breast cancer: a role for tumour markers? Br J Cancer 1993;68:181-5.
90. Robertson JF, Pearson D, Price MR, Selby C, Blamey RW, Howell A. Objective measurement of therapeutic response in breast cancer using tumour markers. Br J Cancer 1991;64:757-63.
91. Ziske C, Schlie C, Gorschluter M, et al. Prognostic value of CA 19-9 levels in patients with inoperable adenocarcinoma of the pancreas treated with gemcitabine. BrJCancer 2003;89:1413-7.
92. Kelly WK, Scher HI, Mazumdar M, Vlamis V, Schwartz M, Fossa SD. Prostate-specific antigen as a measure of disease outcome in metastatic hormone-refractory prostate cancer. J Clin Oncol 1993;11:607-15.
93. Scher HI, Kelly WM, Zhang ZF, et al. Post-therapy serum prostate-specific antigen level and survival in patients with androgen-independent prostate cancer. J Natl Cancer Inst 1999;91:244-51.
94. Smith DC, Dunn RL, Strawderman MS, Pienta KJ. Change in serum prostate-specific antigen as a marker of response to cytotoxic therapy for hormone-refractory prostate cancer. J Clin Oncol 1998;16:1835-43.
95. Bubley GJ, Carducci M, Dahut W, et al. Eligibility and response guidelines for phase II clinical trials in androgen-independent prostate cancer: recommendations from the Prostate-Specific Antigen Working Group. J Clin Oncol 1999;17:3461-7.
96. Small EJ, McMillan A, Meyer M, et al. Serum prostate-specific antigen decline as a marker of clinical outcome in hormone-refractory prostate cancer patients: association with progression-free survival, pain end points, and survival. J Clin Oncol 2001;19:1304-11.
97. Caffo O, Sava T, Comploj E, et al. Estramustine plus docetaxel as second-line therapy in patients with hormone-refractory prostate cancer resistant to docetaxel alone. Urol Oncol 2010;28:152-6.
98. Di Lorenzo G, Buonerba C, Faiella A, et al. Phase II study of docetaxel re-treatment in docetaxel-pretreated castration-resistant prostate cancer. BJU Int 2010.

99. Di Lorenzo G, Pizza C, Autorino R, et al. Weekly docetaxel and vinorelbine (VIN-DOX) as first line treatment in patients with hormone refractory prostate cancer. Eur Urol 2004;46:712-6.
100. Ferrero JM, Foa C, Thezenas S, et al. A weekly schedule of docetaxel for metastatic hormone-refractory prostate cancer. Oncology 2004;66:281-7.
101. Fossa SD, Jacobsen AB, Ginman C, et al. Weekly docetaxel and prednisolone versus prednisolone alone in androgen-independent prostate cancer: a randomized phase II study. Eur Urol 2007;52:1691-8.
102. Kojima T, Shimazui T, Onozawa M, et al. Weekly administration of docetaxel in patients with hormone-refractory prostate cancer: a pilot study on Japanese patients. Jpn J Clin Oncol 2004;34:137-41.
103. Manikandan R, Srirangam SJ, Pearson E, Brown SC, O'Reilly P, Collins GN. Diethylstilboestrol versus bicalutamide in hormone refractory prostate carcinoma: a prospective randomized trial. Urol Int 2005;75:217-21.
104. Nabhan C, Lestingi TM, Galvez A, et al. Erlotinib has moderate single-agent activity in chemotherapy-naive castration-resistant prostate cancer: final results of a phase II trial. Urology 2009;74:665-71.
105. Savarese DM, Halabi S, Hars V, et al. Phase II study of docetaxel, estramustine, and low-dose hydrocortisone in men with hormone-refractory prostate cancer: a final report of CALGB 9780. Cancer and Leukemia Group B. J Clin Oncol 2001;19:2509-16.
106. Small EJ, Fontana J, Tannir N, et al. A phase II trial of gefitinib in patients with non-metastatic hormone-refractory prostate cancer. BJU Int 2007;100:765-9.
107. Kim HS, Park YH, Park MJ, et al. Clinical significance of a serum CA15-3 surge and the usefulness of CA15-3 kinetics in monitoring chemotherapy response in patients with metastatic breast cancer. Breast Cancer Res Treat 2009;118:89-97.
108. Buller RE, Vasilev S, DiSaia PJ. CA 125 kinetics: a cost-effective clinical tool to evaluate clinical trial outcomes in the 1990s. Am J Obstet Gynecol 1996;174:1241-53; discussion 53-4.
109. Buller RE, Berman ML, Bloss JD, Manetta A, DiSaia PJ. Serum CA125 regression in epithelial ovarian cancer: correlation with reassessment findings and survival. Gynecol Oncol 1992;47:87-92.
110. Banu E, Banu A, Medioni J, et al. Serum PSA half-life as a predictor of survival for hormone-refractory prostate cancer patients: modelization using a standardized set of response criteria. Prostate 2007;67:1543-9.
111. Toner GC, Geller NL, Tan C, Nisselbaum J, Bosl GJ. Serum tumor marker half-life during chemotherapy allows early prediction of complete response and survival in nonseminomatous germ cell tumors 1. Cancer Res 1990;50:5904-10.
112. Gregorakis AK, Malovrouvas D, Stefanakis S, Petraki K, Scorilas A. Free/Total PSA (F/T ratio) kinetics in patients with clinically localized prostate cancer undergoing radical prostatectomy. ClinChimActa 2005;357:196-201.
113. Stamey TA, Kabalin JN, McNeal JE, et al. Prostate specific antigen in the diagnosis and treatment of adenocarcinoma of the prostate. II. Radical prostatectomy treated patients. JUrol 1989;141:1076-83.
114. Yedema CA, Kenemans P, Voorhorst F, et al. CA 125 half-life in ovarian cancer: a multivariate survival analysis. Br J Cancer 1993;67:1361-7.
115. Rapellino M, Piantino P, Pecchio F, et al. Disappearance curves of tumor markers after radical surgery. Int J Biol Markers 1994;9:33-7.
116. May M, Gunia S, Helke C, Braun KP, Pickenhain S, Hoschke B. Is it possible to provide a prognosis after radical prostatectomy for prostate cancer by means of a PSA regression model? IntJBiolMarkers 2005;20:112-8.
117. Gadducci A, Cosio S, Fanucchi A, Negri S, Cristofani R, Genazzani AR. The predictive and prognostic value of serum CA 125 half-life during paclitaxel/platinum-based chemotherapy in patients with advanced ovarian carcinoma. Gynecol Oncol 2004;93:131-6.

118. Gadducci A, Zola P, Landoni F, et al. Serum half-life of CA 125 during early chemotherapy as an independent prognostic variable for patients with advanced epithelial ovarian cancer: results of a multicentric Italian study. Gynecol Oncol 1995;58:42-7.
119. Hanninen M, Venner P, North S. A rapid PSA half-life following docetaxel chemotherapy is associated with improved survival in hormone refractory prostate cancer. Can Urol Assoc J 2009;3:369-74.
120. Mano A, Godinho I, Falcao AC. CA 125 half-life breakpoint between a "good" and "poor" prognosis in patients with ovarian cancer. Int J Gynaecol Obstet 2005;88:333-5.
121. Gerl A, Lamerz R, Clemm C, Mann K, Hartenstein R, Wilmanns W. Does serum tumor marker half-life complement pretreatment risk stratification in metastatic nonseminomatous germ cell tumors? Clin Cancer Res 1996;2:1565-70.
122. Ravery V, Meulemans A, Boccon-Gibod L. Clearance of free and total serum PSA after prostatic surgery. Eur Urol 1998;33:251-4.
123. Oesterling JE, Chan DW, Epstein JI, et al. Prostate specific antigen in the preoperative and postoperative evaluation of localized prostatic cancer treated with radical prostatectomy. JUrol 1988;139:766-72.
124. Haab F, Meulemans A, Boccon-Gibod L, Dauge MC, Delmas V. Clearance of serum PSA after open surgery for benign prostatic hypertrophy, radical cystectomy, and radical prostatectomy. Prostate 1995;26:334-8.
125. Lange PH, Vogelzang NJ, Goldman A, Kennedy BJ, Fraley EE. Marker half-life analysis as a prognostic tool in testicular cancer. J Urol 1982;128:708-11.
126. Murphy BA, Motzer RJ, Mazumdar M, et al. Serum tumor marker decline is an early predictor of treatment outcome in germ cell tumor patients treated with cisplatin and ifosfamide salvage chemotherapy. Cancer 1994;73:2520-6.
127. Inanc SE, Meral R, Darendeliler E, Yasasever V, Onat H. Prognostic significance of marker half-life during chemotherapy in non-seminomatous germ cell testicular tumors 1. Acta Oncol 1999;38:505-9.
128. Motzer RJ, Mazumdar M, Bajorin DF, Bosl GJ, Lyn P, Vlamis V. High-dose carboplatin, etoposide, and cyclophosphamide with autologous bone marrow transplantation in first-line therapy for patients with poor-risk germ cell tumors. J Clin Oncol 1997;15:2546-52.
129. Colakovic S, Lukic V, Mitrovic L, Jelic S, Susnjar S, Marinkovic J. Prognostic value of CA125 kinetics and half-life in advanced ovarian cancer. Int J Biol Markers 2000;15:147-52.
130. Brandle E, Hautmann O, Bachem M, et al. Serum half-life time determination of free and total prostate-specific antigen following radical prostatectomy--a critical assessment. Urology 1999;53:722-30.
131. Zagars GK, Pollack A. Kinetics of serum prostate-specific antigen after external beam radiation for clinically localized prostate cancer. Radiother Oncol 1997;44:213-21.
132. Vollmer RT, Montana GS. The dynamics of prostate-specific antigen after definitive radiation therapy for prostate cancer. Clin Cancer Res 1999;5:4119-25.
133. Zagars GK, Pollack A. The fall and rise of prostate-specific antigen. Kinetics of serum prostate-specific antigen levels after radiation therapy for prostate cancer. Cancer 1993;72:832-42.
134. Kaplan ID, Cox RS, Bagshaw MA. A model of prostatic carcinoma tumor kinetics based on prostate specific antigen levels after radiation therapy. Cancer 1991;68:400-5.
135. Vollmer RT, Humphrey PA. Tumor volume in prostate cancer and serum prostate-specific antigen. Analysis from a kinetic viewpoint. Am J Clin Pathol 2003;119:80-9.
136. van Straalen JP, Bossens MM, de Reijke TM, Sanders GT. Biological half-life of prostate-specific antigen after radical prostatectomy. Eur J Clin Chem Clin Biochem 1994;32:53-5.
137. Lein M, Brux B, Jung K, et al. Elimination of serum free and total prostate-specific antigen after radical retropubic prostatectomy. Eur J Clin Chem Clin Biochem 1997;35:591-5.
138. Meek AG, Park TL, Oberman E, Wielopolski L. A prospective study of prostate specific antigen levels in patients receiving radiotherapy for localized carcinoma of the prostate. Int J Radiat Oncol Biol Phys 1990;19:733-41.

139. Ritter MA, Messing EM, Shanahan TG, Potts S, Chappell RJ, Kinsella TJ. Prostate-specific antigen as a predictor of radiotherapy response and patterns of failure in localized prostate cancer. J Clin Oncol 1992;10:1208-17.
140. Hanlon AL, Moore DF, Hanks GE. Modeling postradiation prostate specific antigen level kinetics: predictors of rising postnadir slope suggest cure in men who remain biochemically free of prostate carcinoma. Cancer 1998;83:130-4.
141. Malik R, Jani AB, Liauw SL. Prostate-Specific Antigen Halving Time While on Neoadjuvant Androgen Deprivation Therapy Is Associated with Biochemical Control in Men Treated with Radiation Therapy for Localized Prostate Cancer. Int J Radiat Oncol Biol Phys 2010.
142. Riedinger JM, Eche N, Basuyau JP, Dalifard I, Hacene K, Pichon MF. Prognostic value of serum CA 125 bi-exponential decrease during first line paclitaxel/platinum chemotherapy: a French multicentric study. Gynecol Oncol 2008;109:194-8.
143. Buller RE, Berman ML, Bloss JD, Manetta A, DiSaia PJ. CA 125 regression: a model for epithelial ovarian cancer response. Am J Obstet Gynecol 1991;165:360-7.
144. Markowska J, Manys G, Szewierski Z. CA 125 in monitoring clinical course in ovarian cancer patients. A prospective clinical study. Eur J Gynaecol Oncol 1992;13:201-4.
145. Motzer RJ, Mazumdar M, Gulati SC, et al. Phase II trial of high-dose carboplatin and etoposide with autologous bone marrow transplantation in first-line therapy for patients with poor-risk germ cell tumors. J NatlCancer Inst 1993;85:1828-35.
146. Vogelzang NJ, Lange PH, Goldman A, Vessela RH, Fraley EE, Kennedy BJ. Acute changes of alpha-fetoprotein and human chorionic gonadotropin during induction chemotherapy of germ cell tumors. Cancer Res 1982;42:4855-61.
147. Stevens MJ, Norman AR, Dearnaley DP, Horwich A. Prognostic significance of early serum tumor marker half-life in metastatic testicular teratoma. J Clin Oncol 1995;13:87-92.
148. Mazumdar M, Bajorin DF, Bacik J, Higgins G, Motzer RJ, Bosl GJ. Predicting outcome to chemotherapy in patients with germ cell tumors: the value of the rate of decline of human chorionic gonadotrophin and alpha-fetoprotein during therapy. JClinOncol 2001;19:2534-41.
149. Yuan SQ, Zhou ZW, Wan DS, et al. The role of half-life of carcinoembryonic antigen (CEA) in prognosis prediction of colorectal cancer patients with preoperatively elevated CEA. Ai Zheng 2008;27:612-7.
150. Konishi F. CEA doubling time and CEA half-life in the prediction of recurrences after colorectal cancer surgery. Jpn J Clin Oncol 2002;32:41-2.
151. Choi JS, Min JS. Significance of postoperative serum level of carcinoembryonic antigen (CEA) and actual half life of CEA in colorectal cancer patients. Yonsei Med J 1997;38:1-7.
152. Ellis RJ, Vertocnik A, Sodee B, et al. Combination conformal radiotherapy and radioimmunoguided transperineal 103Pd implantation for patients with intermediate and unfavorable risk prostate adenocarcinoma. Brachytherapy 2003;2:215-22.
153. Crook JM, Szumacher E, Malone S, Huan S, Segal R. Intermittent androgen suppression in the management of prostate cancer. Urology 1999;53:530-4.
154. Ueno S, Namiki M, Fukagai T, Ehara H, Usami M, Akaza H. Efficacy of primary hormonal therapy for patients with localized and locally advanced prostate cancer: a retrospective multicenter study. Int J Urol 2006;13:1494-500.
155. Richardson DL, Seamon LG, Carlson MJ, et al. CA125 decline in ovarian cancer patients treated with intravenous versus intraperitoneal platinum-based chemotherapy. Gynecol Oncol 2008;111:233-6.
156. Frasci G, Conforti S, Zullo F, et al. A risk model for ovarian carcinoma patients using CA 125: time to normalization renders second-look laparotomy redundant. Cancer 1996;77:1122-30.
157. Schmitz MD, Padula GD, Chun PY, Davis AT. Normalization of prostate specific antigen in patients treated with intensity modulated radiotherapy for clinically localized prostate cancer. Radiat Oncol 2010;5:80.

158. Fizazi K, Culine S, Kramar A, et al. Early predicted time to normalization of tumor markers predicts outcome in poor-prognosis nonseminomatous germ cell tumors. JClinOncol 2004;22:3868-76.
159. Mego M, Rejlekova K, Reckova M, et al. Kinetics of tumor marker decline as an independent prognostic factor in patients with relapsed metastatic germ-cell tumors. Neoplasma 2009;56:398-403.
160. Tsuda H, Hashiguchi Y, Nakata S, et al. The CA125 regression rate to predict overall survival differ between paclitaxel-containing regimen and nonpaclitaxel regimen in patients with advanced ovarian cancer. Int J Gynecol Cancer 2002;12:435-7.
161. Mano A, Falcao A, Godinho I, et al. CA-125 AUC as a new prognostic factor for patients with ovarian cancer. Gynecol Oncol 2005;97:529-34.
162. Cappelli G. Mathematical model application to the kinetic study of tumor markers. Int J Biol Markers 1994;9:8-14.
163. Beal, Sl, Sheiner, Lb, Boeckmann AJ. NONMEM users guides. Icon Development Solutions,Ellicott City,Maryland,USA 2006.
164. Ette EI, Williams PJ. Population pharmacokinetics I: background, concepts, and models. Ann Pharmacother 2004;38:1702-6.
165. Sheiner LB. The population approach to pharmacokinetic data analysis: rationale and standard data analysis methods. Drug Metab Rev 1984;15:153-71.
166. You B, Perrin P, Freyer G, et al. Advantages of prostate-specific antigen (PSA) clearance model over simple PSA half-life computation to describe PSA decrease after prostate adenomectomy. Clin Biochemistry 2008;41:785-95.
167. You B, Girard P, Paparel P, et al. Prognostic value of modeled PSA clearance on biochemical relapse free survival after radical prostatectomy. Prostate 2009;69:1325-33.
168. You B, Fronton L, Boyle H, et al. Predictive value of modeled AUC(AFP-hCG), a dynamic kinetic parameter characterizing serum tumor marker decline in patients with nonseminomatous germ cell tumor. Urology 2010;76:423-9 e2.
169. You B, Pollet-Villard M, Fronton L, et al. Predictive values of hCG clearance for risk of methotrexate resistance in low-risk gestational trophoblastic neoplasias. Ann Oncol 2010;21:1643-50.
170. Brendel K, Dartois C, Comets E, et al. Are population pharmacokinetic and/or pharmacodynamic models adequately evaluated? A survey of the literature from 2002 to 2004 4. ClinPharmacokinet 2007;46:221-34.
171. Dartois C, Brendel K, Comets E, et al. Overview of model-building strategies in population PK/PD analyses: 2002-2004 literature survey 1. BrJClinPharmacol 2007;64:603-12.
172. Yano Y, Beal SL, Sheiner LB. Evaluating pharmacokinetic/pharmacodynamic models using the posterior predictive check. JPharmacokinetPharmacodyn 2001;28:171-92.
173. Norman RJ, Buchholz MM, Somogyi AA, Amato F. hCGbeta core fragment is a metabolite of hCG: evidence from infusion of recombinant hCG. J Endocrinol 2000;164:299-305.
174. de WR, Collette L, Sylvester R, et al. Serum alpha-fetoprotein surge after the initiation of chemotherapy for non-seminomatous testicular cancer has an adverse prognostic significance. BrJ Cancer 1998;78:1350-5.
175. Horwich A, Peckham MJ. Transient tumor marker elevation following chemotherapy for germ cell tumors of the testis. Cancer TreatRep 1986;70:1329-31.
176. Sonoo H, Kurebayashi J. Serum tumor marker kinetics and the clinical course of patients with advanced breast cancer. Surg Today 1996;26:250-7.
177. Wu SC, Chou FF, Rau KM. Clinical significance of a serum CA 15-3 surge and the usefulness of CA 15-3 kinetics in monitoring chemotherapy response in patients with metastatic breast cancer. Breast Cancer Res Treat 2010.
178. Kim HJ, Lee KW, Kim YJ, et al. Chemotherapy-induced transient CEA and CA19-9 surges in patients with metastatic or recurrent gastric cancer. Acta Oncol 2009;48:385-90.

179. Sotelo RJ, Mora KE, Perez LH, et al. Assay standardization bias: different prostate cancer detection rates and clinical outcomes resulting from different assays for free and total prostate-specific antigen. Urology 2007;69:1143-6.
180. Loeb S, Chan DW, Sokoll L, et al. Prostate specific antigen assay standardization bias could affect clinical decision making. J Urol 2008;180:1959-62; discussion 62-3.
181. Evans MI, O'Brien JE, Dvorin E, Wapner RJ, Harrison HH. Standardization of methods reduces variability: explanation for historical discrepancies in biochemical screening. Genet Test 2003;7:81-3.
182. Tso E, Elson P, Vanlente F, Markman M. The "real-life" variability of CA-125 in ovarian cancer patients. Gynecol Oncol 2006;103:141-4.
183. Pilo A, Zucchelli GC, Cohen R, Chiesa MR, Bizollon CA. Performance of immunoassays for ca 19-9, ca 15-3 and ca 125 tumour markers evaluated from an international quality assessment survey. Eur J Clin Chem Clin Biochem 1996;34:145-50.
184. Gronlund B, Hansen HH, Hogdall C, Hogdall EV, Engelholm SA. Do CA125 response criteria overestimate tumour response in second-line treatment of epithelial ovarian carcinoma? Br J Cancer 2004;90:377-82.
185. Peters-Engl C, Obermair A, Heinzl H, Buxbaum P, Sevelda P, Medl M. CA 125 regression after two completed cycles of chemotherapy: lack of prediction for long-term survival in patients with advanced ovarian cancer. Br J Cancer 1999;81:662-6.
186. Vicini FA, Vargas C, Abner A, Kestin L, Horwitz E, Martinez A. Limitations in the use of serum prostate specific antigen levels to monitor patients after treatment for prostate cancer. J Urol 2005;173:1456-62.
187. Toner GC. Early identification of therapeutic failure in nonseminomatous germ cell tumors by assessing serum tumor marker decline during chemotherapy: still not ready for routine clinical use. J Clin Oncol 2004;22:3842-5.
188. Sostelly A, Henin E, You B, Girard P, Karlsson MO. Simultaneous modelling of PSA in BPH and cancer patients treated by prostate surgery. Proceedings of 2009 Annual Congress of Population Apprach Group in Europe Abs 1497.

VI. Articles

Available online at www.sciencedirect.com
ScienceDirect
Clinical Biochemistry 41 (2008) 785–795
CLINICAL BIOCHEMISTRY

Advantages of prostate-specific antigen (PSA) clearance model over simple PSA half-life computation to describe PSA decrease after prostate adenomectomy

Benoit You [a,b,c,*], Paul Perrin [d], Gilles Freyer [a,b,c], Alain Ruffion [d], Brigitte Tranchand [a,b,e], Emilie Hénin [a,b], Philippe Paparel [d], Benjamin Ribba [a,b], Marian Devonec [d], Claire Falandry [a,b,c], Cécile Fournel [a,b,c], Michel Tod [a,b,f], Pascal Girard [a,b]

[a] *Université de Lyon, Lyon, F-69003, France*
[b] *Université Lyon 1, EA3738, CTO, Faculté de Médecine Lyon Sud, Oullins, F-69600, France*
[c] *Service d'Oncologie Médicale, Centre Hospitalier Lyon Sud, Hospices Civils de Lyon, F-69310, Pierre-Bénite, France*
[d] *Service d'urologie, Centre Hospitalier Lyon Sud, Hospices Civils de Lyon, F-69310, Pierre-Bénite, France*
[e] *Centre Anticancéreux Léon Bérard, Lyon, F-69008, France*
[f] *Pharmacie-toxicologie, Hôpital Cochin, Paris, France*

Received 10 December 2007; received in revised form 29 March 2008; accepted 2 April 2008
Available online 11 April 2008

Abstract

Objectives: A population kinetic approach based on PSA clearance (CL_{PSA}) may be a more rational strategy to characterize prostate-specific antigen (PSA) decrease profile after prostate surgery than the commonly used method (half-life from mono/bi-exponential models).

Methods: We used 182 post-adenomectomy PSA concentrations from 56 benign prostatic hyperplasia patients to build, with NONMEM software, a multi-exponential and a CL_{PSA} model for comparison.

Results: The best multi-exponential model was $PSA(t)=4.96e^{-0.269t}+3.10e^{-0.16t}+0.746e^{+0.0002t}$ with a stable median residual PSA at 0.64 ng/mL. The best model parametrized with clearance was $CL_{PSA}=0.0229*(AGE/69)^{3.78}$. Akaike information criteria and standard errors favored the CL_{PSA} model. Median peripheral zone and transitional zone productions were 0.034 ng/mL/cm^3 and 0.136 ng/mL/g. A threshold at 2 ng/mL on day 90 allowed for a diagnostic of biochemical relapse diagnostic.

Conclusions: The population CL_{PSA} model was superior to the multi-exponential approach for investigating individual post-adenomectomy PSA decreases.

Keywords: Prostate-specific antigen; Prostatic hyperplasia; Kinetics; Metabolite clearance rate; Prostatectomy; Biomarker

Introduction

Since the Stamey report in 1987 suggesting the usefulness of prostate-specific antigen (PSA) as a biomarker of prostate diseases [1], the value of PSA as a surrogate marker remains in question [2,3]. Recently, many authors focused on the value of PSA kinetic parameters to characterize PSA dynamics, such as PSA doubling time and PSA velocity for PSA increase [3–5], or PSA half-life (HL) for PSA decrease [6–8]. However, questions remain about the optimal method for investigating PSA kinetics, in particular PSA decrease after surgery for benign prostatic hyperplasia (BPH) or prostate cancer. Indeed, most reports have involved graphical determination of PSA HL [6,9–12] or even mono or bi-exponential models for the most sophisticated studies [6,8–15]. Even if it is not mentioned, the concept of the HL determination relies on the linearization of a mono-exponential model. For instance, the commonly used mono-

* Corresponding author. Service d'oncologie médicale, Centre Hospitalier Lyon Sud, Chemin du Grand Revoyet, 69495 PIERRE-BENITE, France. Fax: +33 4 78 86 43 56.
E-mail address: benoit.you@chu-lyon.fr (B. You).

0009-9120/$ - see front matter © 2008 The Canadian Society of Clinical Chemists. Published by Elsevier Inc. All rights reserved.
doi:10.1016/j.clinbiochem.2008.04.001

exponential equation is $PSA(t) = A\,e^{-\alpha * t}$ where HL equals $Ln2/\alpha$. These analyses are limited by the unknown influence of the number and timepoints of PSA sampling on the calculated HL (often 3 or 4 per patient) and the bias arising from the simplification of the bi-exponential model to the mono-exponential model. In addition, these analyses take no account of the inter-individual and intra-individual variability. These limitations certainly alter the prognostic value of PSA kinetic parameters investigated with such approaches.

For this reason, we propose a new method for characterizing PSA decline after prostate surgery based on a population kinetic model involving apparent PSA clearance (CL_{PSA}). The population kinetic approach, commonly used in pharmacology, compensates the paucity of individual kinetic information, such as the sparseness of individual PSA samples, by the large number of patients with kinetic measurements [16]. In addition, it extracts population kinetic information with models that separate inter and intra-individual variability. This kind of analysis may involve the PSA clearance calculation, which is the rate of elimination of PSA from the whole body using the same modeling approach as applied for drug pharmacokinetics [17].

We present here the results of a comparison of the two strategies (multi-exponential models versus PSA clearance-based models) for post-operative PSA kinetic analysis in BPH patients treated by adenomectomy according to Millin surgery method [18] (which consists of the removal of the prostate transitional zone where BPH is usually developed [19]). Using post-adenomectomy PSA concentrations, we performed a population PSA kinetic study to compare the two strategies and determine the best one. The latter was used to determine the PSA kinetic parameters, including half-lives, CL_{PSA}, prostate zones productions, and biochemical relapses.

Methodology

Patients and treatments

For inclusion in this retrospective study, patients were selected who had undergone a prostate BPH removal with adenomectomy according to the Millin method [19]. Moreover, a pathology examination confirmed the histological diagnosis, and a minimum of two serum PSA assays per patient in post-operative follow-up was required. Exclusion criteria involved any therapy susceptible to changing the PSA decline in the post-operative period, such as hormonotherapy, radiotherapy–brachytherapy, or chemotherapy.

Serum PSA was assayed at various times according to the individual physician's usual practice. For each patient, all available serum PSA measurements were collected. Although the majority of PSA concentration assays were centralized and performed at the Lyon Sud Hospital radio-analysis laboratory (53% of all PSA assays), the rest, assayed after the post-operative 10th day, were determined at the laboratory associated with the respective doctor's office. The Lyon Sud Hospital radio-analysis laboratory uses the equimolar IRMA KIT® (Immunotech-Beckman Coulter, France) whose lower limit of quantification is 0.1 ng/mL. Inter and intra-assays variations are below 6% in the range [2.01 to 44.5 ng/mL] with a CV of 20% at 0.14 ng/mL.

For each patient, clinical, biochemical, radiological, and pathological variables were noted: age, weight, blood cell count, sodium, total protein, serum creatinine (Scr), ultrasound (U/S) pre-operative prostate volume, U/S post-operative residual prostate volume, prostate resected tissue weight, and incidental prostate cancer.

Modeling

The two major objectives of this study were to compare two different modeling strategies (model parameterized with multiple exponentials versus model parameterized with CL_{PSA}) to determine the better one and to validate the selected model with visual and statistical predictive checks. Secondary objectives were to characterize PSA decrease kinetics after adenomectomy (PSA half-life (HL_{PSA}), CL_{PSA}, prostate zones productions) using the better model and to look for a PSA/time threshold for biochemical relapse prediction.

Models parameterized with multi-exponentials

In this situation, PSA decrease was analyzed using a 1-, 2-, or 3-exponential decline model. Moreover, because the peripheral zone (PZ) is not removed by surgery, a residual PSA production exponential was added. For instance, in the case of a 2-exponential decrease model, the equation was:

$$PSA(t) = PSA_1 * \exp^{-K1*t} + PSA_2 * \exp^{-K2*t} + PSA_3 * \exp^{+K3*t}$$

where:

- $[PSA_1 * \exp^{-K1*t} + PSA_2 * \exp^{-K2*t}]$ is the bi-exponential PSA decline model, and
- $[PSA_3 * \exp^{+k3*t}]$ is the observed residual PSA production.

Thus, PSA_1, PSA_2, PSA_3, K1, K2, and K3 are all positive parameters, but both K1 and K2 represent the decline rates of PSA while K3 is the residual production rate of PSA observed after the end of the decrease.

Models parameterized with apparent PSA clearance (CL_{PSA})

Clearance is a pharmacokinetic concept and represents the body volume from which a drug has been totally cleared by time unit [17]. In the present case, PSA is an endogenous molecule with production and release processes that are physiologically identified but quantitatively unknown. Because PSA dose and process inputs are unknown, it is assumed to be simply represented by a bolus of an arbitrary amount of 1 given at the time of prostate surgery. The population kinetic approach is applied to fit PSA decline according to 1-, 2-, or 3-compartment models and to investigate CL_{PSA}, which is an apparent clearance (see Appendix for more details). To describe observed residual PSA production arising from a persistent peripheral zone, we assumed a constant rate production parameter (R).

Table 1
Included patient characteristics

Continuous covariates	Median	1st quartile	3rd quartile	Range
Age (years)	69.0	64.0	74.0	50.0–92.0
Patient's weight (kg)	79.0	70.7	90	54.0–170.0
Serum creatinine (μmol/L)	87.5	81.0	96.2	64.0–190.0
Creatinine clearance (mL/min)	80.6	67.9	91.0	37.0–137.2
Serum total protein (g/L)	62.0	55.0	66.7	31.0–143.0
Hemoglobin (g/dL)	12.7	11.6	13.9	8.2–15.3
White blood cell count (Giga/L)	7670.0	6630.0	9790.0	4760.0–13170.0
Platelet count (Giga/L)	199.5	160.7	251.7	101.0–863
Prostate resected tissue weight (g)	74.0	54.0	105.0	14.0–220.0
Pre-operative U/S prostate volume (cm^3)	105.0	83.0	130.5	40.0–254.0
Post-operative U/S prostate residue (cm^3)	19.5	16.2	26.7	10.0–39.0

Incidental prostate cancer: Yes $n=4/56$ (7.14%), No $n=52/56$ (92.8%).

Computing process

In a first step, the NONMEM program® (NON linear Mixed Effect Model, University of San Francisco, California, USA) version V compiled with Digital Visual Fortran 5.0 was used to analyze concentration-time data with first order (FO) and first order conditional event interaction (FOCEI) methods. This program allows simultaneous estimation of fixed effects parameters (PSA_1, PSA_2, PSA_3, K1, K2, and K3 parameters in the first strategy or CL_{PSA}, central compartment volume (V1), inter-compartmental transfer rates (K12, K21), and R in the second strategy) and random effects (inter-individual as well as intra-individual residual variability arising from assay errors and model misspecifications) [20]. An extensive graphical analysis of predicted versus observed concentrations was performed to test the value of each model. The search was also guided by looking at the differences between the objective functions (OF) given by NONMEM. The NONMEM OF is an approximation of twice the logarithm of the likelihood. When a model can be reduced to a simpler one by fixing some parameters to a given value (e.g., 0), the difference between the 2 NONMEM OF is approximately distributed according to a χ^2 with n degrees of freedom, n being equal to the number of fixed parameters. In addition, the hypotheses of independence or dependence of parameter inter-individual variability were investigated.

In a second step, the main individual covariates collected (patient age, weight, blood cell counts, sodium, total protein, serum, creatinine clearance calculated according to the Cockroft-Gault formula, U/S pre-operative prostate volume, U/S post-operative residual prostate volume, prostate tissue resected

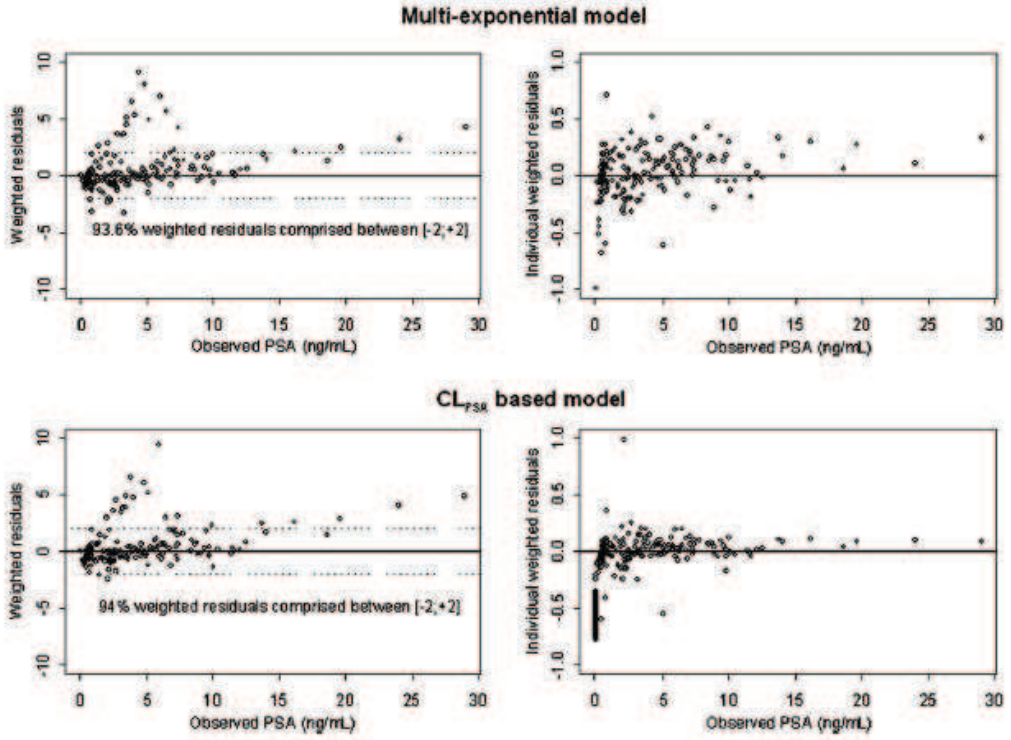

Fig. 1. Weighted residuals and individual weighted residuals versus observed PSA for the multi-exponential and CL_{PSA}-based models, respectively.

Table 2
Parameter values of the bi-exponential model

Parameter	Median value	1st quartile	3rd quartile	CI 95% =	IIV (%)	SE (%)
PSA_1	7.58	2.95	9.88	[5.56–9.60]	63.0%	282.0%
PSA_2	3.25	2.23	4.68	[2.72–3.78]	63.0%	87.0%
PSA_3	0.64	0.46	1.21	[0.40–0.88]	88.6%	18.2%
K1	0.22	0.15	0.50	[0.12–0.32]	97.0%	111.0%
K2	0.16	0.16	0.16	[0.16–0.16]	ND	49.5%
K3	0.0002	$2.088*10^{-4}$	$2.089*10^{-4}$	$[1.7*10^{-4}–2.9*10^{-4}]$	9.0%	71.7%

IIV and SE are the coefficient of variation of inter-individual variability and standard errors, respectively. ND: Not determined by the model.

weight, and incidental prostate cancer) were tested to estimate their impact on PSA kinetic parameters. When a covariate demonstrated significant relationships with any kinetic parameters, it was introduced into the model describing the fixed effects by forward inclusion. The covariate was kept in the model only if the decrease in the NONMEM OF was at least greater than 7, corresponding to a nominal p value <0.01.

For instance, the influence of the "age" covariate on CL_{PSA} was tested with the equation:

$$CL_{PSA} = \Theta 1 * \left(age/age_{med}\right)^{\Theta 2} * \exp(\eta 1)$$

where:

- age is the patient age and age_{med} is the median age of all patients among the cohort;
- $\Theta 1$ and $\Theta 2$ are the fixed-effect parameters; and
- $\eta 1$ is the random-effect parameter.

This equation gives an easy parameter interpretation because $\Theta 1$ is the clearance of a patient whose age equals the age_{med}. Afterwards, a stepwise backward elimination procedure was performed to keep in the model only the significant covariates, producing an OF decrease of at least 11, corresponding to a $p<0.001$.

Modeling strategy comparison

Once the best model had been defined for each strategy, the models were compared to each other. To achieve this aim, several criteria were assessed and compared:

- Akaike Information Criterion (AIC), which is calculated by the following equation: $AIC = 2*P - 2$ log (likelihood) where P is the number of parameters.
- Coefficient of variation (CV) of standard errors of all parameters.

Model validation

The best model should be validated in terms of its ability to predict correctly PSA distribution values [21,22]. For this, we simulated 500 PSA decline profiles using the final parameters

Table 3
Steps of the NONMEM analysis

Model type	OF	ΔOF	Statistical p =	η1 for CL_{PSA} (SD)	η2 for V1 (SD)	η3 for R (SD)	E (SD)
Basic model $CL_{PSA} = \Theta 1$							
FO diag. matrix	298	–	–	0.014	0.54	4E-8	0.22
FOCEI Diag. matrix	221	–	–	5.8E-13	0.22	0.45	0.019
FOCEI Block matrix	221	–	–	0.43 (65.6%)	0.685 (82.7%)	0.680 (82.4%)	0.019 (13.78%)
Covariate testing							
Creatinine clearance CCL (mL/min) $CL_{PSA} = \Theta 1*(CCL/80.6)^{\Theta 2}$	220	1	NS	–	–	–	–
Serum creatinin (μmol/L) $CL_{PSA} = \Theta 1*(Scr/87.5)^{\Theta 2}$	220	1	NS	–	–	–	–
Patient weight (PW) (kg) $CL_{PSA} = \Theta 1*(PW/79)^{\Theta 2}$	221	0	NS	–	–	–	–
Age (years) $CL_{PSA} = \Theta 1 * (Age/69)^{\Theta 2}$	208	−13	<0.001	–	–	–	–
Adenoma weight WGT (g) $CL_{PSA} = \Theta 1 *(WGT/74)^{\Theta 2}$	220	1	NS	–	–	–	–
Prostate cancer PC (yes/no) $CL_{PSA} = \Theta 1 + \Theta 2*PC$	220	1	NS	–	–	–	–
Pre-operative prostate volume (VOL) (cm^3) $CL_{PSA} = \Theta 1 + \Theta 2*VOL$	221	0	NS	–	–	–	–
Post-operative U/S residue (RES) (cm^3) $CL_{PSA} = \Theta 1 + \Theta 2*RES$	219	2	NS	–	–	–	–
Serum protein (PROT) (g/L) $CL_{PSA} = \Theta 1 + \Theta 2*PROT$	220	1	NS	–	–	–	–
Sodium NA (g/L) $CL_{PSA} = \Theta 1 + \Theta 2*NA$	221	0	NS	–	–	–	–
Final model							
FOCEI, covariate, block matrix $CL_{PSA} = \Theta 1 * (Age/69)^{3.78}$	208	–	–	0.39 (62.4%)	0.668 (81.7%)	0.646 (80.4%)	0.02 (14.14%)

Objective function (OF) changes (ΔOF) with model types and with some patient covariate inclusion. Inter-individual (η1 to η3) and residual variabilities (ε) are presented for main models. FO: first order; FOCEI: first order conditional event interaction; SD: standard deviation; diag. matrix: diagonal matrix (independent of the η); block matrix (correlations between the η); and NS: not significant.

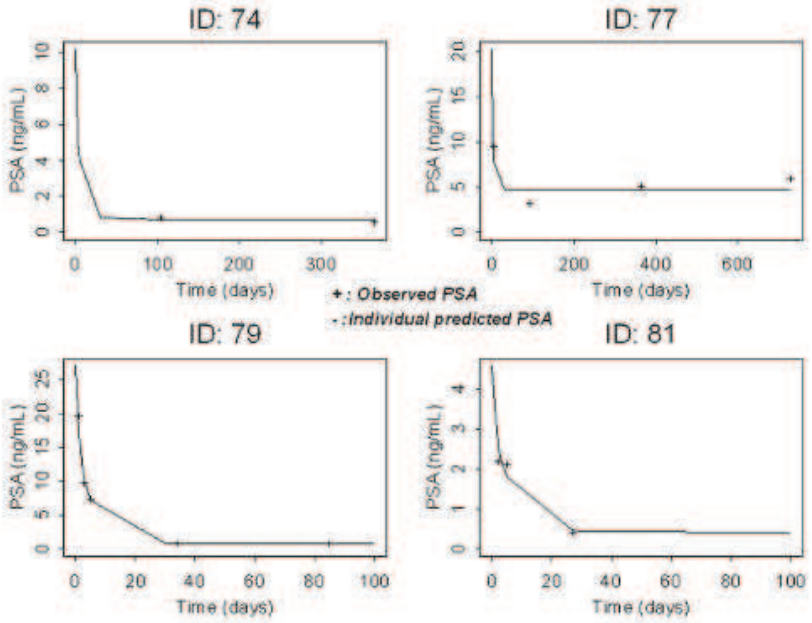

Fig. 2. PSA values versus time for four typical patients. The plots are the observed PSA, and the line represents the modelized PSA values determined with the CL_{PSA} model.

estimated from the best model. Two methods of qualification were used [23,24]:

- *Visual predictive check*: observed PSA values were compared to a 95% confidence interval (CI) of PSA from the 500 simulated replicates.
- *Statistical predictive check*: distributions of PSA computed from the simulated datasets were compared to the corresponding observed PSA values for the prediction of the first PSA before day 5 and the last PSA after day 90.

PSA production by the different prostate zones

PSA peripheral zone production

If surgery was complete, only the prostate PZ was expected to remain. Therefore, the modelized residual PSA after the end of the decrease represented the PSA arising from PZ production. Indeed, when time tends toward infinity, PSA is modelized by PSA_3e^{+K3t} in the case of the multi-exponential model or by R with the CL_{PSA} model. In addition, because prostate residual volume (cm^3) after surgery, as determined by U/S, had been noted for each patient, it was possible to characterize individual PZ production with:

$$\text{Individual PSA PZ production ng/mL/cm}^3 = (\text{individual modelized residual PSA}) \div (\text{individual U/S prostate residue})$$

PSA transition zone production

Adenomectomy was expected to have removed all prostate transition zones (TZ). The PSA difference between initial PSA at time 0 (just before surgery) and PSA residual value represented the PSA linked to the TZ. In addition, because prostate resected tissue weight had been noted, the PSA TZ production was calculated by:

$$\text{Individual PSA TZ production (ng/mL/g)} = (\text{individual PSA difference}) \div (\text{individual resected tissue weight}).$$

Results

Patients and follow-up

A total of 196 serum PSA values from 59 BPH patients treated between November 2000 and December 2006 with Millin prostate adenomectomy [19] were studied. Among these 59 patients, data from 56 patients could be fully analyzed. The median follow-up was 643 days (21.43 months). A total of 182 PSA assays were investigated with a median of 3 PSA values per patient. These PSA levels were assayed at various times,

Table 4
PSA decrease kinetic parameters calculated by the CL_{PSA}-based model

Parameter	Median value	1st quartile	3rd quartile	CI 95% =	IIV (%)	SE (%)
CL_{PSA}	0.019	0.013	0.029	[0.012–0.026]	62.4%	21.48%
V1	0.105	0.070	0.014	[0.744–0.136]	81.7%	26.85%
Residual PSA	0.668	0.507	1.23	[0.398–0.938]	80.4%	17.48%
K12	0.320	ND	ND	ND	ND	101.0%
K21	0.873	ND	ND	ND	ND	90.61%

IIV and SE are the coefficient of variation of inter-individual variability and standard errors, respectively; ND: not determined by the model.

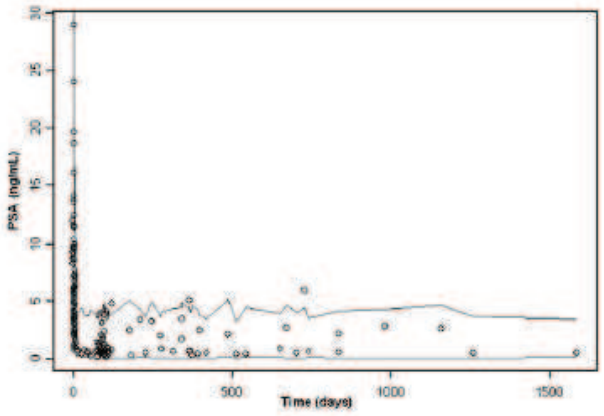

Fig. 3. Visual predictive check. The majority of observed PSA (O) are included in the 95% CI of 500 modelized PSA (grey lines are the inferior and superior limits).

from Day 0 (surgery day) up to Day 1584 (52.8 months after the surgery) with a median of day 8.

Patient characteristics are presented in Table 1. Patient median age was 69 years, and 50% patients were between 64 and 74. The median prostate resected tissue weight, corresponding to the median adenoma weight, was 74 g with a large inter-individual variability; 25% of patients had an adenoma weight below 54 g and 25% over 105 g. The median U/S residual prostate volume available for 30 patients (53.6%) was 19.5 cm^3. Because this value is very close to the mean literature value (20 cm^3), we decided to assign a PZ volume of 19.5 cm^3 to the 24 patients for whom we did not have these data. A histological diagnosis of a small prostate cancer was found in four patients, but they all had negative surgical margins.

Modeling

Multi-exponential model

The best multi-exponential model describing PSA decline after adenomectomy was bi-exponential. Because the FO algorithm produced biased estimates and predictions, model parameters were estimated using FOCEI. Moreover, 1- and 3-exponential models were inappropriate. The inter-individual variability and residual error models were log-normal. No covariate significantly influenced model parameters. The only covariate that showed a trend to reducing inter-individual variability was age. However, this improvement disappeared when inter-individual correlations between parameters were considered. Therefore, no covariate was included in the final model, which was

$$\mathrm{PSA}(t) = 4.96e^{-0.269t} + 3.10e^{0.16t} + 0.746e^{+0.0002t}$$

Fig. 1 shows weighted residuals and individual weighted residuals of the model. The correlation coefficient of individual

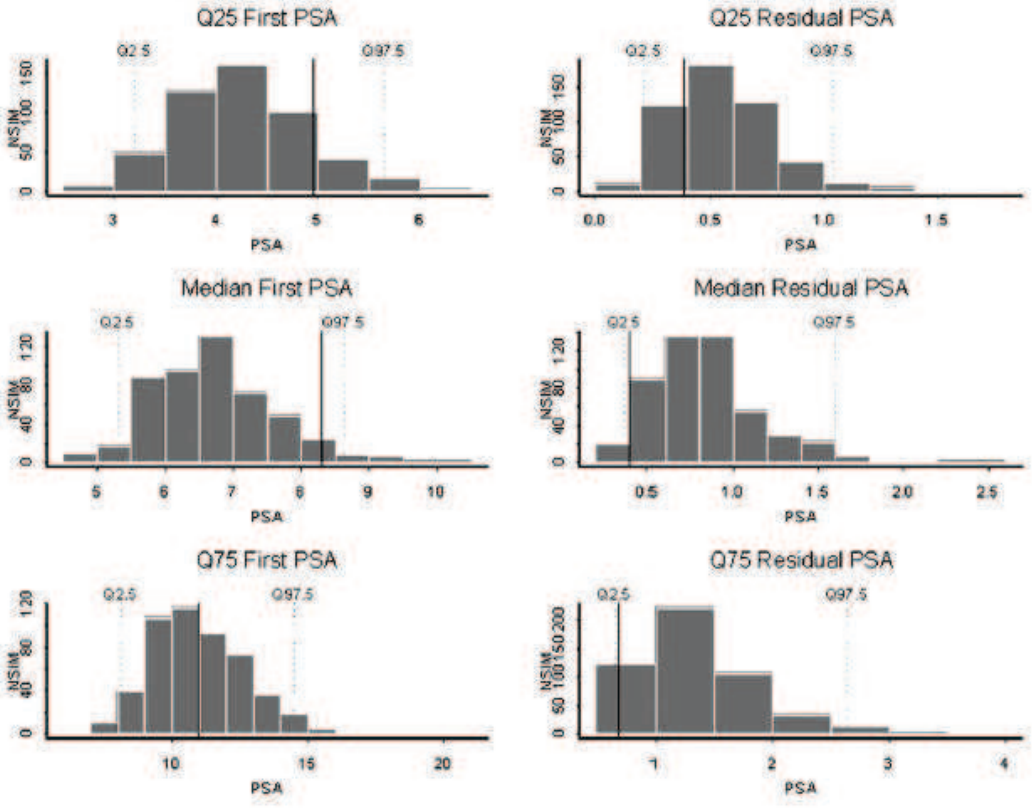

Fig. 4. Statistical predictive check. Three charts (left column) present distribution histograms of median, first quartile, and third quartile simulated data for the first part of the PSA decline curve (first PSA before day 5) and 3 charts (right column) for the last part of the curve (residual PSA after day 90). CI 95% limits of the modelized PSA distribution are presented with dotted lines while black lines represent the corresponding observed PSA (NSIM: number of simulations).

Table 5
Peripheral zone and transitional zone PSA production according to the PSA decline profile

Studied patients	Concerned PSA prostate zone	Median PSA production	Unit	1st quartile	3rd quartile
All patients	Peripheral zone	0.034	ng/mL/cm^3	0.025	0.096
	Transitional zone	0.136	ng/mL/g	0.081	0.260
Patients with "abnormal" PSA decline	Peripheral zone	0.141	ng/mL/cm^3	0.107	0.204
	Transitional zone	0.111	ng/mL/g	0.085	0.280
Patients with normal PSA decline	Peripheral zone	0.032	ng/mL/cm^3	0.024	0.052
	Transitional zone	0.146	ng/mL/g	0.075	0.234

predicted PSA values versus observed PSA was 0.93. Moreover 93.5% of weighted residuals were between −2 and +2. The parameter values and the CVs of inter-individual variability and of standard errors are presented in Table 2. Because parameter K3 is close to zero, the third exponential term $e^{+0.0002t}$ is close to one, and so $PSA_3 = 0.746$ represents the residual constant PSA concentration which appeared to be quite stable with time once the PSA decline had been achieved. Moreover, the HL_{PSA} decrease was inferred from the model with the equation ($HL = \ln 2/K$). The HL of the quick first phase was 3.15 days and of the second phase was 4.33 days.

The model parameterizing PSA clearance

The best model describing CL_{PSA} was a 2-compartment model with a log-normal error model for inter-individual estimation and mixed-error model for residual variability. The FOCEI algorithm gave the best unbiased estimates. Only the covariate age significantly influenced the CL_{PSA}. Indeed, the inclusion of this variable induced an OF decrease of 13 (corresponding to $p < 0.001$). As shown in Table 3, this gain was kept when considering inter-individual correlations between parameters. Therefore, the final equation was

$$CL_{PSA} = 0.0229 * (AGE/69)^{3.78}$$

and an increase of 1 year in age induced an increase of CL_{PSA} of 0.015 units. The inclusion of age allowed reducing the CL_{PSA}, V1, and R inter-individual variability by 3.2%, 1%, and 2%, respectively, but the residual variability was not modified. Fig. 1 presents the weighted residuals and individual weighted residuals of the final CL_{PSA}-based model. The correlation coefficient of individual predicted PSA values versus observed PSA was 0.98. As shown in Fig. 2 for four typical patients, individual Bayesian modelized PSA values were very close to observed values. In addition, 94% weighted residuals were between −2 and 2. As shown in Table 4, the median CL_{PSA} and apparent central compartment volume as well as residual PSA were 0.019 (95% CI = [0.012–0.026]), 0.105 (95% CI = [0.744–0.136]), and 0.668 ng/mL (95% CI = [0.398–0.938]), respectively. Moreover, the coefficients of variation of standard errors were between 17% and 27% for these parameters.

Comparison of the modeling strategies

Number of estimated parameters and Akaike criteria

In the multi-exponential model, a total of six parameters were investigated (PSA_1, PSA_2, PSA_3, K1, K2, and K3), and the OF was 249. Thus, AIC was 2*6+249 = 261. Because five parameters were fitted in the CL_{PSA}-based model (CL_{PSA}, V1, K12, K21, and R) and OF was 208, the AIC was 2*5+208 = 228. The smaller AIC for the clearance-based model compared to the multi-exponential model suggested use of the former strategy.

CV of standard errors linked to model misspecifications

In the multi-exponential model, the CVs of standard errors due to model inaccuracies were 282%, 87%, 18.2%, 111%, 49.5%, and 71.7% for PSAs 1 to 3 and K1 to K3, respectively. In the CL_{PSA}-based model, the CVs of standard errors were 21.48%, 26.85%, 17.48%, 101%, and 90.61% for CL_{PSA}, V1, R, K12, and K21, respectively.

Therefore, all comparison criteria, including AIC, standard errors, and goodness-of-fit-plots, showed the superiority of the CL_{PSA} model for description of the PSA decrease kinetic profile.

Model validation

A total of 500 simulations of a PSA decrease profile were completed using the population parameters of the CL_{PSA} model. Fig. 3 presents the visual predictive check that compared the 95% CI of simulated PSA to observed PSA. A large majority of observed PSA values were included in the 95% CI simulated PSA, suggesting the accuracy of the model. As explained in the Methods, the statistical predictive check involved the prediction of the first part (first PSA before day 5) and the last part of the

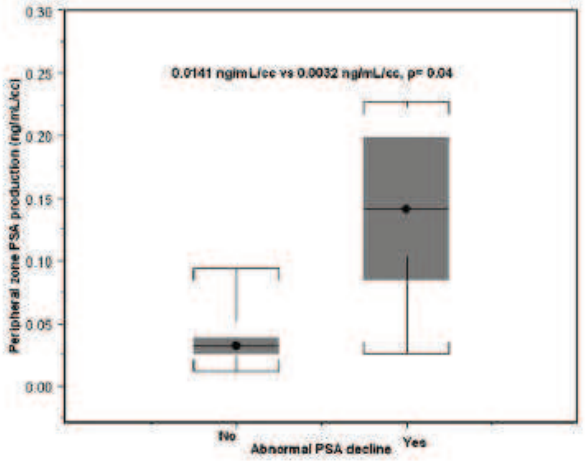

Fig. 5. Peripheral zone PSA productions (median and 95% CI) according to the PSA decline profile (normal vs abnormal).

PSA decline curve (residual PSA after day 90). Fig. 4 presents histograms of median and first and third quartile simulated data. All lines corresponding to the corresponding observed data were comprised in the 95% CI of the simulated values. This statistically significant predictive check confirms the accuracy of the model for the prediction of the first and the last part of the PSA decrease curve.

PSA prostate zone production

The CL_{PSA} model was used to characterize prostate zone production.

PSA peripheral zone production

Once PSA decline had been achieved, the residual PSA was given by a model. This residual PSA (median: 0.668 ng/mL, CI 95% = [0.398–0.938]) was assumed to be produced by the prostate PZ. Thus, the median individual PZ production was 0.034 ng/mL/cm^3 (1st quartile = 0.025, 3rd quartile = 0.096).

PSA transitional zone production

The PSA change from initial value to residual value was assumed to be due to the TZ removal. This median PSA difference was 9.55 ng/mL (1st quartile = 6.76, 3rd quartile = 14.15). Thus, the median PSA individual TZ production was 0.136 ng/mL/g (1st quartile = 0.081, 3rd quartile = 0.260).

Biochemical relapse concept

The modelized PSA decrease curves showed that PSA decline was almost achieved on day 30 and that the day-90 PSA value equaled the stable residual PSA value. Among the 56 studied patients, 11 patients (19.64%) presented an abnormal PSA decrease defined by a day-90 observed PSA over 3 ng/mL and/or a PSA re-increase after day 90. Only two of them had a histological diagnosis of prostate cancer. All but two patients presenting an abnormal PSA decrease had a day-90 modelized PSA over 2 ng/mL. On the other hand, if we exclude these 11 patients, the remaining 45 patients had a modelized PSA < 2 ng/mL on day 90. As shown in Table 5 and Fig. 5, using Student's *t* tests, the calculated PZ productions were statistically different in both groups (0.141 vs 0.032 ng/mL/cm^3, $p = 0.04$) while the calculated TZ productions were very close (0.111 vs 0.146 ng/mL.g, $p = 0.20$).

Discussion

For characterization of PSA kinetics after surgery, two strategies have to be discussed and compared. The standard strategy in reports until now involved the use of an arbitrary determination of 3 to 8 PSA per patient [6,7,10,14]. One or two HLs, according the number of suspected phases in the decline shape, are calculated for each patient using semi-logarithmic paper or a formula such as $[HL = Ln(2) * (T2 - T1)/(Ln(PSA_2) - Ln(PSA_1))]$ [1,25](Fig. 6). Thus, an HL can be determined for each patient and a mean or a median calculated for the population. Because this approach presents the advantage of simplicity, anyone can perform this kind of study. However, it is also the cause of many biases that lead to mistakes.

First of all, 3 or 8 points per patient, in the best studies, are not enough to calculate with accuracy two kinetic parameters in the case of a mono-exponential decrease (the decrease rate α and the intercept PSA_1) or four kinetic parameters for bi-exponential models (decrease rates K1 and K2 as well as intercepts PSA_1 and PSA_2). In addition, because the timing of PSA determinations greatly influences the calculated HL and no one knows when PSA should be sampled, different clinicians may choose different timepoints, leading to different HL values (Fig. 6). Thus, the calculated kinetic parameter includes an unknown inaccuracy that will be amplified by the number of patients for the mean population parameter determination. For this reason, no conclusion is possible about the prognostic value of this kinetic parameter.

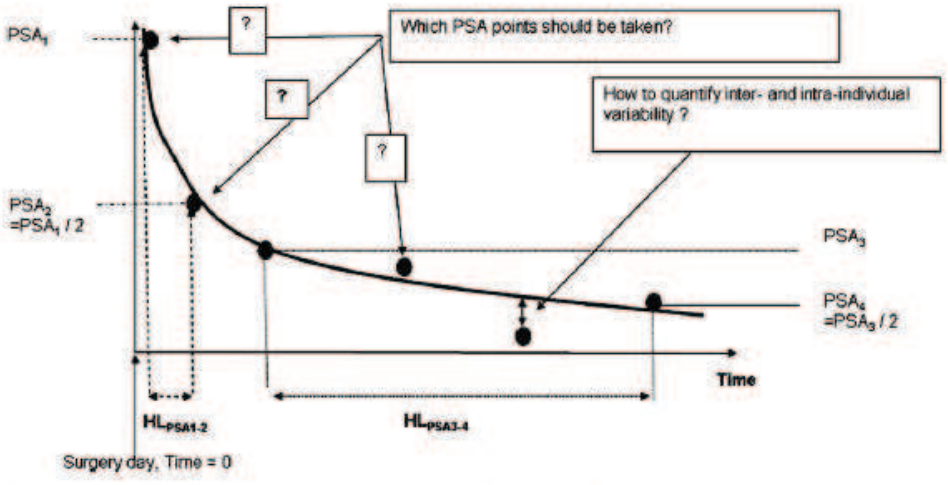

Fig. 6. Limits of the individual method based on multi-exponential decrease. According to the timepoints of the PSA assays used, the calculated HL_{PSA} differs a great deal. For example, we note a large difference between the half-life HL_{1-2} based on point PSA_1 and PSA_2 and the HL_{3-4} based on PSA_3 and PSA_4. Moreover, inter and intra-individual variability are not quantified, leading to unknown inaccuracies, amplified at a population scale.

The strategy we propose presents two advantages. First, the population kinetic approach, which uses all available information, compensates the paucity of individual kinetic information with the large number of patients. This method uses models calculating inter- and intra-individual variability that secondarily allows for determination of the individual decline curve profile as well as the individual covariates influencing the kinetic parameters. It has demonstrated its superiority over the individual method in drug pharmacokinetic studies [26]. On the other hand, a dynamic process such as a clearance-based model may be more accurate because it may be less dependent on the timing of assays and more informative because it integrates the entire decline curve, rather than only a part, as described by an HL.

We had to compare the two strategies knowing that only a population kinetic approach might allow the comparison because only that method could determine the inter-individual variability and standard errors. Both strategies were applicable for post-adenomectomy PSA kinetic characterization. The first approach, based on multi-exponential models, showed that the bi-exponential decrease model was the better of the two. In addition, once the PSA decrease had been achieved, the PSA re-increase coefficient (K3) was quite close to 0, meaning that residual PSA production linked to PZ production was stable over time. This result is consistent with that of Marks et al., who investigated PSA velocity up to 5 years after adenomectomy and found a post-operative velocity of 0.01 ng/mL [27].

On the other hand, the second approach based on CL_{PSA} allowed investigation of the apparent clearance after adenomectomy. Note that it was impossible to give an exact estimation of the PSA clearance because we did not know the amount of the bolus of the assimilated PSA drug (see Appendix for more details). Thus, the CL_{PSA} value integrated both the PSA body elimination and the prostate PSA production, which explained the increase of CL_{PSA} with patient age. The most accurate model, based on CL_{PSA}, was the second strategy. Indeed, it was characterized by smaller CVs of the standard errors and fewer model parameters, and thus a smaller AIC. For this reason, we think that PSA kinetic decrease analyses should now be investigated with CL_{PSA} models, as is commonly done for drug pharmacokinetics.

Surprisingly, PSA decrease kinetics after adenomectomy in prostate adenoma patients has been poorly studied. Only three groups have investigated PSA decline, reporting contradictory results using mono-exponential models (HL_{PSA} between 0.55 and 10.34 days [6,7,28]). Because PSA decline has been extensively described according to bi-exponential models after radical prostatectomy in prostate cancer patients [6,9–14], a mono-exponential PSA decline curve after adenomectomy would be very surprising.

The strategy we describe is not simply theoretical but may be applied for useful and clinical parameter determinations. In the case of prostate adenoma, it included the TZ PSA production, which was close to data in the literature (between 0.096 and 0.31 ng/mL/g [27–32]), especially the largest study results on 190 patients whose PSA TZ production was 0.122 ng/mL/g [33]. The current study also involved the PSA PZ production determination, which had been described only once in the literature, by Recker et al., at 0.052 ng/mL/g [32].

More interestingly, our approach allowed for determination of long-term PSA kinetics so that we could hypothesize about a PSA threshold for post-adenomectomy biochemical relapse. To our knowledge, this concept has never been addressed in the literature. Indeed, because the goal of surgery in BPH is to address symptoms and does not involve patient survival, PSA follow-up is rarely performed after surgery as a clinical routine. However, 11 patients in our cohort presented an abnormal PSA decrease defined by a re-increasing PSA after day 90 or/and high residual PSA values after day 90. This kind of PSA kinetic profile suggested that surgery was not optimal and left TZ cells in the surgery field. A total of 82% of patients in the abnormal PSA decrease group had a modelized day 90 PSA value over 2 ng/mL. Conversely, all patients in the other group had achieved their PSA decline at day 90 and presented a modelized day 90 PSA value under 2 ng/mL. Patients in the two groups had significantly different PZ production, suggesting that an additional PSA production increased PSA PZ residual value in patients in the abnormal PSA decrease group. This additional production may be the consequence of persistent transitional cells in the prostate. Therefore, according to results with our cohort, a threshold of 2 ng/mL on day 90 would be a good limit to distinguish patients having had a complete surgery and those experiencing a biochemical relapse. Of course, this hypothesis should be confirmed with prospective studies.

Our results have to be interpreted with caution. Indeed, it is a non-randomized retrospective study on a small cohort. Moreover, despite the advantages of the population approach, we had a limited number of PSA assays per patient, which increased the inter-individual variability. We did not assay free PSA decline because this parameter was not collected in routine practice by urologists. Another limitation is linked to PSA immunoassay methods, which were certainly different between patients, especially for PSA assayed more than 10 days after surgery. However, the residual variability (Table 3) that includes the intra-individual variability is moderate (14.14%). It suggests that PSA concentration variations linked to the different methods of assay may not have largely influenced our data and results. In the

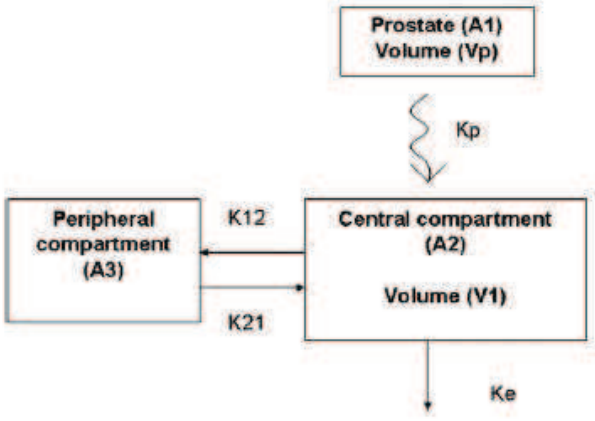

Fig. 7. The optimal specification for the PSA decrease model. Kp is the rate constant of PSA release from prostate to serum; K12 and K21 are the PSA transfer rate constants between the peripheral compartment and central compartment; and Ke is the elimination rate constant. C_{PSA} is the PSA concentration assayed in the central compartment.

contrary we should have observed a large intra-individual residual variability. By taking advantage of the population model approach, we could have taken it into account by considering that each patient has his own residual variance, in other words that the variance of residual variability is prone to inter-individual variability. But this sophistication was not required. As shown in Fig. 1, weighted residuals were over 2 for a group of 9 PSA predictions in the CL_{PSA}-based model. Because all these points only involved patients having experienced a biochemical relapse and concerned PSA sampled after day 90 for 8/9 points, biochemical relapse prediction can be done with a threshold fixed on day 90.

To conclude, the results of this study suggest that further PSA decrease kinetic analysis after surgery should rationally be based on CL_{PSA} because this approach is more accurate than computing the HL decrease without a model, or even with the multi-exponential models used previously. This strategy may lead to improvement in PSA kinetic parameter characterization for their diagnostic value as much as for their prognostic value. The concept of biochemical relapse after adenomectomy should be confirmed in further studies, but a PSA threshold of 2 ng/mL on day 90 would be a rational value, according to our data.

Acknowledgments

Pascal Girard is funded by INSERM, France. The authors would like to thank Paul Kretchmer for help in English editing.

Appendix

To model the PSA decrease, it would have been ideal to build a model as described in Fig. 7. The prostate compartment releases PSA with a first-order rate constant Kp to the central compartment. The latter is characterized by its volume V1 and serum PSA concentrations C_{PSA}. Because PSA decline is generally fitted by a bi-compartmental model, an additional peripheral compartment is required to describe the PSA changes. This compartment exchanges PSA with K12 and K21 transfer rate constants. The PSA is eliminated from the central compartment with a Ke first-order elimination rate. Thus, the central compartment PSA concentration changes over time are described by the equation:

$$dC_{PSA}/dt=(Kp*A1+K21*A3-(Ke+K12)A2)/V1$$

where:

- V1 is the central compartment volume;
- A1 is the amount of PSA in the prostate;
- A2 is the amount of PSA in the central compartment; and
- A3 is the amount of PSA in the peripheral compartment.

Yet, data are unavailable to identify the Kp rate value, the beginning date of PSA release from prostate to serum, and the PSA steady-state concentration. For these reasons, PSA production can be assimilated into an intravenous bolus arbitrarily set at 1, with an unknown bioavailability F that is greater than 1.

In this case, the apparent volume of distribution and clearance corresponding to CL/F=Ke V1 and V1/F can be determined, where V1 and CL are the true unknown volume of distribution and clearance.

References

[1] Stamey TA, Yang N, Hay AR, McNeal JE, Freiha FS, Redwine E. Prostate-specific antigen as a serum marker for adenocarcinoma of the prostate. N Engl J Med 1987;317:909–16.
[2] Kelloff GJ, Coffey DS, Chabner BA, et al. Prostate-specific antigen doubling time as a surrogate marker for evaluation of oncologic drugs to treat prostate cancer. Clin Cancer Res 2004;10:3927–33.
[3] D'Amico AV, Moul J, Carroll PR, Sun L, Lubeck D, Chen MH. Prostate specific antigen doubling time as a surrogate end point for prostate cancer specific mortality following radical prostatectomy or radiation therapy. J Urol 2004;172:S42–6.
[4] Eastham JA. Prostate-specific antigen doubling time as a prognostic marker in prostate cancer. Nat Clin Pract Urol 2005;2:482–91.
[5] Maffezzini M, Bossi A, Collette L. Implications of prostate-specific antigen doubling time as indicator of failure after surgery or radiation therapy for prostate cancer. Eur Urol 2007;51:605–13.
[6] Haab F, Meulemans A, Boccon-Gibod L, Dauge MC, Delmas V, Boccon-Gibod L. Clearance of serum PSA after open surgery for benign prostatic hypertrophy, radical cystectomy, and radical prostatectomy. Prostate 1995;26:334–8.
[7] Ravery V, Meulemans A, Boccon-Gibod L. Clearance of free and total serum PSA after prostatic surgery. Eur Urol 1998;33:251–4.
[8] Vollmer RT, Humphrey PA. Tumor volume in prostate cancer and serum prostate-specific antigen. Analysis from a kinetic viewpoint. Am J Clin Pathol 2003;119:80–9.
[9] Lein M, Brux B, Jung K, et al. Elimination of serum free and total prostate-specific antigen after radical retropubic prostatectomy. Eur J Clin Chem Clin Biochem 1997;35:591–5.
[10] May M, Gunia S, Helke C, Braun KP, Pickenhain S, Hoschke B. Is it possible to provide a prognosis after radical prostatectomy for prostate cancer by means of a PSA regression model? Int J Biol Markers 2005;20:112–8.
[11] Stamey TA, Kabalin JN, McNeal JE, et al. Prostate specific antigen in the diagnosis and treatment of adenocarcinoma of the prostate. II. Radical prostatectomy treated patients. J Urol 1989;141:1076–83.
[12] van Straalen JP, Bossens MM, de Reijke TM, Sanders GT. Biological half-life of prostate-specific antigen after radical prostatectomy. Eur J Clin Chem Clin Biochem 1994;32:53–5.
[13] Brandle E, Hautmann O, Bachem M, et al. Serum half-life time determination of free and total prostate-specific antigen following radical prostatectomy—a critical assessment. Urology 1999;53:722–30.
[14] Gregorakis AK, Malovrouvas D, Stefanakis S, Petraki K, Scorilas A. Free/Total PSA (F/T ratio) kinetics in patients with clinically localized prostate cancer undergoing radical prostatectomy. Clin Chim Acta 2005;357:196–201.
[15] Oesterling JE, Chan DW, Epstein JI, et al. Prostate specific antigen in the preoperative and postoperative evaluation of localized prostatic cancer treated with radical prostatectomy. J Urol 1988;139:766–72.
[16] Sheiner LB. The population approach to pharmacokinetic data analysis: rationale and standard data analysis methods. Drug Metab Rev 1984;15:153–71.
[17] Rowland M, Rowland R, Tozer. Clinical pharmacokinetics: concepts and applications. Sub 1995;3 (mai 1995).
[18] Kuritzky L. Role of primary care clinicians in the diagnosis and treatment of LUTS and BPH. Rev Urol 2004;6(Suppl 9):S53–9.
[19] Millin T. Retropubic prostatectomy: a new extravesical technique report on 20 cases. 1945. J Urol 2002;167:976–9.
[20] Beal S, Sheiner L. NONMEM users guides; 1992.
[21] Dartois C, Brendel K, Comets E, et al. Overview of model-building strategies in population PK/PD analyses: 2002–2004 literature survey. Br J Clin Pharmacol 2007;64(5):603–12.

[22] Brendel K, Dartois C, Comets E, et al. Are population pharmacokinetic and/or pharmacodynamic models adequately evaluated? A survey of the literature from 2002 to 2004. Clin Pharmacokinet 2007;46:221–34.
[23] Yano I, Beal SL, Sheiner LB. The need for mixed-effects modeling with population dichotomous data. J Pharmacokinet Pharmacodyn 2001;28: 389–412.
[24] Yano Y, Beal SL, Sheiner LB. Evaluating pharmacokinetic/pharmacodynamic models using the posterior predictive check. J Pharmacokinet Pharmacodyn 2001;28:171–92.
[25] Oudard S, Banu E, Scotte F. Prostate-specific antigen doubling time before onset of chemotherapy as a predictor of survival for hormone-refractory prostate caner patients. Ann Oncol 2007:1828–33.
[26] Vozeh S, Steimer JL, Rowland M, et al. The use of population pharmacokinetics in drug development. Clin Pharmacokinet 1996;30: 81–93.
[27] Marks LS, Dorey FJ, Rhodes T, et al. Serum prostate specific antigen levels after transurethral resection of prostate: a longitudinal characterization in men with benign prostatic hyperplasia. J Urol 1996;156: 1035–9.
[28] Vollmer RT, Humphrey PA. The relative importance of anatomic and PSA factors to outcomes after radical prostatectomy for prostate cancer. Am J Clin Pathol 2001;116:864–70.
[29] Furuya Y, Akakura K, Ichikawa T, Masai M, Igarashi T, Ito H. Effect of prostatic biopsy on free-to-total prostate-specific antigen ratio in patients with prostate cancer. Int J Urol 2000;7:49–53.
[30] Hammerer PG, McNeal JE, Stamey TA. Correlation between serum prostate specific antigen levels and the volume of the individual glandular zones of the human prostate. J Urol 1995;153:111–4.
[31] Lloyd SN, Collins GN, McKelvie GB, Hehir M, Rogers AC. Predicted and actual change in serum PSA following prostatectomy for BPH. Urology 1994;43:472–9.
[32] Recker F, Kwiatkowski MK, Pettersson K, et al. Enhanced expression of prostate-specific antigen in the transition zone of the prostate. A characterization following prostatectomy for benign hyperplasia. Eur Urol 1998;33:549–55.
[33] Aus G, Bergdahl S, Frosing R, Lodding P, Pileblad E, Hugosson J. Reference range of prostate-specific antigen after transurethral resection of the prostate. Urology 1996;47:529–31.

The Prostate 69:1325 – 1333 (2009)

Prognostic Value of Modeled PSA Clearance on Biochemical Relapse Free Survival After Radical Prostatectomy

Benoit You,[1,2,3]* Pascal Girard,[1,2] Philippe Paparel,[4] Gilles Freyer,[1,2,3] Alain Ruffion,[4] Anne Charrié,[5] Emilie Hénin,[1,2] Michel Tod,[1,2,6] and Paul Perrin[4]

[1]Université de Lyon, Lyon, France
[2]Université Lyon I, EA3738, CTO, Faculté de Médecine Lyon Sud, Oullins, France
[3]Service d'Oncologie Médicale, Centre Hospitalier Lyon Sud, Hospices Civils de Lyon, Pierre-Bénite, France
[4]Service d'urologie, Centre Hospitalier Lyon Sud, Hospices Civils de Lyon, Pierre-Bénite, France
[5]Laboratoire de Techniques nucléaires et Biophysiques, Centre Hospitalier Lyon Sud, Hospices Civils de Lyon, Pierre-Bénite, France
[6]Pharmacie-toxicologie, Hôpital Cochin, Paris, France

PURPOSES. Using population kinetic approach, we modeled PSA decline equations in patients with prostate cancer after radical prostatectomy (RP). We looked for relationships between early PSA decrease profile, characterized by PSA clearance (CL_{PSA}) or half-life (HL_{PSA}), and the 2-year biochemical relapse free survival (bRFS).

PATIENTS AND METHODS. We performed a retrospective study on 55 patients treated with RP and with at least 2 PSA measurements in the post-operative month. A population kinetic model was investigated with NONMEM®. The prognostic factors regarding bRFS were assessed using univariate and multivariate analyses.

RESULTS. The best model describing the PSA post-operative decrease was bi-compartmental and fit patient data well. Median CL_{PSA} was 0.034 (terciles were 0.023 and 0.048). The significant prognostic factors associated with a better bRFS with univariate analysis were lower CL_{PSA} terciles (2-year bRFS = 100% vs. 85.1% vs. 66.7% if $CL_{PSA} < 0.023$, $0.023 \leq CL_{PSA} < 0.048$ or $CL_{PSA} \geq 0.0480$, $P = 0.006$) as well as initial PSA < 7 ng/ml, pT2 stage (vs. pT3), pN0 (vs. pN1) and low main Gleason score (3/5 vs. 4/5). Among these factors, CL_{PSA} was the only independent prognostic factor with multivariate analysis regarding bRFS (HR = 0.92, 95%CI = [0.86–0.98], $P = 0.0088$).

CONCLUSION. CL_{PSA} determined with 4 PSA concentrations in the first month following the RP may predict the biochemical relapse risk of prostate cancer patients, thus enabling early identification of high-risk patients requiring adjuvant treatment. A prospective validation of these results is required. *Prostate 69: 1325–1333, 2009.* © 2009 Wiley-Liss, Inc.

Abbreviations: RP, radical prostatectomy; PSA, prostate specific antigen; C_{LPSA}, apparent psa clearance; V1, apparent central compartment volume; HL_{PSA}, PSA half-life (days); $HL_{PSA(5-30)}$, PSA half-life between day 5 and 30 after surgery (days); bRFS, biochemical relapse free survival (months); pTNM, pathology tumor node metastasis score; D0, day of surgery; D1, day 1 (after surgery); OF, objective function; FO, first order; FOCEI, first order conditional estimation with interaction; Scr, serum creatinine (μmol/L); CV, coefficient of variation (%); HR, hazard ratio; 95%CI, 95% confidence interval.

Institution at which work was performed: Centre Hospitalier Lyon-Sud, Hospices Civils de Lyon, Pierre-Bénite, France and Faculté de médecine de Lyon-Sud, Université Claude Bernard Lyon 1, Lyon, France.

Conflict of interest statement: All authors disclose any financial and personal relationships with other researchers or organizations that could inappropriately influence or bias the study.

*Correspondence to: Benoit You, Service d'oncologie médicale, Centre Hospitalier Lyon-Sud, Chemin du Grand Revoyet, 69495 PIERRE-BENITE, France. E-mail: benoit.you@chu-lyon.fr

Received 5 February 2009; Accepted 7 April 2009
DOI 10.1002/pros.20978
Published online 27 May 2009 in Wiley InterScience (www.interscience.wiley.com).

KEY WORDS: biomarker; metabolite clearance rate; prostate specific antigen; prostate cancer; prostatectomy; prognosis

INTRODUCTION

Patients with localized prostate cancers are commonly treated with radical prostatectomy (RP), which leads to a decrease in concentration of prostate specific antigen (PSA) to undetectable levels if surgery was complete [1]. Among these patients, 20–30% will experience a biochemical relapse, defined as a residual PSA value over 0.2–0.4 ng/ml and re-increase after surgery [2,3]. Of patients with a biochemical relapse, 30% will develop distant metastasis [4,5]. Although adjuvant prostate field external beam radiotherapy can reduce biochemical and locoregional relapse risk by 22% in patients with high risk prostate cancer [6], no clear prognostic factors have been identified so far that can distinguish patients requiring an adjuvant treatment and those requiring a simple follow-up.

One common assumption is that the post-operative PSA profile, as a result of persistence of residual tumor, likely correlates with relapse risk. Yet, methods commonly used to investigate the decline of PSA after surgery (half-life (HL) determined from mono/bi-exponential models) are prone to biases and inaccuracies [7]. In order to investigate individual PSA kinetic after RP, we propose to use modeling and population pharmacokinetic (PK) principles. They are commonly used in PK studies investigating serum drug concentration decline after administration [8]. Assimilating tumor marker decrease to a drug administered with an intravenous bolus, it is possible to model the individual tumor marker decline equation and to characterize it with a simple kinetic parameter such as the apparent elimination clearance. We successfully applied this method for PSA decline analysis in patients with prostate adenoma after adenomectomy. This approach allowed a dynamic investigation, independent on selected time points, of the whole post-operative PSA decline curve, and an estimation of inter/intra-individual variability [7].

To further assess the relationship between PSA clearance (CL_{PSA}) and relapse risk, we performed a retrospective exploratory study investigating post-radical prostatectomy PSA decline in patients with prostate cancer. The main objective was to assess the feasibility of PSA decrease modeling after RP using a population kinetic approach parameterized in CL_{PSA}. Moreover this study aimed at performing a survival analysis to determine if the post-operative PSA decline profile, especially PSA half-life (HL_{PSA}) and/or CL_{PSA}, could have a prognostic value on the 2-year biochemical relapse free survival (bRFS).

PATIENTS AND METHODS

Patients

We retrospectively reviewed data of all patients treated with a RP for prostate cancer in the urology department of Centre Hospitalier Lyon-Sud (France) between February 2004 and March 2006. To be included in this retrospective analysis, patients should have been treated with a RP for a prostate adenocarcinoma, and have had a minimum of 2 PSA assays in the post-operative first month period. The starting date of PSA monitoring was considered to be the surgery day. No time limit was fixed for patient PSA follow-up. Patients were excluded if they received any adjuvant treatment that could potentially modify PSA kinetics, including hormone therapy, chemotherapy, brachytherapy, or external beam radiotherapy. Moreover if such a treatment was begun in the follow-up of an included patient, the PSA assays collected after start of the above-mentioned treatments were not included in our analysis.

In addition to PSA assays, the following data were collected: age, weight, serum creatinine, total protein, sodium, blood cell count, prostate weight without seminal vesicles, tumor volume, surgical margins, pTNM stage, and Gleason score. PSA concentrations were measured in *Centre Hospitalier Lyon-Sud* radio-immuno-laboratory during the early post-operative period (until 10 days after RP) and in the patient's analysis laboratory afterwards. The *Centre Hospitalier Lyon-Sud* radio-analysis laboratory uses the equimolar PSA IRMA KIT®, which has a lower limit of quantification of 0.1 ng/ml. Inter- and intra-assays variations are below 6% in the range of 2.01 to 44.5 ng/ml, with a coefficient of variation (CV) of 20% at 0.14 ng/ml.

PSA Kinetic Analysis

Since the final aim of the study was to develop a useful routine tool for physicians, HL_{PSA} and CL_{PSA} models were built with PSA assayed between day 0 (D0) and day 30 (D30) after surgery. Indeed, prediction of the relapse risk in the month following surgery would provide enough time to plan a post-operative adjuvant treatment (hormonotherapy and/or external beam radiotherapy).

Apparent PSA Clearance (CL_{PSA})

Assimilating PSA decline to a drug given with an intravenous bolus, we parameterized apparent PSA

elimination in term of apparent clearance (CL_{PSA}). Notice that determination of true PSA clearance is not feasible because we do not know the production endogenous rate of PSA. Thus, the apparent CL_{PSA} is a parameter that mixes both the PSA body elimination and the prostate PSA production [7].

The analysis was performed using nonlinear mixed-effects modeling strategy as implemented in NONMEM (Version 6, University of California, San Francisco, California, Unix Operating System) to estimate the population parameters (mean and inter-subject variability), the residual variability and to identify potential covariates to explain inter-subject variability in the parameters [9]. A series of linear PK models were evaluated including 1-, 2-, and 3-compartment models for disposition with zero order absorption. Data analysis was performed using the first order conditional estimation method with interaction computational method (FOCE INTERACTION). Inter-subject variability in the PK parameters was modeled using exponential random effects (i.e., PK parameters are assumed to be log-normal distributed). Comparison of two nested models was based on the minimum value of the objective function (OF), agreement between predicted and observed concentrations, the magnitude of randomness of residual values as assessed by visual inspection, and the precision of the parameter estimates.

In a second step, the main individual covariates collected (age, weight, serum creatinine, creatinine clearance calculated with Cockroft and Gault formula, total protein, prostate weight, tumor volume, surgical margins, pTNM staging, Gleason score, biochemical relapse) were tested to estimate their impact on PSA kinetic parameters, for reducing unexplained inter-individual variability. Analysis of covariates was guided by visual inspection for potential relationships between inter-individual variability and the subject factor. When a covariate demonstrated significant relationships with any kinetic parameters, it was introduced into the model describing the fixed effects by forward inclusion. The covariate was kept in the model only if a significant decrease in the NONMEM OF was obtained (decrease > 7, $P < 0.01$). For instance, influence of age covariate on CL_{PSA} was tested by implementation: $CL_{PSA} = (\Theta 1 \times (\text{patient age/cohort median age})^{\Theta 2} \times \exp(\eta 1)$ where:

- $\Theta 1$ and $\Theta 2$ are the fixed effect parameters of CL_{PSA} and age covariates influencing CL_{PSA},
- $\eta 1$ is the random effect parameters expressing inter-individual variability with 0 mean and ω^2 variance.

The modeling methodology has been described in detail elsewhere [7].

PSA Half-Lives (HL_{PSA})

No clear recommendations have been reported regarding the time points to use for HL_{PSA} calculation after RP. However most of authors calculated HL_{PSA} using PSA values measured between D0 and D10 [10–13]. In the largest study involving 77 patients, May et al. determined two half-lives, between D0 and D5 and between D5 and D10 [13]. Considering patient post-operative PSA decline curves, which presented bi-exponential inflexion around day five, we decided to calculate three HL_{PSA} per patient using the following formula: [HL = Ln2/slope], where Ln is the natural logarithm [13–15]. The first PSA half-life, $HL_{PSA}(0–30)$, was calculated between D0 and D30 and was connected to the overall PSA decrease, while the second, $HL_{PSA}(5–30)$, was determined between D5 and D30 and reflected the terminal HL. Finally we calculated $HL_{PSA}(5–10)$ because its prognostic value was reported by May et al. [13]:

- $HL_{PSA(0-30)} = Ln(2) \times (30–0)/(Ln(PSA_{D0}) - Ln(PSA_{D30}))$
- $HL_{PSA(5-30)} = Ln(2) \times (30–5)/(Ln(PSA_{D5}) - Ln(PSA_{D30}))$
- $HL_{PSA(5-10)} = Ln(2) \times (10–5)/(Ln(PSA_{D5}) - Ln(PSA_{D10}))$

where PSA_{D0}, PSA_{D5}, PSA_{D10}, and PSA_{D30} are modeled PSA on D0, D5, D10, and D30 after surgery.

CL_{PSA} Model Internal Validation

The PSA kinetic model was validated by a predictive check consisting of simulation of 500 PSA decline profiles using the final model parameters [16,17]. Two methods of qualification were used in the validation:

- Visual predictive check: observed PSA values were compared to 95% confidence interval (95%CI) of the 500 simulated replicates.
- Statistical predictive check: distributions of a PSA statistics computed from the simulated dataset were compared to the corresponding PSA observed statistics. These statistics involved prediction of two parts of PSA decline curve, including the initial portion defined as first PSA before day 5, as well as the curve slope (calculated with: slope = first PSA − last PSA/change in time). Distribution histograms of the lower quartiles, medians, and upper quartiles of simulated values were drawn with their 95%CI. The model was considered able to properly predict decline curve if all corresponding observed values were included in the 95%CI of simulated values.

Statistical Survival Analysis

Biochemical and clinical follow-up were implemented according to surgeon habit. The bRFS was calculated as the time elapsed between the surgery day (D0) and the day of the first event, such as the patient death or the clinical/biochemical relapse. Biochemical relapse was defined as a post-operative PSA larger than 0.4 ng/ml [3].

Since half the biochemical relapses are observed in the first 2 years after surgery, and as these relapses are associated with the highest risk of distant metastasis [13], our survival analysis included the 2-year bRFS. The following potential prognostic factors were investigated by univariate analysis using a log-rank test: patient age, Gleason scores, pTNM stage, prostate weight, tumor volume, initial PSA, $HL_{PSA(0-30)}$, $HL_{PSA(5-30)}$, $HL_{PSA(5-10)}$, and CL_{PSA} inferred from the model.

As log-rank test requires categorical data, all continuous covariates were split into two groups according to the median, except for CL_{PSA}, which was split into terciles to take into account the continuity of the prognostic value of the variable in the survival analysis.

To test the independence of prognostic factors, those found with univariate analysis ($P < 0.05$) were included in a multivariate analysis using a Cox model according to a backward elimination procedure. The results of Cox model were confirmed using a bootstrap. Hence, covariate hazard ratios were calculated in 1000 repeated random resampling of the original dataset. All tests were performed using the S-PLUS® program with a two-sided 0.05 α risk.

Optimal Sampling Strategy

If a PSA kinetic parameter had a prognostic value on the 2-year bRFS, a prospective study should confirm its predictive value. To achieve such an aim, we determined the sampling times required to reach the best estimation of the concerned parameter.

We used the WinPopt® program that sought the sampling protocol (number of samples and sample times), which maximized the accuracy of the population model parameters estimation [18]. The optimal number of samples was first determined by assessing various protocols, including testing between 1 and 5 samples over the post-operative first month. We also examined the maximum criteria given by the *Exchange Algorithm* program and the minimum CV for estimation of the fixed parameters, random parameters and residual variability. Once the optimal number of samples was determined, the program identified the optimal sampling times with the *simulated annealing* method.

RESULTS

Patients and Follow-up

Data of 55 patients treated with RP between February 2004 and March 2006 and with a minimum of 2 PSA values between D0 and D30 were available. A total of 162 PSA concentrations were measured at various times between D0 and D673 (more than 22.4 months after the surgery) with a median of 3 PSA measurements per patient. The median follow-up was 780 days. The characteristics of the included patients are presented in Table I.

Modeling

The best model describing PSA decrease after RP was a bi-compartmental one. The FOCEI method was used to estimate inter-individual variabilities for CL_{PSA} and V1 with log-normal distribution and residual distribution with mixed models, respectively.

All covariates susceptible to influence the PSA profile were tested. None of them significantly decreased unexplained inter-individual variability except for biochemical relapse (yes/no) which decreased unexplained inter-individual variability of CL_{PSA} by 10%. Yet it was not kept in the model since one of the study aims was to test the value of CL_{PSA} as a predictor of relapse.

The CV of inter-individual variabilities of CL_{PSA} and V1 were 106.3 and 77.0 %, respectively, whereas the CV of the residual variability was estimated at 3.5 %. Addition of a block matrix for the random effect parameters reduced unexplained inter-individual variability of CL_{PSA} and V1 by 3 and 5% respectively. Modeled median CL_{PSA} was 0.034 and CL_{PSA} terciles were 0.023 and 0.048. Figure 1 presents the final model results including weighted residuals versus observed PSA values. It also shows individual predicted versus observed PSA values for all patients as well as for three typical patients, including one who experienced a biochemical relapse 6 months after surgery (patient 18). Table II presents the results of post hoc fixed parameters with inter-individual variability, standard errors, and residual variability.

Half-Lives Calculation

We used PSA on day 0, day 5, day 10, and day 30 derived from the model to calculate $HL_{PSA(0-30)}$, $HL_{PSA(5-30)}$, and $HL_{PSA(5-10)}$ for all patients. Results are shown in Table II.

Internal Model Validation

A total of 500 PSA decline profiles were simulated using the population parameters of the CL_{PSA} model.

TABLE I. Patient Characteristics

Covariate	Median	Q25%	Q75%	Range
Age (years)	61.7	57.4	66.0	40.8–73.6
Patient weight (kg)	82.0	71.0	90.0	57.0–112.0
Serum creatinine (μmol/L)	93.0	83.0	101.0	62.0–136.0
Creatinine clearance (ml/min)	83.6	69.8	93.9	46.9–18.7
Prostate weight (g)	34.0	28.0	48.6	16.8–84.0
Tumor volume (cc)	2.3	1.5	6.0	0.1–20.0
Gleason score	7.0	7.0	8.0	6.0–9.0
	Number of patients	Percentage		
Biochemical relapse				
Yes	8	14.5%		
No	47	85.4%		
Positive surgical margins				
Yes	24	43%		
No	31	57%		
Involved lymph nodes				
Yes (N1)	8	14.5%		
No (N0)	47	85.4%		
Pathology tumor stage				
pT2	31	56.3%		
pT3	24	43.6%		
Gleason score				
3+3	9	16.3%		
3+4	20	36.3%		
4+3	11	20.0%		
4+4	7	12.7%		
4+5	8	14.5%		

Q25% = first quartile, Q75% = fourth quartile

Figure 2 presents the visual predictive check, which compared 95%CI bounds of simulated PSA to observed PSA. A large majority (96 %) of the observed PSA were included in the 95%CI simulated PSA, supporting the accuracy of the model.

Regarding the statistical predictive check, all observed PSA values were comprised in the 95%CI bounds of simulated values. This statistical predictive check confirmed the ability of the model to predict the first portion of the PSA decline curve as well as its decrease slope.

Survival Analysis

All patients were included in the 2-year bRFS analysis, and all were alive as of February 2009, date of the last update. Eight patients (14.5%) experienced a biochemical relapse after a median time of 11.2 months. All of these relapses were observed in the 2 years following the surgical procedure. An additional treatment with external beam radiotherapy and/or hormonotherapy was prescribed at biochemical relapse diagnosis in 63% of the cases. Table III presents the results of univariate analysis using the log-rank test. The significant factors included pT stage, nodal invasion, global Gleason score, major Gleason score, modeled initial PSA, and CL_{PSA} terciles (2-year bRFS = 100% vs. 85.1% vs. 66.7% if $CL_{PSA} \geq 0.048$, $0.023 \leq CL_{PSA} < 0.048$, or $CL_{PSA} < 0.023$ respectively, $P = 0.006$). Figure 3 presents the 2-year bRFS Kaplan-Meier curves according to CL_{PSA} terciles. Note that $HL_{PSA(0-30)}$, $HL_{PSA(5-30)}$, or $HL_{PSA(5-30)}$, commonly parameterized in the literature, did not present any prognostic value in our analysis.

The covariates found to be statistically significant by univariate analysis (CL_{PSA}, pT stage, nodal invasion, and major Gleason score) were included in a Cox multivariate model. Since CL_{PSA} and initial PSA were correlated, only CL_{PSA} was kept in the multivariate model.

Among all the potential prognostic factors, only the CL_{PSA} covariate presented a significant independent prognostic value. This Cox model prognostic value was continuous and a 0.001 unit CL_{PSA} increase was associated with a 9% decrease in the relative risk of biochemical relapse (hazard ratio = 0.91, 95%CI = [0.86–0.98], $P = 0.0088$). The bootstrap analysis confirmed the independent and statistically significant prognostic value of CL_{PSA} with an observed HR = 0.9258, 95%CI = [0.825–0.9980].

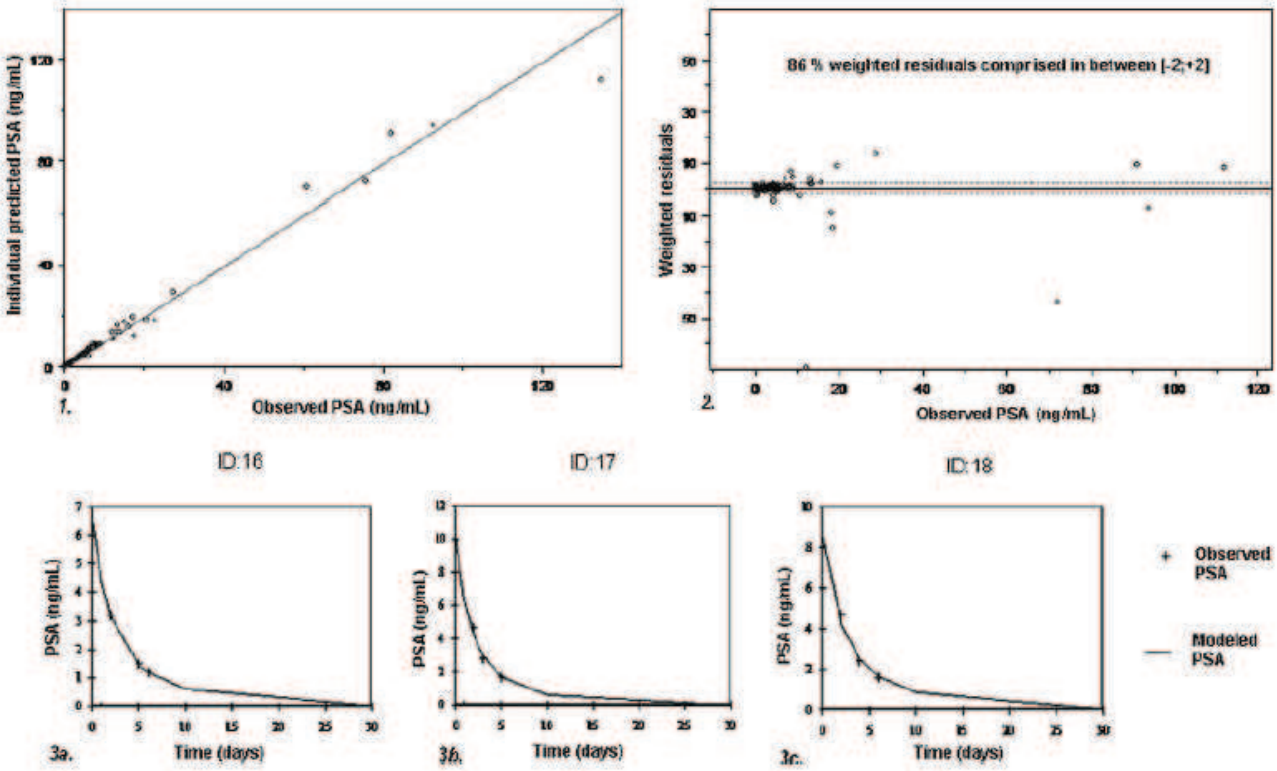

Fig. 1. Individual predicted PSA values versus observed PSA values for all patients (1) and for three typical patients (3a.–3c.). Patient number 18 (3c.) experienced a biochemical relapse 6 months after surgery. Weighted residuals versus observed PSA values (2).

Optimal Sampling Strategy

The 1-, 2-, or 3-sample strategies estimated CL_{PSA} with a larger CV than did the 4 sample protocol. A 5-sample strategy did not improve CL_{PSA} prediction, as the WinPopt program proposed two identical time points. Thus, we chose the 4-sample protocol to characterize patient post-operative PSA decrease. Using the *simulating annealing* method, we entered the following initial sample times: D0 (before surgery), D5, D10, and D15 for a 50 patient cohort. The program suggested 4 optimal PSA sample times collected on D0, D2, D7, and D27.

DISCUSSION

Analysis of post-operative PSA kinetic parameters, due to the potential for residual prostate cancer cells after surgery, is not novel. Despite the advantage of its simplicity, the approach based on PSA half-life and commonly reported so far contains biases and inaccuracies. Authors used various individual PSA time-points to calculate 1 or 2 individual HL_{PSA} with the following formula $[HL = Ln(2) \times (T2-T1)/(Ln(PSA_2)-Ln(PSA_1))]$ and then determined a mean or a median for population. This strategy was limited by the lack of quantification of inter/intra-individual variability and

TABLE II. Model Parameter Estimations and CV of Inter-Individual Variabilities and Standard Error Due to Model Inaccuracies

Parameter	Population post hoc values	Median post hoc values	95%CI of post hoc values =	Inter-individual variability	Standard error	Residual variability
CL_{PSA}	0.030	0.034	[0.026–0.043]	106.3%	30.5%	3.5%
Apparent central compartment volume	0.129	0.142	[0.114–0.170]	77.0%	24.4%	
Initial PSA estimation (ng/ml)	ND	7.06	[2.11–12.01]	ND	ND	ND
$HL_{PSA(0-30)}$ (days)	ND	3.90	[2.70–5.10]	ND	ND	ND
$HL_{PSA(5-30)}$ (days)	ND	4.43	[3.21–5.65]	ND	ND	ND
$HL_{PSA(5-10)}$ (days)	ND	4.29	[3.44–5.12]	ND	ND	ND

ND = Not Determined, Q25% = first quartile, Q75% = fourth quartile.

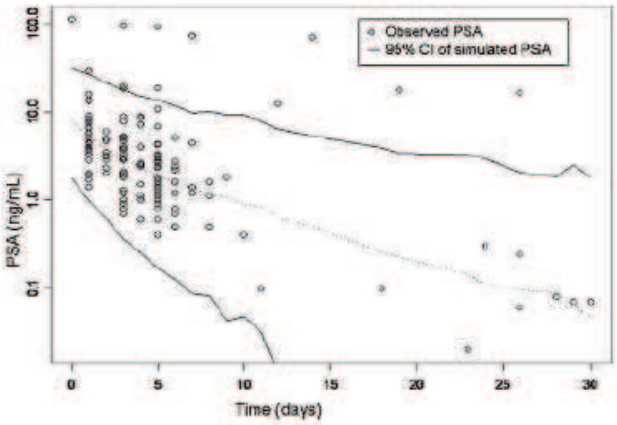

Fig. 2. Visual predictive check. PSA and log (PSA) versus time. As shown, 96% observed PSA values are included in the bounds of 95%CI of the simulated data set.

the dependence of calculated HL on selected time-points. Thus, the calculated kinetic parameter included an unknown inaccuracy that was amplified by the number of patients for the mean population parameter determination, as shown by the large variability of reported results. Indeed, the latter have varied widely in the seven main studies investigating PSA half-lives according to bi-exponential models, with values of HL(α) ranging between 1.45 and 45.36 hours and HL(β) between 52.80 and 182.88 hours [1,10–13,19–23]. In addition, several authors reported the prognostic values of PSA kinetic parameters, but these results were even more heterogeneous. Some found relationships between HL_{PSA} or nadir and relapse risk after RP [13,20,24–27], while others rejected the prognostic value of the post-operative PSA kinetics [13,28]. Consequently these PSA kinetic parameters are currently not used in routine.

In this study, we employed modern tools such as mathematic and computational modeling, already implemented with success in clinical pharmacology, to reconsider tumor biomarker kinetics along with their prognostic value. We previously showed that modeling of the individual post-operative PSA decline profile after prostate adenomectomy using a population kinetic approach was superior to the common

TABLE III. Univariate Analysis on the 2-Year bRFS.

Covariate	Status	n	2-year bRFS(%)	*P*-value
Age (years)	<61.7	28	80.9	0.51
	≥61.7	27	87.6	
Tumor volume (cc)	<2.3	27	95.7	0.050
	≥2.3	28	73.0	
Prostate weight (g)	<34.5 g	30	84.1	0.62
	≥34.5 g	25	83.1	
Disease stage	**pT = 2**	**31**	**95.0**	**0.005**
	pT = 3	**24**	**70.6**	
Surgical margins	R0	31	93.5	0.053
	R1	24	70.0	
Nodal invasion	**N = 0**	**47**	**87.8**	**0.023**
	N ≥ 1	**8**	**67.2**	
Major Gleason score (1–5)	**Gl = 3**	**29**	**95.0**	**0.009**
	Gl = 4	**26**	**72.5**	
Global Gleason score (2–10)	**Gl ≤ 7**	**40**	**90.3**	**0.01**
	Gl ≥ 8	**15**	**66.7**	
$HL_{PSA(0-30)}$(days)	<3.90	27	82.1	0.39
	≥3.90	28	86.5	
$HL_{PSA(5-30)}$(days)	<4.43	27	82.1	0.39
	≥4.43	28	86.5	
HL_{PSA}(5–10) (days)	<4.29	27	78.9	0.58
	≥4.29	28	88.6	
CL_{PSA}	**≥0.048**	**19**	**100**	**0.006**
	0.023–0.048	**18**	**85.1**	
	<0.023	**18**	**66.7**	
CL_{PSA}	**<0.023**	**18**	**66.7**	**0.007**
	≥0.023	**37**	**92.7**	
Initial PSA (ng/ml)	**<7.0**	**27**	**100**	**0.002**
	≥7.0	**28**	**67.6**	

Significant prognostic factors are in bold

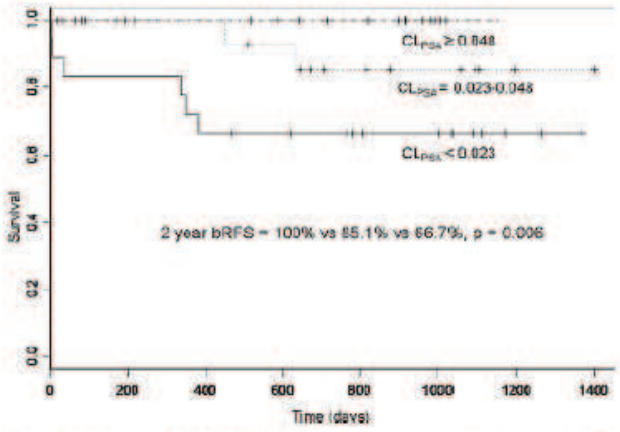

Fig. 3. Two-year bRFS Kaplan-Meier curve according to modeled CL_{PSA} terciles.

half-life strategy. Indeed, our approach allowed the calculation of a simple parameter (modeled clearance) that characterizes the whole biomarker decline curve, in contrast to the static half-life parameter that only represents a part of the curve [7].

We demonstrated the ability to model the individual PSA decline curve using this new approach. Interestingly, in contrast to HL_{PSA}, CL_{PSA} was the only independent prognostic factor on the 2-year bRFS and was stronger than the other common prognostic factors. A group with a high risk of relapse characterized by a low CL_{PSA} was identified (33% risk of 2-year biochemical relapse if $CL_{PSA} < 0.023$), and these patients may benefit from adjuvant treatments such as radiotherapy and/or hormonotherapy. The lower observed CL_{PSA} in patients with biochemical relapse might reflect a persistent PSA production due to residual prostate tissue after surgery and thus explain the higher relapse risk.

If CL_{PSA} prognostic value would be prospectively confirmed, it could easily be calculated by every clinician in the first month of post-operative period thereby allowing adequate time for planning adjuvant treatments. Indeed PSA concentrations obtained at appropriate times during this period could be entered in a model-based software which would immediately determine patient's CL_{PSA}.

These results should be analyzed with caution, as this was a non-randomized study on a small number of patients that included few relapses. A large proportion of included patients had advanced prostate cancer (43% positive margin rate, 15% positive lymph nodes) with high risk of biochemical recurrence. Thus our results may not apply for patients with lower risk prostate cancer treated with RP such as pT1 tumors. Although all relapses were observed in the first 2 years, recurrences may be observed later in follow-up and alter our results. Moreover, it was not possible to investigate well-known prognostic factors, such as the patient's performance status or seminal vesicle invasion. Determination of the PSA concentrations after the 10th post-operative day were not centralized but performed in different analysis laboratories, using different immunoassay kits. However, the residual variability that includes the intra-individual variability is objectively small (3.5%), suggesting that PSA concentration variations linked to the different assay methods may not have largely influenced our data and results.

On the basis of these results, it is impossible to definitively assert the influence of CL_{PSA} on bRFS. A prospective validation of these results is required. However, this is the second study that suggests this new approach offers a promising method to analyze a biomarker decline profile after/during treatment. A prospective study using the optimal sampling strategy is warranted to confirm the relevance of CL_{PSA} in the treatment of localized prostate cancer after surgery. Moreover, retrospective studies are currently being performed to assess the value-modeled clearance of other tumor biomarkers (hCG, CA-125, AFP, and others).

ACKNOWLEDGMENTS

Pascal Girard is funded by INSERM, France. The authors thank Dr Eric Chen (Princess Margaret Hospital, Toronto, Canada) for help in reviewing the manuscript and Paul Kretchmer (San Francisco Edit) for help in English editing.

REFERENCES

1. Stamey TA, Kabalin JN, McNeal JE, Johnstone IM, Freiha F, Redwine EA, Yang N. Prostate specific antigen in the diagnosis and treatment of adenocarcinoma of the prostate II. Radical prostatectomy treated patients. J Urol 1989;141:1076–1083.
2. Freedland SJ, Sutter ME, Dorey F, Aronson WJ. Defining the ideal cutpoint for determining PSA recurrence after radical prostatectomy. Prostate-specific antigen. Urology 2003;61:365–369.
3. Stephenson AJ, Kattan MW, Eastham JA, Dotan ZA, Bianco FJ Jr, Lilja H, Scardino PT. Defining biochemical recurrence of prostate cancer after radical prostatectomy: a proposal for a standardized definition. J Clin Oncol 2006;24:3973–3978.
4. Han M, Partin AW, Zahurak M, Piantadosi S, Epstein JI, Walsh PC. Biochemical, (prostate specific antigen) recurrence probability following radical prostatectomy for clinically localized prostate cancer. J Urol 2003;169:517–523.
5. Zhou P, Chen MH, McLeod D, Carroll PR, Moul JW, D'Amico AV. Predictors of prostate cancer-specific mortality after radical prostatectomy or radiation therapy. J Clin Oncol 2005;23:6992–6998.
6. Bolla M, van PH, Collette L, van CP, Vekemans K, Da PL, de Reijke TM, Verbaeys A, Bosset JF, van VR, Marechal JM, Scalliet P, Haustermans K, Pierart M. Postoperative radiotherapy after radical prostatectomy: a randomised controlled trial (EORTC trial 22911). Lancet 2005;366:572–578.

7. You B, Perrin P, Freyer G, Ruffion A, Tranchand B, Henin E, Paparel P, Ribba B, Devonec M, Falandry C, Fournel C, Tod M, Girard P. Advantages of prostate-specific antigen (PSA) clearance model over simple PSA half-life computation to describe PSA decrease after prostate adenomectomy. Clin Biochem 2008; 41:785–795.
8. Sheiner LB. The population approach to pharmacokinetic data analysis: rationale and standard data analysis methods. Drug Metab Rev 1984;15:153–171.
9. Beal SL, Sheiner LB, Boeckmann A. NONMEM users guides. Ellicott City, Maryland, USA: Icon Development Solutions, 2006.
10. Brandle E, Hautmann O, Bachem M, Kleinschmidt K, Gottfried HW, Grunert A, Hautmann RE. Serum half-life time determination of free and total prostate-specific antigen following radical prostatectomy–a critical assessment. Urology 1999;53: 722–730.
11. Gregorakis AK, Malovrouvas D, Stefanakis S, Petraki K, Scorilas A. Free/total PSA (F/T ratio) kinetics in patients with clinically localized prostate cancer undergoing radical prostatectomy. Clin Chim Acta 2005;357:196–201.
12. Lein M, Brux B, Jung K, Henke W, Koenig F, Stephan C, Schnorr D, Loening SA. Elimination of serum free and total prostate-specific antigen after radical retropubic prostatectomy. Eur J Clin Chem Clin Biochem 1997;35:591–595.
13. May M, Gunia S, Helke C, Braun KP, Pickenhain S, Hoschke B. Is it possible to provide a prognosis after radical prostatectomy for prostate cancer by means of a PSA regression model? Int J Biol Markers 2005;20:112–118.
14. Iwanicki-Caron I, Di Fiore F, Stetiu M, Tougeron D, Tougeron S, Benichou J, Basuyau J, Michel P. Usefulness of the serum carcinoembryonic antigen kinetic for chemotherapy monitoring in patients with unresectable metastasis of colorectal cancer. J Clin Oncol 2008;26:3681–3686.
15. Riedinger JM, Eche N, Basuyau JP, Dalifard I, Hacene K, Pichon MF. Prognostic value of serum CA 125 bi-exponential decrease during first line paclitaxel/platinum chemotherapy: a French multicentric study. Gynecol Oncol 2008;109:194–198.
16. Brendel K, Dartois C, Comets E, Lemenuel-Diot A, Laveille C, Tranchand B, Girard P, Laffont CM, Mentre F. Are population pharmacokinetic and/or pharmacodynamic models adequately evaluated? A survey of the literature from 2002 to 2004. Clin Pharmacokinet 2007;46:221–234.
17. Dartois C, Brendel K, Comets E, Laffont CM, Laveille C, Tranchand B, Mentre F, Lemenuel-Diot A, Girard P. Overview of model-building strategies in population PK/PD analyses: 2002-2004 literature survey. J Clin Pharmacol 2007;64:603–612.
18. Retout S, Duffull S, Mentre F. Development and implementation of the population Fisher information matrix for the evaluation of population pharmacokinetic designs. Comput Methods Programs Biomed 2001;65:141–151.
19. Haab F, Meulemans A, Boccon-Gibod L, Dauge MC, Delmas V, Boccon-Gibod L. Clearance of serum PSA after open surgery for benign prostatic hypertrophy, radical cystectomy, and radical prostatectomy. Prostate 1995;26:334–338.
20. Oesterling JE, Chan DW, Epstein JI, Kimball AW Jr, Bruzek DJ, Rock RC, Brendler CB, Walsh PC. Prostate specific antigen in the preoperative and postoperative evaluation of localized prostatic cancer treated with radical prostatectomy. J Urol 1988;139:766–772.
21. Ravery V, Meulemans A, Boccon-Gibod L. Clearance of free and total serum PSA after prostatic surgery. Eur Urol 1998;33:251–254.
22. van Straalen JP, Bossens MM, de Reijke TM, Sanders GT. Biological half-life of prostate-specific antigen after radical prostatectomy. Eur J Clin Chem Clin Biochem 1994;32:53–55.
23. Vollmer RT, Humphrey PA. Tumor volume in prostate cancer and serum prostate-specific antigen. Analysis from a kinetic viewpoint. Am J Clin Pathol 2003;119:80–89.
24. Di FG, Zezza A, Nicolai M, Lombardi G, Cipollone G, Iantorno R, Boni R, Tenaglia R. Half-life of blood PSA after radical prostatectomy. Correlations with pathological stage and clinical course of the disease. Arch Ital Urol Androl 1997;69 (Suppl 1) 97–100.
25. Pontes JE, Jabalameli P, Montie J, Foemmel R, Howard PD, Boyett J. Prognostic implications of disappearance rate of biologic markers following radical prostatectomy. Urology 1990;36:415–419.
26. Schaefer U, Witt F, Schueller P, Micke O, Willich N. Prostate-specific antigen (PSA) in the monitoring of prostate cancer after radical prostatectomy and external beam radiation. Anticancer Res 2000;20:4989–4992.
27. Semjonow A, Hamm M, Rathert P. Prediction of tumor recurrence after radical prostatectomy using elimination kinetics of prostate-specific antigen. World J Urol 1993;11:218–220.
28. Brandle E, Gottfried HW, Maier S, Flohr P, Steinbach G, Hautmann RE. Is radical prostatectomy a suitable model for determination of PSA half-life?. Urologe A 1995;34:419–423.

Predictive Value of Modeled $AUC_{AFP\text{-}hCG}$, a Dynamic Kinetic Parameter Characterizing Serum Tumor Marker Decline in Patients With Nonseminomatous Germ Cell Tumor

Benoit You, Ludivine Fronton, Helen Boyle, Jean-Pierre Droz, Pascal Girard, Brigitte Tranchand, Benjamin Ribba, Michel Tod, Sylvie Chabaud, Henri Coquelin, and Aude Fléchon

OBJECTIVE The early decline profile of alpha-fetoprotein (AFP) and human chorionic gonadotropin (hCG) in patients with nonseminomatous germ cell tumors (NSGCT) treated with chemotherapy may be related to the risk of relapse. We assessed the predictive values of areas under the curve of hCG (AUC_{hCG}) and AFP (AUC_{AFP}) of modeled concentration–time equations on progression-free survival (PFS).

METHODS Single-center retrospective analysis of hCG and AFP time-points from 65 patients with IGCCCG intermediate-poor risk NSGCT treated with 4 cycles of bleomycin-etoposide-cisplatin (BEP). To determine AUC_{hCG} and AUC_{AFP} for D0-D42, AUCs for D0-D7 were calculated using the trapezoid rule and AUCs for D7-D42 were calculated using the mathematic integrals of equations modeled with NONMEM. Combining AUC_{AFP} and AUC_{hCG} enabled us to define 2 predictive groups: namely, patients with favorable and unfavorable $AUC_{AFP\text{-}hCG}$. Survival analyses and ROC curves assessed the predictive values of $AUC_{AFP\text{-}hCG}$ groups regarding progression-free survival (PFS) and compared them with those of half-life (HL) and time-to-normalization (TTN).

RESULTS Mono-exponential models best fit the patterns of marker decreases. Patients with a favorable $AUC_{AFP\text{-}hCG}$ had a significantly better PFS (100% vs 71.5%, $P = .014$). ROC curves confirmed the encouraging predictive accuracy of $AUC_{AFP\text{-}hCG}$ against HL or TTN regarding progression risk (ROC AUCs = 79.6 vs 71.9 and 70.2 respectively). Because of the large number of patients with missing data, multivariate analysis could not be performed.

CONCLUSION $AUC_{AFP\text{-}hCG}$ is a dynamic parameter characterizing tumor marker decline in patients with NSGCT during BEP treatment. Its value as a promising predictive factor should be validated. UROLOGY 76: 423–429, 2010. © 2010 Elsevier Inc.

The relevance of initial alpha-fetoprotein (AFP) and/or human chorionic gonadotropin (hCG) concentration measurements in the management of nonseminomatous germ cell tumors (NSGCT), included in the International Germ Cell Cancer Collaborative Group (IGCCCG) prognostic classification, is well established.[1] However the relevance of kinetic analysis of serum tumor marker decrease in NSGCT patients treated with chemotherapy is less clear.[2] Most works that have assessed the predictive value of NSGCT marker kinetics have relied on hCG and/or AFP half-life (HL) calculations. The leading HL-based model, described by Murphy et al,[3] is based on HL_{hCG} and/or HL_{AFP} calculated between day 7 (D7; day 1 was the first day of chemotherapy) and D42-56 (completion of the second cycle of treatment). It was used by the Memorial Sloan-Kettering Cancer Center (MSKCC) in 2 dose densification clinical trials.[3-5] Recently, Fizazi et al reported the independent predictive value of marker time to normalization (TTN), a kinetic parameter very similar to HL, on progression-free survival (PFS).[6] Yet these studies may be limited by the methodology used to characterize serum tumor

Presented in part at the American Society of Clinical Oncology Annual Meeting, May 29-June 2, 2009, Orlando, FL (Abstract 5085).

From the Université de Lyon, Lyon, France; Faculté de Médecine Lyon Sud, Oullins, France; Service d'Oncologie Médicale, Centre Hospitalier Lyon Sud, Hospices Civils de Lyon, Pierre-Bénite, France; Princess Margaret Hospital, Drug Development Program, Toronto, Ontario, Canada; Département de Médecine, Département d'Oncologie Médicale, Centre Léon Bérard, Lyon, France; Centre Léon Bérard, Lyon, France; INRIA Grenoble, Rhône-Alpes, Saint Ismier Cedex, France; Unité de Biostatistiques et d'Evaluation thérapeutique, Centre Léon Bérard, Lyon, France; and Service de Biologie Médicale, Hôpital Saint Joseph-Saint Luc, Lyon, France

Reprint requests: Benoit You, M.D., Ph.D., Centre Hospitalier Lyon Sud, Service d'oncologie médicale, 69495, Pierre-Benite, France. E-mail: benoit.you@chu-lyon.fr

Submitted: October 28, 2009, accepted with revisions: February 15, 2010

0090-4295/10/$34.00
doi:10.1016/j.urology.2010.02.049

Table 1. Patient characteristics and available data*

Patient Characteristics According to IGCCCG Risk Grouping	Intermediate (n = 38)		Poor (n = 27)	
Covariates	No. of Patients	% of Patients	No. of Patients	% of Patients
Primary site				
Testis + retroperitoneum	38	100	16	59.2
Mediastinum	0	0	11	40.7
Visceral metastases other than lung metastases	0	0	10	37.0
Lung metastasis	16	42.1	15	55.5
LDH (ULN)				
<1.5	9	23.6	7	25.9
1.5-10	28	73.7	17	62.3
>10	0	0	3	11.1
Missing†	1	2.6		
AFP between day 7 and day 0 (AFP_{J0}) (IU/mL)				
Available†	32		26	
Abnormal	23	84.2	18	96.3
Median of abnormal AFP_{J0}	365.9	71.9	1995.7	69.2
Range	[12.1-6625.3]		[42.1-66,777]	
hCG between day 7 and day 0 (hCG_{J0}) (IU/L) available†	31		26	
Abnormal	22	81.5	16	96.3
Median of abnormal hCG_{J0}	1002.5	70.9	1375.05	61.5
Range	[20-24,296]		[16.1-753,758]	
Total number of available hCG time-points per patient				
Median	13		12	
Range	[4-23]		[2-30]	
Total number of available AFP time-points per patient				
Median	14		12.5	
Range	[4-23]		[6-29]	
Number of available hCG time-points per patient between day 7 and day 42	5 [2-8]		5 [2-11]	
Number of available AFP time-points per patient between day 7 and day 42	5 [2-8]		5 [2-11]	

Abbreviations: IGCCCG, International Germ Cell Cancer Collaborative Group; LDH, lactate dehydrogenase; ULN, upper limit of normal; AFP, alpha-fetoprotein; hCG, human chorionic gonadotropin.

* When hCG and AFP concentrations were unavailable in the week before the start of chemotherapy (19% and 4% patients in intermediate-risk and poor-risk groups, respectively), serum tumor marker levels measured more than 1 week before beginning the BEP regimen were used to classify patient into ICCCCG groups.

† Patient was classified into the intermediate risk group by his physician on the basis of LDH measured in the physician's private office laboratory.

‡ When not available, hCG and AFP measured more than 1 week before chemotherapy were used to classify patients into the IGCCCG group.

marker decreases, as suggested by the large heterogeneity in the reported kinetic parameter results and their predictive values.[2,6-11]

We propose a population kinetic approach, relying on modeling and pharmacokinetic principles, to assess individual serum tumor marker decreases dynamically in NSGCT patients treated with chemotherapy. In previous works involving prostate-specific antigen (PSA) in patients with prostate tumors treated with surgery[12,13] and hCG in patients with trophoblastic tumors treated with methotrexate,[14] we showed that this method was superior to other traditional approaches. It combines all patient time-points to model a population decline profile, quantifies inter- and intraindividual variability, and then determines the individual decline curve equations. Using this method, it might possible to calculate individual areas under the curve (AUCs) for hCG and AFP (AUC_{hCG} and AUC_{AFP}, respectively) for each patient. We postulated that AUCs, which are independent of selected marker time-points, would predict more accurately the disease progression risk.

We performed a retrospective analysis of hCG and/or AFP declines in patients with intermediate or poor risk NSGCT who were treated with the standard 4 cycles of bleomycin-etoposide-cisplatin (BEP), to assess the feasibility of characterizing individual serum tumor marker decrease profiles using AUC_{AFP} and AUC_{hCG}. In addition, we performed survival and receiver operating characteristic (ROC) curve analyses to assess the predictive values of AUC_{AFP} and AUC_{hCG} regarding 2-year PFS.

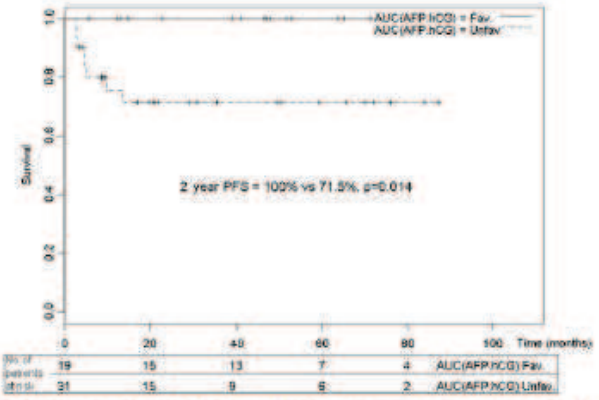

Figure 1. Kaplan–Meier Curve of probability of progression-free survival (PFS) according to patient $AUC_{AFP\text{-}hCG}$ grouping (Favorable (Fav) vs Unfavorable (Unfav)).

PATIENTS AND METHODS

Patients

We reviewed data of all patients treated with 4 cycles of BEP for IGCCCG intermediate- or poor-risk group NSGCT at the Centre Léon Bérard of Lyon (France) after January 1997. To be enrolled in our retrospective study, patients were required to have been treated for NSGCT with 4 cycles of BEP and to have had a minimum of 2 abnormal titers of either tumor markers (hCG >5 IU/mL and/or AFP >5 IU/L) between D0 (first day of cycle 1) and D42 (first day of cycle 3). No time limit was fixed for the patient serum tumor marker follow-up. Concentrations of hCG and AFP were centrally determined. Imaging assessments with computed tomography (CT) scans were performed after 2 and 4 cycles of chemotherapy. Because there are no recommendations regarding the optimal sampling strategy of NSGCT tumor markers, times of sampling of AFP and hCG were chosen at the treating physicians' discretion. Measurements were usually made every week.

Serum Tumor Marker Kinetic Analysis

Kinetic models were built using marker concentrations assayed between the week before chemotherapy (assumed to be baseline serum tumor marker concentration on D0) and D42. Indeed, determining progression risk during the first 2 courses of chemotherapy would provide enough time to adapt treatment in patients with a high risk of failure.

Because 25%-41% patients treated with chemotherapy present a transient surge during first week of treatment,[15,16] we considered patient marker kinetic profiles in 2 separate parts: (1) marker kinetics during the first week were analyzed as a straight line from D0 to D7, and (2) the exponential decreases between D7 and D42 were modeled.

Modeling of Marker Decline Curves Between D7 and D42

Population mixed-effects modeling was applied to fit hCG and AFP decline curves between D7 and D42 according to 1- or 2-compartment models. Thus, 2 independent models were built, 1 for hCG decrease and 1 for AFP decrease (See Appendix online). The analysis was performed using NONMEM to estimate the population parameters (mean and intersubject variability) and the residual variability using the first-order conditional estimation method with interaction (FOCE interaction). Furthermore, it was used to identify potential covariates to explain intersubject variability in the parameters:[17] mediastinal site of primary disease (yes/no), lung metastasis (yes/no), visceral metastasis other than lung metastases (yes/no), initial LDH value, IGCCCG prognostic group (intermediate/poor), and duration between first and second chemotherapy cycles. The modeling methodology has been explained in detail elsewhere.[12] When a covariate demonstrated a significant relationship with any kinetic parameter, it was introduced into the model describing the fixed effects by forward inclusion.

Calculation of AUCs for hCG and/or AFP (AUC_{AFP} and AUC_{hCG})

The total AUC between D0 and D42 was the sum of the 2 subparts of the curve, as described below.

1. AUC between D0 and D7 was calculated using the trapezoid rule (area = 0.5 × base × (H + h)), where that base is equal to 7 days, h is the observed serum tumor marker value on D0, and H is the observed marker value on D7.
2. AUC between D7 and D42 ($AUC_{7\text{-}42}$) was derived by calculating the mathematic integral of the patient-modeled concentration-time curve equation. For example, if $C(t) = A\,e^{-\alpha * t} + B$ (see eq. 1), then $AUC_{7\text{-}42} = (A/\alpha) * A\,e^{-\alpha * 42} + B \times 42 + (A/\alpha) \times A\,e^{-\alpha * 7} - B \times 7$.

Model Internal Validation

We simulated 500 decline profiles for hCG and AFP using the final parameters estimated from the corresponding best models. To qualify these models, visual and predictive checks were used to compare the titers as well as the distribution of observed hCG and AFP to those of the corresponding simulated dataset[18] (See Appendix online).

Other Kinetic Parameters

Times to Normalization. TTN_{AFP} and TTN_{hCG} as well as patient prognostic groups ($TTN_{AFP\text{-}hCG}$: favorable vs unfavorable) were calculated for every patient[2,6] (See Appendix online).

Decrease in Half-Lives. Both HL_{AFP} and HL_{hCG} between D7 and D42 were calculated with the decline exponentials derived from the models. As well, patients were classified into 2 prognostic groups (satisfactory or unsatisfactory $HL_{AFP\text{-}hCG}$) according to HL_{AFP} and HL_{hCG} results[3] (See Appendix online).

Statistical Analysis

The primary endpoint of the study was PFS, calculated as the time elapsed from D0 to the first event, such as the patient death, clinical relapse, or date of last follow-up for patients who were alive and who did not experience relapse. Log-ranks tests were used to assess the prognostic value of potential factors regarding PFS, comprising items included in the IGCCCG prognosis score, duration between first and second chemotherapy cycles, transient serum tumor marker surge after start of chemotherapy, and marker kinetic parameters ($TTN_{AFP\text{-}hCG}$, $HL_{AFP\text{-}hCG}$ and $AUC_{AFP\text{-}hCG}$). Because log-rank test requires categorical data, the continuous covariates, such as AUC_{AFP} and AUC_{hCG}, were split into 2 groups and 3 groups according to the median and the tertiles, respectively. Patients with a higher serum tumor marker AUCs were expected to have worse outcomes. If a clear continuous predictive value was identified for AUC_{hCG} tertiles, the predictive value of AUC_{AFP} was binary and

Table 2. Analysis of kinetic parameters for alpha-fetoprotein (AFP) and human chorionic gonadotropin (hCG)

Parameter	Median	No. of Patients	First Quartile	Fourth Quartile
AUC_{hCG} (IU d/L)	12396.3	38	4216.0	70424.2
AUC_{hCG0-7}	4688.0	45	994.0	22720.0
$AUC_{hCG7-42}$	7551.4	48	1086.2	20895.4
AUC_{AFP} (IU d/mL)	11729.4	40	634.3	41960.8
AUC_{AFP0-7}	4640.6	42	449.2	20795.7
$AUC_{AFP7-42}$	3193.1	47	284.9	21312.0
TTN_{hCG}	4.70	37	3.28	6.22
TTN_{AFP} (weeks)	6.64	41	4.61	12.26
$HL_{AFP7-42}$	5.02	47	4.52	5.62
$HL_{hCG7-42}$ (days)	2.77	45	2.71	2.85

Abbreviations: AUC, area under the curve; TTN, time to normalization; HL, half-life.

discriminated by median. Hence, 2 predictive groups were built for combining AUC_{AFP} and AUC_{hCG} ($AUC_{AFP-hCG}$): favorable $AUC_{AFP-hCG}$ for patients with $AUC_{AFP} \leq$ median value and with $AUC_{hCG} \leq$ upper tertile value; and unfavorable $AUC_{AFP-hCG}$ for patients with AUC_{AFP} > median value and/or with AUC_{hCG} > upper tertile value.

When patients had normal AFP or normal hCG, the AUC value of the non-normal parameter determined the predictive group. Of note, among 47 patients for whom both AFP and hCG were available, 20 patients (42.5%) had normal titers for 1 marker, whereas concentrations the other marker were elevated.

To test the independence of potential predictive factors considered together, we initially planned to perform a multivariate analysis with the predictive factors found to be significant by univariate analysis ($P < .1$). However, because of the retrospective study design, data for several covariates were missing, and only a small number of patients were assessable in the Cox model (n = 34 patients without any missing data for all covariates, including 5 progression events). Because the results would not have been interpretable, we decided not to perform this analysis.

All tests were performed using the S-PLUS program with a two-sided 0.05 alpha risk. To assess accuracies of $AUC_{AFP-hCG}$ (unfavorable vs favorable risk group), $HL_{hCG-AFP}$ (unsatisfactory vs satisfactory), and $TTN_{hCG-AFP}$ (unfavorable vs favorable) for predicting progression risk, we calculated ROC curves using TANAGRA.

RESULTS

Patients and Follow-up

A total of 456AFP and 259 hCG values from 65 patients who were treated with 4 cycles of BEP between February 1997 and June 2008 were analyzed. Medians of 12 hCG and 12 AFP values per patient were available at various times, from 143 days before the start of treatment (D-143) to 1875 days after the start of chemotherapy (D1875). For serum tumor marker modeling, medians of 5 hCG and 5 AFP values per patient were available between D7 and D42. The median follow-up was 939 days (equivalent to 2.6 years). Patient characteristics are presented in Table 1.

Modeling AFP and hCG Decreases Between D7 and D42

Mono-compartmental models with block matrix best described AFP and hCG decreases between D7 and D42. For both markers, bi-compartmental models did not allow significant reduction of unexplained interindividual variability of the kinetic parameter estimates. No individual covariates were significant for influencing either marker decline profile. The final population models were: as follows: $C_{AFP.7-42}(t) = 381 \times e - 0.14 * t + 3.27$ and $C_{hCG.7-42}(t) = 1230 \times e - 0.25 * t + 1.22$, where $C_{AFP.7-42}(t)$ is the population-predicted AFP value at time t (days) between D7 and D42 (IU/mL) and $C_{hCG.7-42}(t)$ is the population-predicted hCG value at time t (days) between D7 and D42 (IU/L).

Results of population parameter estimates, interindividual variability, standard errors, and residual variability are presented in Table 4 in the Appendix. Figure 1 shows time-plots of predicted hCG/AFP versus observed hCG/AFP for 4 typical patients, including 2 patients who experienced clinical relapse.

Calculating AUCAFP and AUChCG Between D0 and D42

Results for all kinetic parameters are shown in Table 2.

Internal Model Validation

Figure 2 in the Appendix shows the visual comparison of the 95% CIs of simulated marker titers to the observed ones. Regarding the statistical predictive checks, all observed hCG and AFP values fell within the 95% confidence interval bounds of the simulated values, confirming the model's ability to predict the first portion of the NSGCT marker decline curve as well as its slope decrease (data not shown).

Survival Analysis

All patients were included in the 2-year PFS analysis. Nine patients (13.8%) experienced disease progression after a median of 146 days (range, 84-1351 days) and 6 patients (9.2%) had died as of February 2009. No patients experienced progression during the first 2 cycles of chemotherapy.

Table 3 presents the results of univariate analysis using the log-rank test. Neither AUC_{hCG} nor AUC_{AFP} were significantly predictive of progression when considered alone. However, the combination factor $AUC_{AFP-hCG}$ (favorable vs unfavorable risk) was significantly predic-

Table 3. Results of univariate analysis with log-rank test

Covariate	Status	No. of Patients	2-y PFS (%)	*P* Value
Primary site				.0007
Mediastinum vs	Yes	11	48.5	
Testis + retroperitoneum	No	54	90.2	
Lung metastasis	Yes	31	79.2	.52
	No	34	87.5	
Nonlung metastases	Yes	10	77.8	.72
	No	55	84.6	
LDH (*ULN)	<1.5	16	100	.31
	1.5-10	45	86.0	
	>10	3	75.0	
Initial AFP values (ng/mL)	<1000	23	91.3	.24
	1000-10,000	18	81.2	
	>10,000	2	50.0	
Initial hCG values (IU/L)	<5000	32	80.8	.47
	5000-50,000	2	100	
	>50,000	6	62.5	
IGCCCG prognosis	Intermediate	38	94.3	.006
	Poor	27	67.0	
Time interval between first and second BEP cycles (days)	≤21	50	85.2	.79
	>21	15	78.8	
hCG surge in the first week	yes	11	75.0	.66
	No	30	81.1	
AFP surge in the first week	yes	13	75.0	.30
	No	29	88.8	
AUC_{hCG} tertiles	≤6,669.7	14	92.3	.17
Median 12,207 (IU d/L)	6,669.7-18,178.4	11	90.9	
	>18,178.4	13	67.7	
AUC_{AFP} tertiles	≤2,265.5	13	100	.34
Median 11,729.4 (IU d/mL)	2,265.5-26,791.7	13	83.9	
	>26,791.7	14	74.3	
AUC_{AFP} tertiles	≤11,729.4	20	95.0	.15
Median 11,729.4 (IU d/mL)	>11,729.4	20	76.9	
$AUC_{AFP-hCG}$ prognostic groups				.014
$AUC_{hCG} \leq 18,178.4$ and $AUC_{AFP} \leq 11,729.4$	Favorable	19	100	
$AUC_{hCG} > 18,178.4$ and/or $AUC_{AFP} > 11,729.4$	Unfavorable	31	71.5	
TTN_{hCG} (weeks)	≤9	28	89.1	.15
	>9	10	67.5	
TTN_{AFP} (weeks)	≤6	25	92.0	.14
	>6	17	72.2	
$TTN_{AFP-hCG}$ prognostic groups	Favorable	29	89.3	.13
	Unfavorable	23	69.1	
HL_{hCG} (days)	≤3	43	85.2	.09
	>3	2	50.0	
HL_{AFP} (days)	≤7	43	89.8	.29
	>7	4	75.0	
$HL_{AFP-hCG}$ prognostic groups	Satisfactory	31	84.9	.07
	Unsatisfactory	6	66.7	

Abbreviations: LDH, lactate dehydrogenase; ULN, upper limit of normal; AFP, alpha-fetoprotein; hCG, human chorionic gonadotropin; IGCCCG, International Germ Cell Cancer Collaborative Group; BEP, bleomycin-etoposide-cisplatin; AUC, area under the curve; TTN, time to normalization; HL, half-life.

tive in univariate analysis. The 2 year PFS was 100% for patients in the favorable risk group against 71.5% for those in the unfavorable risk group ($P = .014$; Fig. 1).

With a sensitivity of 100%, specificity of 45.2%, negative predictive value (NPV) of 100%, and ROC AUC of 79.6, the predictive value of $AUC_{AFP-hCG}$ (unfavorable vs favorable risk) for identifying patients at high risk for progression looked encouraging against the other predictive factors previously described. Indeed, $HL_{AFP-hCG}$ ROC AUC (satisfactory vs unsatisfactory) was 71.9 (sensitivity 88.9%, specificity 44.0%, NPV 95.6%) and $TTN_{AFP-hCG}$ ROC AUC (favorable vs unfavorable) was 70.2 (sensitivity 40.0%, specificity 87.5%, NPV 90.3%) (Fig. 3 in the online Appendix).

COMMENT

Analysis of NSGCT serum tumor marker kinetics during chemotherapy as a reflection of tumor cell chemosensitivity is not novel. The common HL and TTN approaches may present several limitations: (a) simplification of complex hCG and AFP decline kinetics

(including initial surges in 25% of patients) by calculating the median decline slopes between 2 time-points prone to high intra- and interindividual variability[2,6-11]; (b) high interstudy variability in the time-points used to assess NSGCT marker kinetics (D0 and D21 in Fizazi et al,[6] D7 to D42-56 in Murphy et al,[3] D7 and D56 in Mazumdar et al,[9] D7 to another time-point before D90 in Toner et al[10]); (c) no assessment of inter- and intraindividual variability. The consequent heterogeneity of HL-based results, along with their predictive values,[2,7-11] may be of concern when these kinetic parameters are used to adapt treatment. The predictive value of hCG TTN initially reported in 2004 was not confirmed in an independent cohort of NSGCT.[19] In addition, a Scandinavian trial reported disappointing results of treatment intensification in poor IGCCCG risk patients presenting with long marker HL.[20]

The approach that we used, relying on mathematic and computational modeling, allowed the dynamic characterization of the individual marker decline profile, independently on selected time-points. Combining both hCG and AFP AUCs enabled us to determine 2 potential predictive groups. All patients within the $AUC_{AFP\text{-}hCG}$ favorable risk group (defined by low AUC_{AFP} and low AUC_{hCG}) were progression-free at 2 years, whereas patients classified into the unfavorable $AUC_{AFP\text{-}hCG}$ group had a 28.5% risk of relapse at 2 years. Unfortunately, the large number of missing data for the different covariates, owing to the retrospective study design, did not allow us to test the independence of each in a multivariate Cox model. Indeed, a minimum of 4 time-points were required to model the whole marker decrease between D0 and D42: baseline value, D7 value, and 2 values between D7 and D42. If either of the first 2 time-points was missing, we could not assess the whole AUC, but we still could model the decline profile from D7 to D42. These requirements were not met for many patients because of the absence of recommended NSGCT marker sampling strategy, may explain the high number of missing data and heterogeneity in table cohort sizes. Another study that includes a larger number of patients is needed to confirm this hypothesis. If the predictive value of $AUC_{AFP\text{-}hCG}$ were confirmed, this model could be used to identify patients who might benefit from early treatment adaptation. These results may have potential practical and clinical applications. Indeed, hCG and AFP concentrations obtained at appropriate times (D0, D7, D21, and D42) could be entered into a model-based software application that would immediately determine the patient's $AUC_{AFP\text{-}hCG}$ predictive group. ROC curve analyses indicated that $AUC_{AFP\text{-}hCG}$ groupings (nonfavorable vs favorable risk) might be predictive of outcome with both high sensitivity and a high NPV.

Because this was a nonrandomized study of a selected group of patients with IGCCCG intermediate-poor risk NSGCT and abnormal titers of at least 1 serum tumor marker and in which only 9 progression events occurred, the results should be interpreted with caution. The results might not be applicable to other populations of patients with NSGCT. In particular, the high proportion of patients (17%) with mediastinum disease might be linked to the reference center nature of Centre Léon Bérard for treatment of NSGCT and to the study inclusion criteria. Although orchiectomy, performed before chemotherapy, might have also contributed in tumor marker decline before the start of chemotherapy, its effect was not directly measured in our assessment. We considered starting of hCG/AFP decline analysis on D0 of chemotherapy was the only way to standardize patients so that their tumor marker decreases could be compared.

Furthermore, the residual variability was nonnegligible, suggesting that an important part of interindividual variability remained unexplained by our models. We did not assess the impact of $AUC_{AFP\text{-}hCG}$ on tumor response rates because the PFS seemed clinically more relevant with respect to the data available in the literature.[0,6]

CONCLUSIONS

Our results suggest that population kinetic modeling may be a promising method for analyzing hCG and AFP decline profiles during the treatment of patients with intermediate- and poor-risk NSGCT. This modeling approach needs to be validated in a larger trial.

Acknowledgments. Pascal Girard is funded by INSERM, France. The authors thank Paul Kretchmer (San Francisco Edit) for help in English editing.

References

1. International Germ Cell Consensus Classification: a prognostic factor-based staging system for metastatic germ cell cancers. International Germ Cell Cancer Collaborative Group. *J Clin Oncol* 1997;15:594-603.
2. Toner GC. Early identification of therapeutic failure in nonseminomatous germ cell tumors by assessing serum tumor marker decline during chemotherapy: still not ready for routine clinical use. *J Clin Oncol.* 2004;22:3842-3845.
3. Murphy BA, Motzer RJ, Mazumdar M, et al. Serum tumor marker decline is an early predictor of treatment outcome in germ cell tumor patients treated with cisplatin and ifosfamide salvage chemotherapy. *Cancer.* 1994;73:2520-2526.
4. Motzer RJ, Mazumdar M, Gulati SC, et al. Phase II trial of high-dose carboplatin and etoposide with autologous bone marrow transplantation in first-line therapy for patients with poor-risk germ cell tumors. *J Natl Cancer Inst.* 1993;85:1828-1835.
5. Motzer RJ, Mazumdar M, Bajorin DF, et al. High-dose carboplatin, etoposide, and cyclophosphamide with autologous bone marrow transplantation in first-line therapy for patients with poor-risk germ cell tumors. *J Clin Oncol.* 1997;15:2546-2552.
6. Fizazi K, Culine S, Kramar A, et al. Early predicted time to normalization of tumor markers predicts outcome in poor-prognosis nonseminomatous germ cell tumors. *J Clin Oncol.* 2004;22:3868-3876.
7. de Wit R, Sylvester R, Tsitsa C, et al. Tumour marker concentration at the start of chemotherapy is a stronger predictor of treatment failure than marker half-life: a study in patients with disseminated non-seminomatous testicular cancer. *Br J Cancer* 1997;75:432-435.
8. Inanc SE, Meral R, Darendeliler E, et al. Prognostic significance of marker half-life during chemotherapy in non-seminomatous germ cell testicular tumors. *Acta Oncol.* 1999;38:505-509.

9. Mazumdar M, Bajorin DF, Bacik J, et al. Predicting outcome to chemotherapy in patients with germ cell tumors: the value of the rate of decline of human chorionic gonadotrophin and alpha-fetoprotein during therapy. *J Clin Oncol*. 2001;19:2534-2541.
10. Toner GC, Geller NL, Tan C, et al. Serum tumor marker half-life during chemotherapy allows early prediction of complete response and survival in nonseminomatous germ cell tumors. *Cancer Res*. 1990;50:5904-5910.
11. Willemse PH, Sleijfer DT, Schraffordt KH, et al. The value of AFP and HCG half lives in predicting the efficacy of combination chemotherapy in patients with non-seminomatous germ cell tumors of the testis. *Oncodev Biol Med*. 1981;2:129-134.
12. You B, Perrin P, Freyer G, et al. Advantages of prostate-specific antigen (PSA) clearance model over simple PSA half-life computation to describe PSA decrease after prostate adenomectomy. *Clin Biochem*. 2008;41:785-795.
13. You B, Girard P, Paparel P, et al. Prognostic value of modeled PSA clearance on biochemical relapse free survival after radical prostatectomy. *Prostate*. 2009;69:1325-1333.
14. You B, Pollet-Villard M, Boyle H, et al. Predictive values of hCG clearance for risk of methotrexate resistance in low-risk gestational trophoblastic neoplasias. *Ann Oncol*. (in press, doi: 10.1093/annonc/mdq033).
15. de Wit R, Collette L, Sylvester R, et al. Serum alpha-fetoprotein surge after the initiation of chemotherapy for non-seminomatous testicular cancer has an adverse prognostic significance. *Br J Cancer* 1998;78:1350-1355.
16. Horwich A, Peckham MJ. Transient tumor marker elevation following chemotherapy for germ cell tumors of the testis. *Cancer Treat Rep*. 1986;70:1329-1331.
17. Beal SL, Sheiner LB, Boeckmann A. NONMEM users guides. Icon Development Solutions, Ellicott City, MD; 2006.
18. Yano Y, Beal SL, Sheiner LB. Evaluating pharmacokinetic/pharmacodynamic models using the posterior predictive check. *J Pharmacokinet Pharmacodyn*. 2001;28:171-192.
19. Massard C, Huguet H, Kramar A, et al. Cross-validation of new prognostic index integrating tumor marker decline in patients with relapsed disseminated germ cell tumors. Proc Am Soc Clin Oncol 2009. *J Clin Oncol*. 2009(Suppl):27:5086.
20. Olofsson S, Dahl O, Jerkeman M, et al. Individualized intensification of treatment based on tumor marker decline in metastatic nonseminomatous germ cell testicular cancer (NSGCT): A report from the Swedish Norwegian Testicular Group, SWENOTECA. Proc Am Soc Clin Oncol 2009. *J Clin Oncol*. 2009(Suppl):27:5015.

Appendix (on-line only)

Modeling of Marker Decline Curves Between D7 and D42

Mono-exponential models were implemented with the following equation:

$$C_{ij}(t) = (A_i \times e^{-Ki*t} + B) * \varepsilon_{ij} \quad \text{(eq. 1)}$$

Biexponential models were implemented using the following equation:

$$C_{ij}(t) = (A_i \times e^{-\alpha i*t} + B_i \times e^{-\beta i*t} + C) * \varepsilon_{ij} \quad \text{(eq. 2)}$$

where C_{ij} (t) is the jth measurement of marker in patient i at time t, ε_{ij} accounts for the proportional residual variability of patient i at jth measurement, for which the mean is zero and the variance is σ^2. Parameters A_i, B_i, K_i, α_i, β_i, B_i and C were assumed to vary randomly among patients according to a log-normal distribution.

Validation of the Models

Two methods of qualification were used.[18]

Visual Predictive Check

Observed hCG and AFP values were compared with the 95% confidence intervals (CI) of corresponding markers from the 500 simulated replicates.

Statistical Predictive Check

Distributions of hCG and AFP computed from the simulated dataset were compared with the corresponding observed statistics. These statistics involved prediction of the 2 parts of marker decline curves:

1. The initial portion, defined as the first hCG or AFP before day 5.
2. The curve slope (calculated as slope = first marker value − last marker value / change in time). Distribution histograms of the lower quartiles, medians, and upper quartiles of simulated values were drawn with their 95% CIs. The model was considered predictive of the decline curve if all corresponding observed values were within the 95% CIs of simulated values.

2. Other kinetic parameters
   a. Times to normalization (TTN). Fizazi et al described the method of calculating TTN:[5,6] $TTN_{AFP} = 3* (\log(AFP_0) - \log(AFP_n)/(\log(AFP_0) - \log(AFP_{21}))$, where AFP_0 is the AFP value in the week before the first day of the first cycle of chemotherapy, AFP_n is the upper limit of normal range of AFP, and AFP_{21} is the AFP value measured between D18 and D28. Thus, we calculated the TTN_{AFP} and TTN_{hCG} for every patient and determined their combined predictive group as described by Fizazi et al. ($TTN_{AFP\text{-}hCG}$: favorable vs unfavorable).[6]
   b. Half-lives (HL). In MSKCC studies, Murphy et al. reported the prognostic value of AFP and hCG HL calculated between D7 and D42.[3] We calculated both HL_{AFP} and HL_{hCG} between D7 and D42 using the decline exponentials derived from the models. For instance, if AFP were fit by the equation $C_{AFP}(t) = AFP1\ e - K^* t + AFP2$, then $HL_{AFP} = Ln(2)/K$; we could calculate HL_{AFP} and HL_{hCG} for every patient. Two potential predictive groups were determined ($HL_{AFP,hCG}$): a satisfactory group, with patients with $HL_{AFP} \leq 7$ days and $HL_{hCG} \leq 3$ days; and an unsatisfactory group, with patients with $HL_{AFP} > 7$ days and/or $HL_{hCG} > 3$ days.[3]

Table 4. Results of modeling of alpha-fetoprotein (AFP) and human chorionic gonadotropin (hCG) decline curves between day 7 and day 42

Model Parameter	Modeled Population Post Hoc Value	Interindividual Variability (CV %)	Standard Error (CV %)	Residual Variability (CV %)
AFP_1	381.00	261	39.0	21.2
AFP_{res}	3.27	30	28.0	
K1 (AFP)	0.14	24	4.8	
hCG_1	1230.00	254	40.8	42.5
hCG_{res}	1.22	278	49.1	
K1 (hCG)	0.25	4	3.0	

Abbreviations: CV, coefficient of variation; K1 (AFP), exponential decrease constant in AFP between day 7 and day 42; K1 (AFP), exponential decrease constant in hCG between day 7 and day 42.

Annals of Oncology Advance Access published February 12, 2010

original article

Annals of Oncology
doi:10.1093/annonc/mdq033

Predictive values of hCG clearance for risk of methotrexate resistance in low-risk gestational trophoblastic neoplasias

B. You[1,2,3,4*], M. Pollet-Villard[1,2,5,6], L. Fronton[1,2], C. Labrousse[1,2,5,6], A.-M. Schott[1,2,7,8], T. Hajri[1,2,5,6], P. Girard[1,2], G. Freyer[1,2,3], M. Tod[1,2], B. Tranchand[1,2,9], O. Colomban[1,2], B. Ribba[1,2,10], D. Raudrant[1,2,5,6], J. Massardier[1,2,5,6], S. Chabaud[11] & F. Golfier[1,2,5,6]

[1]EA 3738, Université de Lyon, Lyon; [2]Université Lyon 1, Faculté de Médecine Lyon Sud, Oullins; [3]Medical Oncology Department, Hospices Civils de Lyon, Centre Hospitalier Lyon Sud, Pierre-Bénite, France; [4]Medical Oncology Department, Drug Development Program, Princess Margaret Hospital, Toronto, Ontario, Canada; [5]Gynecology-Obstetrics Department, Hospices Civils de Lyon, Hôtel Dieu, Centre de Référence des Maladies Trophoblastiques, Lyon; [6]Hospices Civils de Lyon, Centre Hospitalier Lyon Sud, Pierre Bénite; [7]EA 4129, Université Lyon 1; [8]Hospices Civils de Lyon, Réseau d'Epidémiologie Clinique International Francophone, Lyon; [9]Centre Anticancéreux Léon Bérard, Lyon; [10]INRIA Grenoble Rhône-Alpes, Montbonnot, Saint Ismier Cedex and [11]Biostatics Department, Unité de Biostatistique et d'évaluation thérapeutique, Centre Anticancereux Léon Bérard, Lyon, France

Received 29 September 2009; revised 8 December 2009; accepted 8 January 2010

Background: Early identification of patients at high risk for chemoresistance among those treated with methotrexate (MTX) for low-risk gestational trophoblastic neoplasia (GTN) is needed. We modeled human chorionic gonadotropin (hCG) decline during MTX therapy using a kinetic population approach to calculate individual hCG clearance (CL_{hCG}) and assessed the predictive value of CL_{hCG} for MTX resistance.

Patients and methods: A total of 154 patients with low-risk GTN treated with 8-day MTX regimen were retrospectively studied. NONMEM™ was used to model hCG decrease equations between day 0 and day 40 of chemotherapy. Receiver operating characteristic curve analysis defined the best CL_{hCG} threshold. Univariate/multivariate survival analyses determined the predictive value of CL_{hCG} and compared it with published predictive factors.

Results: A monoexponential equation best modeled hCG decrease: $hCG(t) = 3900 \times e^{-0.149 \times t}$. Median CL_{hCG} was 0.57 l/day (quartiles: 0.37–0.74). Only choriocarcinoma pathology [yes versus no: hazard ratio (HR) = 6.01; 95% confidence interval (CI) 2.2–16.6; $P < 0.001$] and unfavorable CL_{hCG} quartile (≤0.37 versus >0.37 l/day: HR = 6.75; 95% CI 2.7–16.8; $P < 0.001$) were significant independent predictive factors of MTX resistance risk.

Conclusion: In the second largest cohort of low-risk GTN patients reported to date, choriocarcinoma pathology and CL_{hCG} ≤0.37 l/day were major independent predictive factors for MTX resistance risk.

Key words: kinetics, methotrexate, predictive value of tests, biological serum tumor markers, survival analysis, trophoblastic neoplasms

introduction

In 2002, the International Federation of Gynecology and Obstetrics (FIGO) committee classified gestational trophoblastic neoplasias (GTN) as high-risk and low-risk tumors according to the risk of relapse. Classification into one of these two groups is determined by a combination of eight prognostic factors graded from 0 to 4 [1, 2]. In France, low-risk tumors, characterized by a FIGO score ≤6, are commonly treated with monotherapy, usually the 8-day methotrexate (MTX) regimen modified by Bagshawe et al. and Chalouhi et al. [3, 4]. In cases of MTX resistance or intolerance, patients are switched to actinomycin D (ACT-D) or to etoposide, methotrexate, actinomycin, cyclophosphamide, and vincristine regimen (EMA-CO) regimens, including ACT-D, etoposide, methotrexate, and folinic acid [5]. Although tumor chemoresistance is often defined as an increase or stagnation of human chorionic gonadotropin (hCG) levels over a 2- to 3-week period, there are no clear guidelines concerning the optimal method for analyzing hCG kinetics [5]. Identification of predictive factors that could provide early information about the risk of MTX resistance would be useful [5].

Recently, authors have proposed hCG titer thresholds as potential predictive factors of chemoresistance. Using hCG

*Correspondence to: Dr B. You, Medical Oncology Department, Drug Development Program, Princess Margaret Hospital, 610 University Avenue, Toronto, Ontario, Canada M5G 2M9. Tel: +1-416-531-8557; Fax: +1-416-946-4607; E-mail: benoit.you@laposte.net, benoit.you@chu-lyon.fr, benoit.you@uhn.on.ca

decline corridors and receiver operating characteristic (ROC) analyses, hCG cut-offs measured during the seventh week of MTX therapy were proposed: 56 μg/l equivalent to 520.24 mIU/ml in Van Trommel et al. [6], 737 mIU/ml in Kerkmeijer et al. [7], and 500 mIU/ml in Savage et al. [8] studies. These studies might have been limited by the methodology used to characterize hCG decreases, especially by their dependence on a single time point prone to high inter/intraindividual variability. It may explain the heterogeneity in the reported cut-offs.

Herein, we propose a population kinetic approach, relying on modeling and pharmacokinetic principles [9], to assess individual hCG decrease profiles dynamically. Application of this method has been described for kinetic assessment of other tumor markers [10–12]. Briefly, combining all patient time points allows to model a population decline profile, to quantify inter- and intraindividual variability, and to determine the individual decline curve equations. The apparent tumor marker clearance (CL), a kinetic parameter, related to marker residual production and elimination, and independent of selected time points, can then be determined.

We postulate that hCG clearance (CL_{hCG}) would predict accurately the MTX resistance risk in patients with low-risk GTN. The objective of the present study was to assess the feasibility of characterizing MTX resistance using hCG kinetics.

patients and methods

patients

All patient data were derived from the French national registry of the Centre de Référence des Maladies Trophoblastiques based in Lyon [2]. All patients had been treated in French centers for chemonaive low-risk GTN according to 2000 FIGO classification [13] between January 2000 and February 2008. Exclusion criteria included treatment with two or less courses of MTX, patients whose treatment was changed without resistance criteria fixed by the Centre de Référence des Maladies Trophoblastiques or whose treatment differed from the conventional MTX regimen, patients with inadequate hCG follow-up, and historical diagnosis of a placental site trophoblastic tumor.

All patients were treated with the 8-day MTX regimen defined by Bagshawe et al. [3]: intramuscular MTX (1 mg/kg) on days 1, 3, 5, and 7 along with oral folinic acid (10 mg) on days 2, 4, 6, and 8, every 2 weeks. hCG levels were determined once each week. Treatment was stopped if hCG values normalized (≤5 mIU/ml) or switched to a second treatment (EMA-CO, ACT-D, or a platinum-based regimen) in the case of tumor MTX resistance or biochemical relapse. If the treatment was altered, further hCG titers were not included in the analysis. Choriocarcinoma diagnoses were confirmed by a pathologist, whereas non-choriocarcinoma diagnoses were defined biologically and not histologically according to 2000 FIGO hCG criteria [1].

analysis of hCG kinetics

A population pharmacokinetic model was developed using a dataset consisting of plasma concentrations of total hCG following MTX administration. The analysis was carried out using data collected between day 0 (day of chemotherapy start) and day 40. Indeed, predicting the resistance risk after three courses of chemotherapy would provide enough time to quickly adapt treatment in patients at high risk of resistance.

The analysis was carried out using a nonlinear mixed-effects modeling strategy, implemented in NONMEM version 6, to estimate the population parameters (mean and intersubject variability) as well as the residual variability. Moreover, it was used to identify potential covariates that could explain intersubject variability of parameters [14]. Linear pharmacokinetic models were evaluated, including one- and two-exponential models for disposition and elimination of hCG. Because the rate of endogenous hCG production was unknown, no attempt was made to characterize it before time 0. Monoexponential models were implemented with the following equation:

$$hCG_{ij}(t) = \left(hCG0_i \times e^{-K_i \times t}\right)\left(1+\varepsilon 1_{ij}\right)+\varepsilon 2_{ij},$$

whereas biexponential models were implemented with

$$hCG_{ij}(t) = \left(hCG1_i \times e^{-\alpha_i \times t} + hCG2_i \times e^{-\beta_i \times t}\right)\left(1+\varepsilon 1_{ij}\right)+\varepsilon 2_{ij},$$

where $hCG_{ij}(t)$ is the jth measurement determined in patient i at time t, and $\varepsilon 1_{ij}$ and $\varepsilon 2_{ij}$ are the proportional and additive residual variability of patient i at the jth measurement, which has a mean of zero and variance of σ^2. Parameters $hCG0_i$, K_i, $hCG1_i$, $hCG2_i$, α_i, and β_i were assumed to vary randomly between patients according to a normal log distribution. Once individual parameters $hCG0_i$ and K_i or $hCG1_i$, $hCG2_i$, α_i, and β_i are estimated, it is possible to determine the individual apparent clearance (CL_{hCGi}). In the monoexponential model, this is equal to the product of K_i and the volume of distribution (Vd), where Vd is estimated to be 3.4 l, as described previously [15]. Data analysis was carried out using the first-order conditional estimation method with an interaction computational method algorithm (FOCE INTERACTION). Comparison of two nested models was based on differences between the minimum value of the objective function. The following individual covariates were tested to estimate their impact on hCG kinetic parameters for reducing unexplained interindividual variability: items included in the FIGO score as well as tumor pathology (choriocarcinoma versus non-choriocarcinoma), number of children, hysterectomy (yes versus no), interval between first and second MTX cycle, and hCG surge after MTX start (yes versus no). The modeling methodology has been described in detail elsewhere [11].

internal validation of the model: visual predictive check

The predictive performance of the final model was evaluated by visual predictive check (VPC) [16, 17]. We simulated 100 decline profiles for hCG using the final parameters estimated from the best model. The predictive ability of the population pharmacokinetic model was assessed using graphical comparison of the 90% confidence intervals (CIs) of predictions built from simulated data with an overlay of the observed data.

assessment of predictive value of CL_{hCG}

A normal hCG value was considered ≤5 mIU/ml. MTX resistance is defined by the Centre de Référence des Maladies Trophoblastiques as an increase or a plateau in two consecutive hCG values over a 2-week interval. This definition was chosen to minimize the effects of weekly hCG concentration fluctuations and to establish a similar time interval between two MTX cycles.

One of the aims of the study was to define a CL_{hCG} threshold that could discriminate patients at high risk of MTX resistance from those at lower risk. We used ROC curves to test the diagnostic accuracies of different cut-offs. To optimize statistical power, the thresholds tested were derived from the median and quartiles of CL_{hCG}. Once the best cut-off was identified, we assessed the diagnostic accuracy of the CL_{hCG} ['less than or equal to' (≤) threshold versus 'more than' (>) threshold] against other kinetic

parameters reported in literature (seventh-week hCG value ≤520.24 versus >520.24 mIU/ml [6], or ≤737.0 versus >737.0 mIU/ml [7]) for predicting MTX resistance risk. Because patient distributions were similar when seventh-week hCG cut-off was fixed at 500 or 520 mIU/ml, we did not study the predictive value of threshold reported by Savage et al. (9).

Moreover, we assessed the predictive value of CL_{hCG} on MTX resistance-free survival (MRFS) using univariate/multivariate survival analyses. MRFS was calculated as the time elapsed between the first MTX course on day 0 and the first event, such as MTX biochemical resistance day or death due to any cause.

The following potential predictive factors were investigated using survival log-rank tests:

- Parameters included in the FIGO score except for the previous chemotherapy item because all patients were chemonaive.
- Other potential predictive covariates: hysterectomy (yes/no), tumor pathology (choriocarcinoma or non-choriocarcinoma), number of MTX courses, number of uterine evacuations, number of children, uterus invasion depth, transient hCG surge after start of MTX (yes/no), interval between first and second MTX courses (≤14 versus >14 days), pretreatment hCG scored according to the Chan et al. threshold reported as a predictive factor of failure after one single MTX dose (≤5000 versus >5000 mIU/ml) [18], and hCG level in the seventh week, scored according to the Van Trommel et al. threshold (≤520.24 versus >520.24 mIU/ml, equivalent to ≤56 versus >56 μg/l) [6] and according to Kerkmeijer et al. cut-off (≤737.0 versus >737.0 mIU/ml) [7]. Seventh-week hCG values were available for 125 patients. We also assessed the predictive value of CL_{hCG} threshold defined with the ROC curve analysis (≤ versus > lower quartile). Because the log-rank test requires categorical data, continuous covariates were split into two groups according to the median except for CL_{hCG}, which was split according to the lower quartiles for the ROC curve analysis.

To determine independent predictive factors, variables found to be statistically significant in univariate analysis ($P < 0.05$) were included in multivariate analysis using Cox models with backward elimination. Median follow-up was calculated using a reverse Kaplan–Meier estimate [19]. All tests were carried out with S-PLUS™ and SPSS™ using a two-sided 0.05 alpha risk. The ROC curves were generated using TANAGRA™ software.

results

patients and follow-up

Data for 154 patients with low-risk GTN were analyzed; 5574 hCG concentration determinations were recorded between October 1999 and March 2008. Modeling analysis was carried out using 845 hCG concentrations determined between day 0 (day of chemotherapy start) and day 40, with a mean of 5.5 observations per patient. Because the data included concentrations below the limit of quantification (BLOQ), the first concentration in a series of BLOQ observations was replaced by LOQ/2 and later observations were censored [20, 21]. Patient characteristics are summarized in Table 1.

modeling

The best model describing the hCG decrease between day 0 and day 40 was a one-compartment model. All covariates likely to influence the hCG decline profile were evaluated. Only the pretreatment hCG value, scored according to FIGO criteria (shCG0), significantly decreased the unexplained interindividual variability of the modeled hCG0. However, shCG0 could not be inserted into the model as a covariate because it was equivalent to hCG0 grouped by classes. Thus, the final population model was

$$hCG(t) = 3900 \times e^{-0.149 \times t},$$

where $hCG(t)$ was the population-predicted hCG value (mIU/ml) at time t (days) for data collected between day 0 and day 40. Figure 1 shows the plots leading to the final model selection.

The results for modeled parameters, interindividual variability, 95% CIs, and residual variability are shown in Table 2. Figure 2 shows the VPC: 96.7% of observed hCG levels fell within the 90% prediction interval, supporting the accuracy of the model.

predictive value of CL_{hCG}

After a median follow-up of 12.7 months (95% CI 11.5–13.4), 133 patients (86%) were not MTX resistant and 21 (14%) had become resistant to MTX. All resistances developed within the first year of initiating treatment (median time to resistance = 83 days; range 48–195 days). These patients all received second-line treatment: EMA-CO, $n = 13$ (62%); ACT-D, $n = 6$ (29%); bleomycin, etoposide, cisplatin regimen, $n = 1$ (5%), or had a hysterectomy, $n = 1$ (5%). One patient died 91 days after start of chemotherapy.

ROC curve analysis

Several different thresholds, using CL_{hCG} median and quartiles, were evaluated for diagnostic accuracy of MTX resistance by ROC curve analysis. The best area under the ROC curve (AUC) was observed when the lower CL_{hCG} quartile was used (≤0.37 versus >0.37 l/day): AUC = 74.5, sensitivity = 66.7%, specificity = 81.2%, positive predictive value (PPV) = 35.9%, and negative predictive value (NPV) = 93.9%.

Because none of the three other tests reported in literature offered a better diagnostic accuracy for detecting resistance risk, we decided to use the cut-off described previously in univariate and multivariate analyses. The seventh-week hCG cut-off of Van Trommel et al. (≤520.24 versus >520.24 mIU/ml) had an AUC of 74.5 (sensitivity 44.4%, specificity 91.7%, NPV 89.9%, PPV 50.0%), whereas the seventh-week hCG cut-off of Kerkmeijer et al. (≤737.0 versus >737.0 mIU/ml) had an AUC of 72.5 (sensitivity 38.9%, specificity 92.8%, NPV 89.1%, PPV 50.0%; supplemental Figure S1, available at *Annals of Oncology* online).

survival analyses

Table 3 shows the predictive factors significant in univariate survival analysis using the log-rank test. Six factors predictive of hCG resistance risk were identified: unfavorable CL_{hCG}, less than or equal to lower quartile (0.37 l/day), choriocarcinoma tumor pathology, term or abortion pregnancy history, hCG surge after start of chemotherapy, seventh-week hCG >520.2 mIU/ml, and seventh-week hCG >737.0 mIU/ml. These covariates were included in a multivariate survival Cox model. As shown in Table 3, four factors were initially significant; backward elimination identified two of these as independent significant predictive factors: (i) choriocarcinoma versus non-choriocarcinoma pathology [hazard ratio (HR) = 6.01; 95% CI

Table 1. Patient characteristics

Covariate	Status	*n*	%
MTX tumor response	Sensitive	133	86.4
	Resistant	21	13.6
Age (years; median = 31;	≥40	30	18.8
25% quartile = 28; 75% quartile = 34)	<40	124	81.2
Pregnancy history	Hydatidiform mole	147	95.4
	Term	4	2.5
	Abortion	3	2
Interval between end of	<4	127	82.5
previous pregnancy and	4–6	20	12.9
start of chemotherapy (months)	7–12	7	4.5
	>12	0	0
Baseline hCG (shCG0 in	$<10^3$	46	29.9
mIU/ml; median = 7461.5)	10^3–10^4	43	27.9
	10^4–10^5	54	35.0
	$>10^5$	11	7.1
Sites of metastases (144 patients	Lung	CT scan: 48, X-ray: 9	CT scan: 33.3, X-ray: 6.2
evaluated by CT)	Spleen, kidney	0	0
	GI tract	1	0.6
	Liver and/or brain	0	0
Largest tumor (cm)	<3	106	68.8
	3–5	34	22.1
	>5	14	9.1
No. of metastases	0	137	88.9
	1–4	14	9
	5–8	2	1.2
	>8	1	0.6
FIGO score (median = 2)	0	15	9.7
	1	40	25.9
	2	42	27.2
	3	28	18.2
	4	10	6.5
	5	9	5.8
	6	10	6.5
Hysterectomy	Yes	12	7.7
	No	142	92.3
Tumor pathology	Non-choriocarcinoma	144	93.5
	Choriocarcinoma	10	6.5
No. of children (median = 1)	≤1	105	68.2
	≥2	49	31.8
Uterus invasion depth	≤50% myometrium	32	20.8
	>50% myometrium	47	30.5
	Serosa	3	1.9
	Unknown	72	46.7
No. of MTX courses (median = 6)	≤6	98	63.3
	>6	56	36.3
No. of uterus evacuations (median = 2)	1	59	38.3
	2	78	50.6
	3	8	5.1
	Unknown	9	5.8
hCG surge after MTX start	Yes	10	6.5
	No	144	93.5
Interval between 1st and 2nd MTX course	≤15 days	135	87.6
	>14 days	19	12.3
Total		154	100

MTX, methotrexate; hCG, human chorionic gonadotropin; CT, computed tomography; GI, gastrointestinal; FIGO, International Federation for Gynecology and Obstetrics.

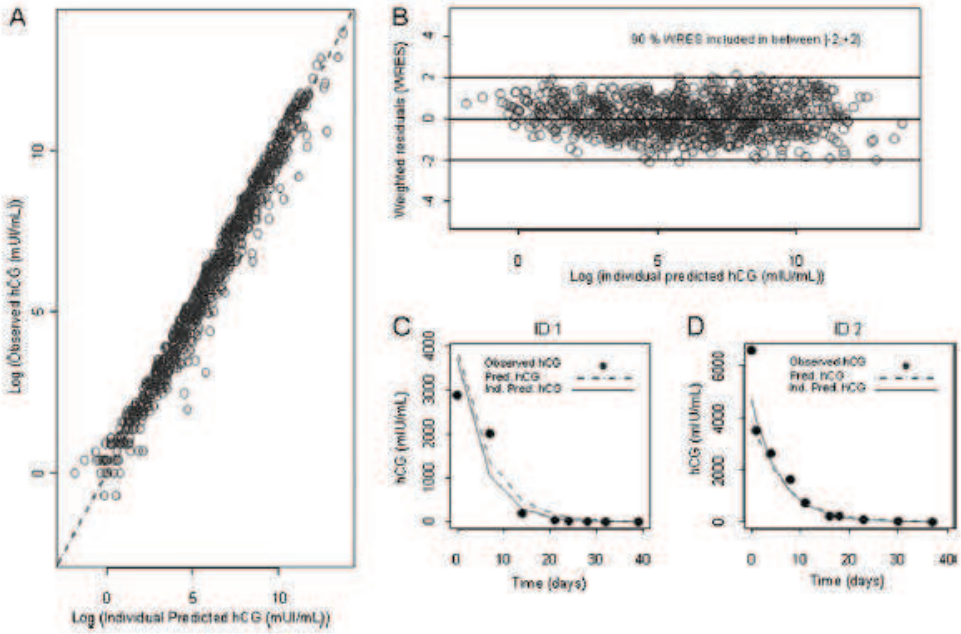

Figure 1. Goodness-of-fit plots: (A) log (observed hCG concentrations) versus log (individual predicted hCG concentrations); (B) weighted residual versus log (individual predicted hCG concentrations); (C and D) observed hCG, predicted hCG (Pred. hCG), and individual predicted hCG concentrations (Ind. Pred. hCG) concentrations for two representative patients; and (D) patient ID 2 expressed MTX resistance 62 days after start of treatment. hCG, human chorionic gonadotropin.

Table 2. Final model parameter estimates

Final model			
MOF	11 017.039		
Variation from base model	-214.456		
Parameters	Population mean	95% CI	IIV (%)
hCG0 (IU/l) (θ1)	3900	2269.28–5530.72	273.50
K (day 1) (θ5)	0.149	0.135–0.163	52.92
V (l) (θ6)	3.4	—	—
Eprop (CV%)	67.08	64.93–69.17	—
Eadd (IU/l)	1.16	0.37–1.95	—

MOF, minimum objective function; CI, confidence interval; IIV (%), interindividual variability expressed as a percentage; *K*, elimination shCG0, concentration of human chorionic gonadotropin at time 0; *V*, volume of distribution; Eprop (CV%), % of proportional residual variability; Eadd (IU/l), additive component of residual variability.

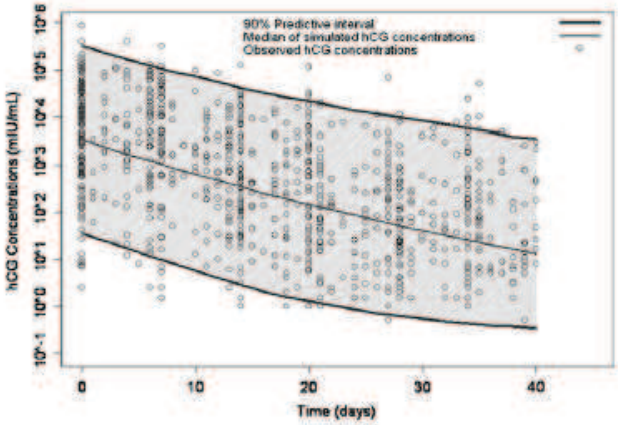

Figure 2. Results of the visual predictive check: 96.7% of observed human chorionic gonadotropin (hCG) values are within the 90% prediction interval.

2.17–16.6; $P = 0.0005$] and (ii) CL_{hCG} (unfavorable versus favorable: HR = 6.75; 95% CI 2.71–16.8; $P = 0.00004$). Figure 3 shows the Kaplan–Meier curves of MRFS according to tumor pathology and CL_{hCG} lower quartile threshold.

conclusions

Although there is consensus regarding the use of monotherapy (MTX or ACT-D) for treating low-risk GTN, many aspects of treatment for this patient subgroup remain unclear [5]. Early identifying patients at high risk for MTX resistance would enable rational individualization of treatment protocols [22]. Recently, several studies have identified potential predictive factors of chemoresistance in poor-risk GTN [6–8, 23, 24].

However, the cut-offs reported in these trials might be limited by their intimate dependences on static and single hCG measurements, prone to high unconsidered inter/intraindividual variability. It could explain the heterogeneity in the reported thresholds. Moreover, none of the latter studies incorporated survival analysis or regression models to test the predictive values of cut-offs with respect to other prognostic covariates, which is the standard method for validating such factors.

In the present study, we identified two independent predictive factors. Because 50% of patients with a choriocarcinoma were resistant to MTX, this pathology appeared to be a strong negative predictive factor. We also

Table 3. Results of univariate (log-rank test) and multivariate survival analyses (Cox model) for 1-year methotrexate resistance-free survival

Univariate analysis					Multivariate analysis		
Covariate	Status	No. of patients	1-year MRFS (%)	*P* value	Hazard ratio	95% CI	*P* value
Age (years)	<40	124	85.5	0.87	—	—	—
	≥40	30	86.3				
Pregnancy history	**Hydatidiform mole**	**147**	**87.1**	**0.02**	**5.06**	**1.23–20.79**	**0.024**
	Abortion	**3[a]**	**66.7**				
	Term	**4[a]**	**50.0**				
Interval between end of previous pregnancy and start of chemotherapy (months)	<4	127	86.8	0.30	—	—	—
	4–6	20	84.2				
	7–12	7	71.4				
	>12	0	ND				
Initial hCG (mIU/ml; median = 7461.5)	$<10^3$	46	88.2	0.86	—	—	—
	10^3–10^4	43	90.2				
	10^4–10^5	54	77.1				
	$>10^5$	11	100				
Lung metastasis (144 patients evaluated by CT)	Yes	48	85.0	0.82	—	—	—
	No	96	86.7				
Largest tumor (cm)	<3	106	83.9	0.33	—	—	—
	3–5	34	88.2				
	>5	14	91.7				
No. of metastases	0	137	84.1	0.62	—	—	—
	1–4	14	100				
	5–8	2	ND				
	>8	1	100				
FIGO score (median = 2)	0	15	93.3	0.80	—	—	—
	1	40	86.0				
	2	42	85.0				
	3	28	82.1				
	4	10	78.7				
	5	9	88.9				
	6	10	88.9				
Hysterectomy	Yes	12	75.0	0.26	—	—	—
	No	142	86.8	0.26			
Tumor pathology (unknown, $n = 4$)	**Choriocarcinoma**	**10**	**50.0**		**6.57**	**2.00–21.51**	**0.0018**
	Non-choriocarcinoma	**140**	**87.9**	**0.00025**			
No. of children (median = 1)	≤1	105	83.9	0.38	—	—	—
	≥2	49	89.3				
No. of MTX courses (median = 6)	≤6	98	83.9	0.27	—	—	—
	>6	56	89.0				
No. of uterus evacuations (median = 2; unknown, $n = 9$)	1	59	87.3	0.77	—	—	—
	2	78	85.2				
	3	8	100				
hCG surge after MTX start	**Yes**	**10**	**60.0**	**0.01**	1.81	0.40–8.00	0.44
	No	**144**	**87.5**				
Pretreatment hCG value (mIU/ml)	≤5000	68	88.8	0.32	—	—	—
	>5000	86	83.2				
hCG value in the 7th week (mIU/ml)	**>520.2**	**26**	**66.8**	**0.0056**	**4.71**	**1.52–14.56**	**0.007**
	≤520.2	**99**	**89.6**				
hCG value in the 7th week (mIU/ml)	**>737.0**	**14**	**50.0**	**0.0009**	0.36	0.10–1.26	0.11
	≤737.0	**101**	**88.8**				
Interval between 1st and 2nd MTX course	≤14 days	135	84.6	0.30	—	—	—
	>14 days	19	93.8				
CL_{hCG} (l/day; median = 0.57; quartiles = 0.37, 0.74	**≤0.37**	**38**	**64.5**	**<0.00001**	**6.05**	**1.88–19.42**	**0.0025**
	>0.37	**116**	**92.8**				

Significant predictive factors are written in bold.

[a]Term and abortion covariates were grouped together for Cox model analysis.

CI, confidence interval; CL_{hCG}, hCG clearance; CT, computed tomography; FIGO, International Federation of Gynecology and Obstetrics; hCG, human chorionic gonadotropin; MRFS, methotrexate resistance-free survival; MTX, methotrexate; ND, not determined.

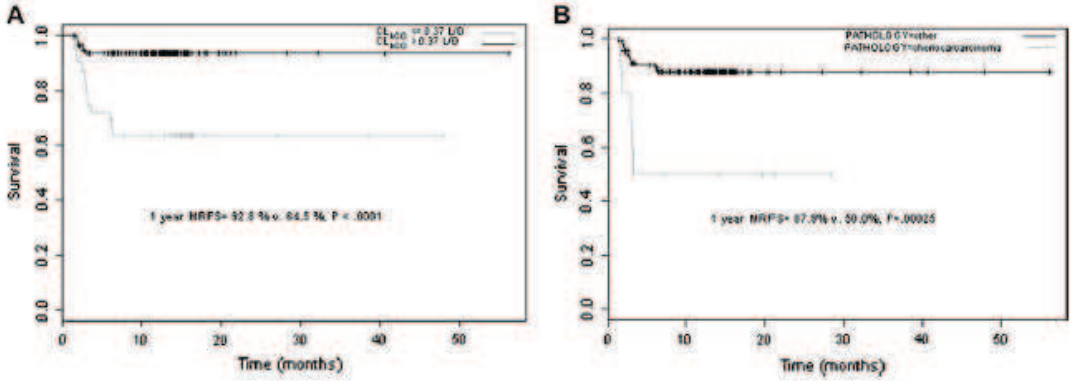

Figure 3. Kaplan–Meier curve of probability of methotrexate resistance-free survival according (MRFS) to (A) CL_{hCG} (≤37 versus >37 l/day) and (B) tumor pathology (choriocarcinoma versus non-choriocarcinoma). CL_{hCG}, human chorionic gonadotropin clearance.

identified a group of patients with a high risk of resistance characterized by a low CL_{hCG} (35.5% risk of biochemical resistance at 1 year if CL_{hCG} ≤0.37 l/day). As asserted by the Cox model, this predictive value was independent of tumor pathology and was stronger than the other expected prognostic factors, such as FIGO score components or the cut-offs reported previously. ROC curve analyses confirmed the predictive value of CL_{hCG} for resistance risk with respect to other published factors. The high specificity and NPV indicate that this marker may be used to identify the patients with favorable hCG decline, thereby unlikely to present further MTX resistance. The risk of resistance (false-negative rate) in patients with high CL_{hCG} was only 6%. For routine practice, the patient's risk group could be calculated by every clinician easily. Indeed, hCG concentrations obtained at appropriate times (day 0, day 15, day 30, and day 40 after start of MTX) could be entered into a model-based software program that would immediately determine patient's group. If the predictive value of CL_{hCG} were confirmed, it might give the opportunity to reduce MTX exposure in patients with satisfactory hCG declines. Some investigators have advocated for one single dose of MTX in all low-risk GTN patients, but the risk of failure has been concerning [18, 25, 26]. Early MTX discontinuation might rather be considered in patients with MTX-sensitive tumors and thereby more likely to be cured. Stop of treatment might thus be considered after three chemotherapy cycles in patients with high CL_{hCG}, whereas MTX continuation until hCG normalization or change of chemotherapy regimen could be discussed in patients with low CL_{hCG}. Of course, this assumption was not directly raised in the present study and will have to be assessed in other studies.

These results reported herein should be interpreted with caution because this study included small numbers of patients and MTX resistance events, although it is the second largest study on this particular subgroup to date. The results we present relate to our cohort but might not be applicable to another group of patients. The data used in the analysis were not derived from a specifically designed study with highly selected patients and favorable conditions likely to aid in predictive factor identification but conformed to 'real-life' patient data (treatment in various French hospitals, hCG concentrations determined in different laboratories using various immunoassay kits). Despite these limitations that were likely to increase inter- and intraindividual variability and to scatter modeled CL_{hCG} values, our results were highly statistically significant. CL_{hCG} values were calculated on the assumption that body hCG distribution was equal to the blood volume distribution, as indicated by Norman et al. [15]. Three elements could explain the 'traditional' prognostic factors, such as FIGO items, FIGO score [25, 27], or metastasis status [18], that were not found significant in the multivariate analysis. The limited number of patients might have contributed to the reduced statistical power of analysis. Moreover, these factors were reported in studies carried out before the definition of low-risk GTN by FIGO in 2000, thereby including patients with various disease stages. Finally, these factors have not been confronted with hCG kinetic parameters in univariate/multivariate analyses within articles published so far.

This study confirms that it is possible to model individual hCG decline curves using a kinetic population approach in low-risk GTN patients. Using univariate and multivariate survival analyses, our results showed that patients with choriocarcinoma and treated with MTX have a high risk of MTX resistance. Using this modeled CL_{hCG} approach, it might be possible to identify a subgroup of patients likely to develop MTX resistance who might benefit from early treatment alterations. Other retrospective studies involving higher numbers of patients, potentially followed by prospective trials, are warranted to confirm the relevance of CL_{hCG} in managing patients with low-risk GTN.

funding

Institut National de la Santé et de la Recherche Médicale to P.G.

acknowledgements

The authors thank Paul Kretchmer (*San Francisco Edit*) for help in English editing.

disclosure

All authors disclose no conflict of interest or financial and personal relationships with other researchers or organizations that could inappropriately influence or bias the study.

references

1. FIGO staging for gestational trophoblastic neoplasia 2000. FIGO Oncology Committee. Int J Gynaecol Obstet 2002; 77: 285–287.
2. Golfier F, Raudrant D, Frappart L et al. First epidemiological data from the French Trophoblastic Disease Reference Center. Am J Obstet Gynecol 2007; 196: 172–175.
3. Bagshawe KD, Dent J, Newlands ES et al. The role of low-dose methotrexate and folinic acid in gestational trophoblastic tumours (GTT). Br J Obstet Gynaecol 1989; 96: 795–802.
4. Chelouhi GE, Golfier F, Soignon P et al. Methotrexate for 2000 FIGO low-risk gestational trophoblastic neoplasia patients: efficacy and toxicity. Am J Obstet Gynecol 2009; 200: 643–646.
5. Foulmann K, Guastalla JP, Caminet N et al. What is the best protocol of single-agent methotrexate chemotherapy in nonmetastatic or low-risk metastatic gestational trophoblastic tumors? A review of the evidence. Gynecol Oncol 2006; 102: 103–110.
6. van Trommel NE, Massuger LF, Schijf CP et al. Early identification of resistance to first-line single-agent methotrexate in patients with persistent trophoblastic disease. J Clin Oncol 2006; 24: 52–58.
7. Kerkmeijer LG, Thomas CM, Harvey R et al. External validation of serum hCG cutoff levels for prediction of resistance to single-agent chemotherapy in patients with persistent trophoblastic disease. Br J Cancer 2009; 100: 979–984.
8. Savage P, Seckl M, Short D. Practical issues in the management of low-risk gestational trophoblast tumors. J Reprod Med 2008; 53: 774–780.
9. Sheiner LB. The population approach to pharmacokinetic data analysis: rationale and standard data analysis methods. Drug Metab Rev 1984; 15: 153–171.
10. You B, Girard P, Paparel P et al. Prognostic value of modeled PSA clearance on biochemical relapse free survival after radical prostatectomy. Prostate 2009; 69: 1325–1333.
11. You B, Perrin P, Freyer G et al. Advantages of prostate-specific antigen (PSA) clearance model over simple PSA half-life computation to describe PSA decrease after prostate adenomectomy. Clin Biochemistry 2008; 41: 785–795.
12. Boyle H, You B, Fronton L et al. Major prognostic value of modeled $AUC_{hCG-AFP}$, a dynamic kinetic marker characterizing tumor marker decline of non seminomatous germ cell tumors (NSGCT) intermediate-poor risk patients according to the IGCCCG. Proc ASCO 2009. J Clin Oncol 2009; 27(Suppl): 5085.
13. Kohorn EI. The new FIGO 2000 staging and risk factor scoring system for gestational trophoblastic disease: description and critical assessment. Int J Gynecol Cancer 2001; 11: 73–77.
14. Beal SL, Sheiner LB, Boeckmann A. NONMEM Users Guides. Ellicott City, MD: Icon Development Solutions 2006.
15. Norman RJ, Buchholz MM, Somogyi AA et al. hCGbeta core fragment is a metabolite of hCG: evidence from infusion of recombinant hCG. J Endocrinol 2000; 164: 299–305.
16. Brendel K, Dartois C, Comets E et al. Are population pharmacokinetic and/or pharmacodynamic models adequately evaluated? A survey of the literature from 2002 to 2004. Clin Pharmacokinet 2007; 46: 221–234.
17. Dartois C, Brendel K, Comets E et al. Overview of model-building strategies in population PK/PD analyses: 2002-2004 literature survey. Br J Clin Pharmacol 2007; 64: 603–612.
18. Chan KK, Huang Y, Tam KF et al. Single-dose methotrexate regimen in the treatment of low-risk gestational trophoblastic neoplasia. Am J Obstet Gynecol 2006; 195: 1282–1286.
19. Schemper M, Smith TL. A note on quantifying follow-up in studies of failure time. Control Clin Trials 1996; 17: 343–346.
20. Duval V, Karlsson MO. Impact of omission or replacement of data below the limit of quantification on parameter estimates in a two-compartment model. Pharm Res 2002; 19: 1835–1840.
21. Beal SL. Ways to fit a PK model with some data below the quantification limit. J Pharmacokinet Pharmacodyn 2001; 28: 481–504.
22. Tham KF, Ratnam SS. The classification of gestational trophoblastic disease: a critical review. Int J Gynaecol Obstet 1998; 60 (Suppl 1): S39–S49.
23. Berkowitz RS, Goldstein DP. Current management of gestational trophoblastic diseases. Gynecol Oncol 2009; 112: 654–662.
24. Growdon WB, Wolfberg AJ, Goldstein DP et al. Evaluating methotrexate treatment in patients with low-risk postmolar gestational trophoblastic neoplasia. Gynecol Oncol 2009; 112: 353–357.
25. Berkowitz RS, Goldstein DP. Current management of gestational trophoblastic diseases. Gynecol Oncol 2009; 112: 654–662.
26. Garrett AP, Garner EO, Goldstein DP et al. Methotrexate infusion and folinic acid as primary therapy for nonmetastatic and low-risk metastatic gestational trophoblastic tumors. 15 years of experience. J Reprod Med 2002; 47: 355–362.
27. Matsui H, Suzuka K, Yamazawa K et al. Relapse rate of patients with low-risk gestational trophoblastic tumor initially treated with single-agent chemotherapy. Gynecol Oncol 2005; 96: 616–620.